The Dissertation Committee for Gurtej Singh Saini Certifies that this is the approved version of the following dissertation:

Digital Twinning of Well Construction Operations for Improved Decision-Making

Committee:

____

Eric van Oort, Supervisor

____

Carlos Torres-Verdin

____

Michael J. Pyrcz

____

Pradeepkumar Ashok

____

Parham Pournazari

Digital Twinning of Well Construction Operations for Improved Decision-Making

by

Gurtej Singh Saini

DISSERTATION

Presented to the Faculty of the Graduate School of

The University of Texas at Austin

in Partial Fulfillment

of the Requirements

for the Degree of

DOCTOR OF PHILOSOPHY

The University of Texas at Austin

December 2020

Dedication

Dedicated to my parents who have always believed in me, pushed me to go above and beyond, and encouraged me to ‘ਚੱਕ ਦੇ ਫੱਟੇ’ (just go for it), to my brother who has been my inspiration, and also to my amazing and supportive wife, Urja.

Acknowledgments

I want to start by thanking Dr. Eric van Oort for allowing me to be a part of the Rig Automation and Performance Improvement in Drilling (RAPID) group. Being part of such a diverse and talented team provided me with the opportunities to explore new multi-disciplinary ideas, work on the cutting edge of drilling automation research, and work alongside some of the smartest researchers in the world. I am very grateful to Dr. van Oort for his continuous guidance, supervision, and mentorship throughout my Ph.D.

I would also like to acknowledge Dr. Pradeepkumar Ashok for his valuable insights, support, and regular feedback throughout my research. Dr. Ashok's initial guidance on digital twinning, and his pushing me to lead the undergraduate research teams in the early days of my Ph.D. helped me a lot with my data analytics and modeling skills. Another person I am greatly appreciative of is Dr. Parham Pournazari for the many brainstorming sessions, and guidance on reinforcement learning concepts. I want to thank Dr. Pyrcz and Dr. Verdin for bringing up some valuable points during my proposal, addressing which have helped make this dissertation better.

I much appreciate the administrative and logistical support provided by Ms. Tesse Smitherman, one of the most important members of the RAPID group. Also, all the help provided by Ms. Amy Stewart over the past four years of my graduate school has been invaluable. It has been an honor to work alongside some of the brightest and the most hard-working lab mates and friends, from whom I have learned a lot. A special thanks to my fellow lab mates, Sercan Gul and Melissa Lee, for providing valuable feedback on some of my early publication drafts. Also, I am grateful to our RAPID sponsors for their financial support of my work, and their regular feedback, direction, and data.

I am incredibly grateful to my parents and my brother for their moral support and encouragement. Finally, I would like to thank my amazing wife for her unwavering support through all the ups and downs of my Ph.D.

And of course, coffee!

Abstract

Digital Twinning of Well Construction Operations for Improved Decision-Making

Gurtej Singh Saini, Ph.D.

The University of Texas at Austin, 2020

Supervisor: Dr. Eric van Oort

Well construction is a highly technical, inherently unpredictable, and non-holonomic multi-step process with vast state and action spaces, that requires complex decision-making and action planning at every step. Action planning demands a careful evaluation of the vast action-space against the system's long-term objective. Current human-centric decision-making introduces a degree of bias, which can result in reactive rather than proactive decisions. This can lead from minor operational inefficiencies all the way to catastrophic health, safety, and environmental issues. A system that can automatically generate an optimal action sequence from any given state to meet an operation's objectives is therefore highly desirable. Moreover, an intelligent agent capable of self-learning can offset the computation and memory costs associated with evaluating the action space. This dissertation details the development of such intelligent planning systems for well construction operations by utilizing digital twinning, reward shaping and reinforcement learning techniques.

To this effect, a methodology for structuring unbiased purpose-built sequential decision-making systems for well construction operations is proposed. This entails formulating the given operation as a Markov decision process (MDP), which demands carefully defining states and action values, defining goal states, building a digital twin to model the process, and appropriately shaping reward functions to measure feedback. An iterative method for building digital twins, which are vital components of this MDP structure, is also developed. Finally, a simulation-based search decision-time planning algorithm, the Monte Carlo tree search (MCTS), is adapted and utilized for learning and planning.

The developed methodology is demonstrated by building and utilizing a finite-horizon decision-making system with discrete state- and action-space for hole cleaning advisory during well construction. A digital twin integrating hydraulics, cuttings transport, and rig-state detection models is built to simulate hole cleaning operations, and a non-sparse reward function to quantify state-action transitions is defined. Finally, the MCTS algorithm, enhanced by a well-designed heuristic function tailored for hole cleaning operations, is utilized for action planning. The plan (action sequence) output by the system, results in significant performance improvement over the original decision maker's actions, as quantified by the long-term reward and the final system state.

Table of Contents

List of Tables

List of Figures

Chapter 1: Introduction

Well construction is a multi-step process of drilling and completing wells in the subsurface for applications such as extracting hydrocarbons or accessing geothermal energy. It is highly complex since each step has multiple co-occurring sub-processes and various systems interacting with each other. Furthermore, drilling deep in the subsurface into variable geological environments adds unpredictability to the process. The highly involved and unpredictable nature of well construction can result in operational inefficiencies or safety and environmental issues, potentially leading to non-productive time (NPT). The cost of NPT can easily span from a few thousand to several million dollars. Currently, real-time data streams, advanced process models, and sophisticated simulation techniques are utilized for monitoring well construction operations (Mayani et al., 2018). Decision-making, however, is still primarily performed by humans, with little automation. The decisions are based on the understanding of the processes by the subject matter expert (e.g., engineer, or the driller out in the field) in control of the process. They are made not only based on interpretations of the model outputs, but also to a large extent on past experiences or 'rules of thumb', and sometimes 'gut feelings.' They are also affected by other human factors, such as situational awareness or even the physical and mental state of the decision-maker (with, e.g., fatigue playing a significant role (Chan et al., 2020)). Consequences of making erroneous decisions can range from poor operational efficiency to catastrophic failures and accidents, as was witnessed in the blowout on Macondo well in the Gulf of Mexico in 2010 (Griggs, 2010). Therefore, careful surveillance of process and equipment data for performance tracking and building intelligent systems for decision-making and action planning is essential. These objectives can be accomplished by developing decision-engines, which are automated intelligent sequential decision-making and action planning systems.

1.1 BACKGROUND

Well construction is guided by an engineering plan called the drilling program, which includes information about the current well's directional plan, the bottom hole assembly (BHA) design, subsurface geology, fluid and hydraulics plan, well control measures, casing design, cementing plans, as well as relevant information from offset wells (Dunn & Payne, 1986). Apart from specifying making the hole with a drill bit attached to a hollow flexible drillstring, which is rotated via a motor at the surface (top drive or rotary table), the drilling program guides many other processes, such as (Bourgoyne, 1986; Maidla & Haci, 2004; Mitchell & Miska, 2011):

- **'tripping'** the drillstring in and out of the borehole using a drilling rig's hoisting system (drawworks, hook, traveling block, etc.);
- making or breaking **'connections'**, to add or remove discrete drillstring elements called stands using pipe handling systems (hydrarackers and hydratongs);
- **directional drilling**, to control the trajectory of the well using either mud motors (rotary and slide drilling operating modes) or rotary steerable systems;
- **circulating** the drilling fluid (or drilling mud), to maintain its equivalent circulation density (ECD) within a drilling margin (as shown in **Figure 1**) using the rig's hydraulic system (reciprocating positive displacement mud pumps, standpipe, etc.);
- **hole cleaning**, to remove the drilled cuttings from the borehole by controlling the mud flowrate, mud properties and surface drilling parameters;

- **well logging**, to make high fidelity downhole measurements such as formation evaluation logs, near-bit drilling parameter measurements, and directional surveys using measurement and logging while drilling (MLWD) tools.

Throughout the process, various drilling parameters such as weight on bit (WOB), drillstring rotation speed (RPM), applied torque, rate of penetration (ROP) and standpipe pressure are measured directly or calculated using a suite of sensors installed on the drilling equipment (Cayeux & Daireaux, 2009; Gul et al., 2020). Once a section of the well has been drilled, the next steps involve securing it by running casing and then cementing the casing in place (Mitchell & Miska, 2011).

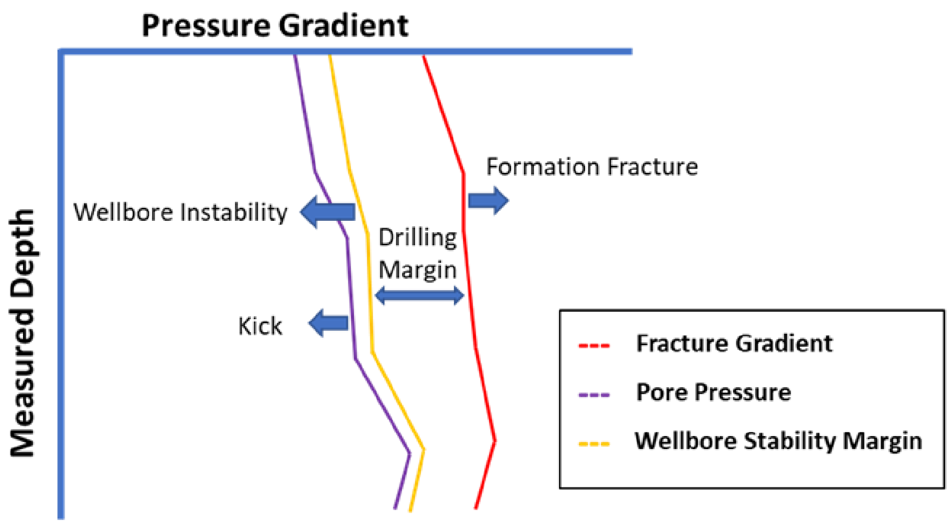

Figure 1 A simple representation of the drilling margin. Exceeding the fracture gradient can fracture the rock formation (Formation fracture), whereas a drop in pressure below the pore pressure can lead to an influx of formation fluids into the wellbore (called a kick).

1.1.1 Hole cleaning

One major issue that can lead to severe problems, potentially resulting in NPT, is inefficient or poor hole cleaning. Hole cleaning is the process of removing solids (cuttings, cavings, or metal shavings) from the borehole by circulating a drilling fluid in and out of the well. Drilling fluid or mud is a water or oil or synthetic-based mixture of solids and chemicals. It serves many functions, the main ones being to provide well control, lubrication of the drillstring, and hole cleaning by carrying the generated rock cuttings back to the surface. Removal of solids is critical in ensuring different well construction operations (such as drilling, tripping, casing, and cementing) are performed safely and efficiently. Poor hole cleaning can lead to such problems as (Erge et al., 2015; Naganawa, 2017; Nazari et al., 2010):

- Cuttings bed accumulation, which can lead to high torque and drag while moving the drillstring in or out of the borehole
- Deteriorating wellbore quality
- Damage to the downhole formations
- Damage to downhole drilling assembly
- Decreased rate of penetration
- Adversely affect the drilling mud properties
- Increased ECD, which can result in wellbore stability issues
- In severe cases, it can result in stuck pipe issues or pack-offs around the larger BHA elements

Annually, hole cleaning issues result in several hundred million dollars in NPT costs (Ahmed et al., 2019; Forshaw et al., 2020). Therefore, building a decision-engine for hole cleaning advisory that permits proactive action planning is of considerable practical importance and value.

1.1.2 Current state of process monitoring and decision-making in well construction

Currently, in the well construction domain, many algorithms and systems are utilized for performing calculations and process monitoring. To assist with decision-making, approaches such as case-based reasoning (Sadlier et al., 2013; Shokouhi & Skalle, 2009), performance tracking using digital twins (Mayani et al., 2020; Nadhan et al., 2018; Saini, et al., 2018), knowledge graphs and decision-trees (Danner, 2020; Miller & Gouveia, 2019), and type curve matching (Cordoso et al., 1995; Zhang et al., 2015) are being utilized. Remote process monitoring and multidisciplinary collaboration among domain experts have been enabled by the use of real-time (RT) data streams, advanced process and system models, and machine learning techniques (Abbas et al., 2019; Da Cruz Mazzi et al., 2020; Fjellheim, 2013). Cayeux et al. (2011, 2012), discuss the development and application of a system that defines and estimates some key indicators using physical models and real-time data to detect deviations from normal expected behavior. Other examples of such decision-assist tools and methods include the storyboarding process (Saini et al., 2018) complemented with the spider-bots technique (Saini et al., 2018) to calculate appropriate key performance indicators (KPIs) and present only the relevant information to the user in the form of a storyboard.

While such methodologies assist the decision-maker, the final decision, however, is based on the decision maker's understanding and interpretation of the data, KPIs, and model outputs. Moreover, decision-making for effective hole cleaning is based on many rules of thumbs or best-practices that have been established over the years based on the experiences of drillers or rig site engineers. This human-centered decision-making not only introduces a degree of bias but also results in reactive, short-term decisions instead of proactive long-term action planning.

1.1.3 Decision-making and action planning in other domains

The recent technological advances in the fields of big data, artificial intelligence, IoT hardware, and sensor technology have resulted in accelerating digitalization in many industries. Building intelligent decision-making and action planning systems using the concept of digital twinning is becoming the norm.

1.1.3.1 Digital twinning

The term ‘digital twin’ was first coined by Michael Greives and John Vickers (Grieves, 2014; Grieves & Vickers, 2016), initially to assist in product lifecycle management. It was introduced to model a physical system such as a jet propulsion engine or wind turbine. However, this concept has seen wider adoption across multiple industries because of many reasons, primary ones being:

- Advancement in sensor technology;
- Increased modern computational power;
- Increased data storage capability;
- Industry experience and expertise in the ability to handle big data.

The literature describes the digital twinning process as having three main components (Grieves & Vickers, 2016, 2017):

- The real physical system (process or equipment) and the associated sensors for data collection;
- The virtual representation of integrated models of the system to digitally replicate its behavior (called its digital twin) to enable performance tracking and scenario analysis;
- A data-stream to exchange data and information between the real system and its twin.

A valuable property of digital twins is their ability to be updated in real-time (RT) based on the most recent data. This feature allows for their application in RT decision-making systems (Chinesta et al., 2020; Datta, 2016; Jones et al., 2020). The concept of digital twinning is successfully implemented in other industries across a variety of applications. Some practical applications include Formula One racing simulations and strategy planning (Boxall, 2016; Breuer, 2018), twinning wind turbines for digital wind farm management (Schmidt, 2017), twinning gas turbines to predict failures (Power Digital Solutions, 2016; Schmidt, 2017), aerospace asset maintenance (Etong, 2019; Tuegel et al., 2011), product lifecycle management (Lim et al., 2019; Lu et al., 2020; Macchi et al., 2018), and developing integrated models for weather forecasting (Hoffman & Atlas, 2016; Rasheed et al., 2019).

1.1.3.2 Intelligent systems

Intelligent decision-making and action planning systems have resulted in overall performance improvement in various other fields. For instance, areas such as microgrid energy management (Ji et al., 2019; Kuznetsova et al., 2013), economic dispatch and large-scale power dispatch problems (Guan et al., 2020; Jasmin et al., 2011), electric vehicle systems management (Qi et al., 2019; Vandael et al., 2015), and smart grid management (Kang et al., 2009), utilize reinforcement learning (RL) methods. More recently, very high complexity adversarial board games (e.g., chess and Go), and complex RT strategy games (e.g., AlphaStar, Dota, and Pac Man) have been solved using a combination of deep neural networks and tree-based search techniques (Arulkumaran et al., 2019; Moerland et al., 2018; Ontanon et al., 2013; Silver et al., 2012, 2017, 2018).

Figure 2 demonstrates one such application of a digital twinning system for Formula One racing strategy planning and management. The physical system is the race car interacting with other competitor race cars and the racetrack. The race car itself has over 300 sensors that stream data about different aspects of the car (such as engine and tire temperatures, racetrack conditions, etc.) in real-time to the team's control room at their headquarters (Boxall, 2016). This data is then fed into an integrated multi-model system (the digital twin) representing the car and its interaction with the environment, to run many thousands of simulations per second. These simulations analyze multiple scenarios and decide on the best race strategy going forward. Also, throughout the race weekend, starting from the practice sessions on Friday until the final race on Sunday, many hundred gigabytes of data are collected. This data is used to update the understanding of the environment and the car, thereby improving the digital twin's performance for future racing events (a process known as enrichment).

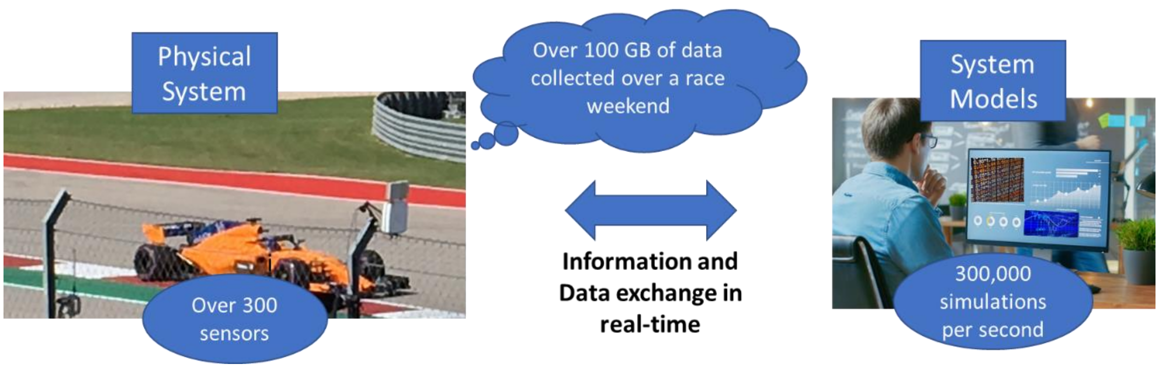

Figure 2 The three components of digital twining demonstrated through application in race strategy planning (Boxall, 2016).

1.2 Research Objectives

To summarize, well construction is a highly technical process that requires continuous complex decision-making and multi-step action planning. Action selection at every step demands a careful evaluation of the vast action space, while guided by achieving long-term objectives and desired outcomes. Although there exist multiple tools and systems that assist the rig site personnel with decision-making, there is no system yet that can continually quantify the state of the well construction operation, evaluate a set of actions to analyze the various possible scenarios, and suggest an optimal action sequence to meet the operation's objectives. A system that can automatically generate an optimal action sequence from any given state to meet an operation's objectives is highly desirable. In other domains, however, the use of sophisticated decision-making systems, coupled with digital twins of operations or equipment have resulted in an overall improvement in operational efficiency and safety. Therefore, the development of such *automated intelligent decision-making and action planning systems* (or **decision-engines**, as depicted in **Figure 3**) for improved well construction safety and performance is the overarching objective of the research presented in this dissertation.

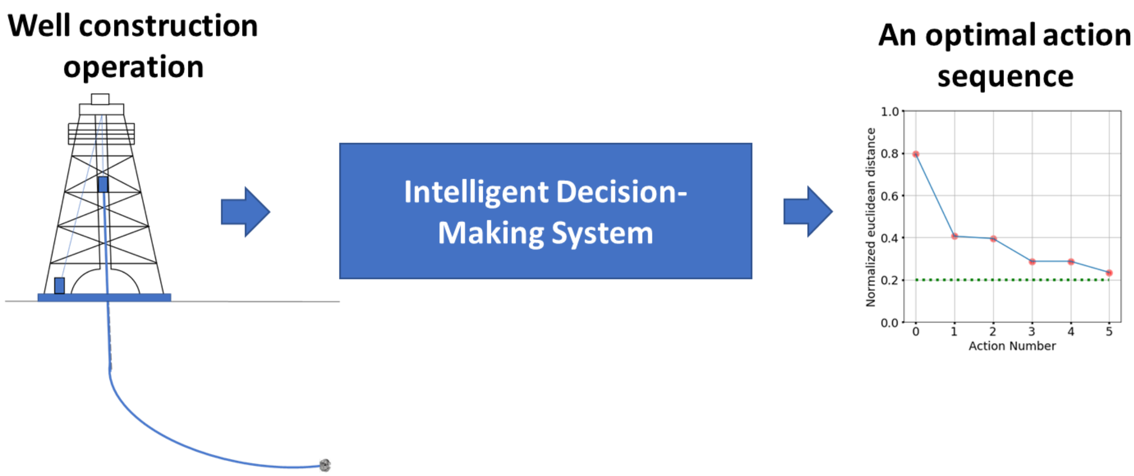

Figure 3 The objective of this research: development of intelligent decision-making systems for well construction operations.

Recent advances in sensors and data processing technologies at the rig site allow more reliable access to operational and equipment data. This data can be used in conjunction with historical data and appropriate system models to build **digital twinning systems** of the various well construction processes. These twinning systems serve as basic building blocks to help improve operational performance by allowing more informed decision-making. These twinning systems can then be utilized to **structure intelligent planning systems as Markov decision processes (MDPs).** The development of such systems requires:

- Integrating multiple sources of information (including data and process models) to quantify the system state;
- An unambiguous definition of goal or desirable states based on the operations' long term objective;
- Defining control variables or actions to manipulate these states, and using digital twins of the underlying process (or the environment) to simulate state-action transitions;
- A well-crafted non-sparse normalized reward function to evaluate action-sequences.

This MDP structure is then **solved by an appropriate planning algorithm** to output a policy or action plan in the form of a recommended action-sequence. Simulation-based search algorithms are a category of planning algorithms that can be utilized to solve MDPs with vast state and action spaces, as is the case in well construction.

1.2.1 Scope

The methodology proposed in this dissertation is demonstrated by structuring a decision-engine for **hole cleaning advisory**. First, a digital twin for hole cleaning operations is built by integrating multiple data streams with analytical implementations of the cuttings transport, hydraulics, and rig-state detection models. Subsequently, an MDP for the hole cleaning system is set up by appropriately defining its various components. Finally, the Monte Carlo tree search (MCTS), a type of simulation-based search algorithm that has successfully been used across other domains, is used for planning. The MCTS's performance is enhanced by the development of a heuristic function tailored for the hole cleaning system. This decision-engine is then tested on multiple real-world oil well cases that exhibited hole cleaning issues.

1.3 Dissertation Outline

The dissertation is structured as follows:

- Chapter 2 reviews hole cleaning operations and discusses the different components of building an intelligent decision-making and planning system. For hole cleaning, the various cuttings transport, hydraulics, and torque and drag modeling approaches are presented. The current state of digital twinning in the well construction domain is reviewed, and finally, the concept of planning and building intelligent planning systems is discussed.
- Chapter 3 defines a generalized iterative methodology for setting up digital twins for any well construction operation and demonstrates the same by building a twinning system for hole cleaning advisory. The application of such twinning systems is shown by performing a single-step scenario analysis.
- Chapter 4 details the steps in structuring unbiased purpose-built sequential decision-making systems in an MDP formulation by utilizing digital twins and non-sparse normalized reward design. The application of this system is shown for the quantification of different multi-step scenarios or action sequences.
- Chapter 5 builds on the Markov decision process formulation of a well construction operation by using the MCTS planning algorithm to develop decision-engines capable of self-learning. This decision-engine is then utilized for performance tracking and intelligent action planning for hole cleaning operations.
- Chapter 6 summarizes the contributions of this dissertation and suggests recommendations for further work in this area.

- The various appendix sections supplement the dissertation by detailing the nomenclature as well as discussing the development and utilization of a digital twin for logistics and planning.

Chapter 2: Literature Review

In well construction, there has been a significant amount of research in the areas of cuttings transport, hydraulics, and torque and drag modeling. Over the past few decades, due to the evolution of computational technology and the advent of many advanced modeling techniques, the models have become more sophisticated and can more accurately replicate the different drilling processes. Also, over the past few years, due to significantly improved computational power, increased data storage ability, advancements in sensor technology, and industry-wide expertise to handle big data, the concept of digital twinning has been adopted widely across multiple industries. However, only recently, the oil and gas industry has begun to recognize the incredible potential of digitally twining various equipment and processes. The following sections discuss the many cuttings transport, hydraulics, and torque and drag modeling approaches in the industry, followed by applications of digital twinning in drilling, and finally, the different methods available for sequential decision-making and action planning.

2.1 Hole Cleaning

As previously discussed, the primary goal of hole cleaning is to remove solids from the wellbore to the extent that various operations such as drilling, tripping, running casing and cementing can be performed safely and efficiently. Therefore, it is vital to monitor the condition of the borehole from a hole cleaning standpoint, which can be quantified by deriving metrics using a digital twin comprising of the cuttings transport, hydraulics, and torque and drag models.

2.1.1 Cuttings transport modeling

There are two main mechanisms for cuttings transport: dispersion of cuttings into the drilling mud and mechanical removal of cuttings. Cuttings transport mechanism is different in different wellbore sections, and wellbore inclination significantly affects the cuttings transport efficiency. These differences can be understood by dividing the wellbore into three distinct sections based on the inclination angles: 0 to 30 degrees (near-vertical section), 30 to 60 degrees (curve or the build section), and 60 to 90 degrees (near-lateral or horizontal section).

In the near-vertical section of the wellbore, the principal method of suspending and carrying cuttings up-hole in the mud is by overcoming the particle slip velocity, and no cuttings bed can exist. Hole cleaning is primarily due to viscosity and flowrate of the drilling fluid. There have been multiple studies to quantify the effect of annular velocity on cuttings transport. Williams and Bruce (1951) studied the effects of mud properties on cuttings removal capacity and the minimum annular velocity required to lift the cuttings. Since then, there have been multiple studies to model the cuttings slip velocity by considering different factors such as cuttings size and density, drilling fluid density and rheology, cuttings shape, Reynold’s number, etc. (Baldino et al., 2015; Larsen et al., 1997a; Walker & Mayes, 1975; Zeidler, 1970). A key advantage with predicting cuttings particle settling velocity is the ability to estimate the depth from where cuttings would have generated. In the curve section, an unstable cuttings bed can form below the angle of repose. However, there is a high possibility that when the mud circulation stops, the cuttings avalanche back down the annulus, which can pack-off around the bottom-hole assembly, causing a stuck pipe incident. For this section, the hole cleaning design requires tackling and preventing this cuttings avalanche. In the near-horizontal section, above the angle of repose for the cuttings, a stable cuttings bed will form on the low-side of the hole. The primary hole cleaning requirement is to move this bed up and out of the hole continuously (Sanchez et al., 1997; Sifferman & Becker, 1992). There has been extensive experimental work and model development in trying to understand the cuttings transport mechanisms for deviated and horizontal wells. **Figure 4** summarizes the cuttings transport in the different sections of the wellbore.

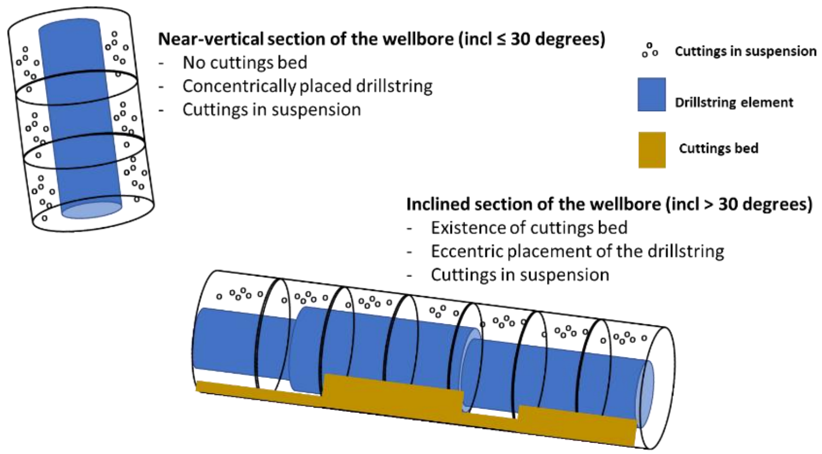

Figure 4 Cuttings bed distribution in different inclination segments of the well.

In deviated and horizontal sections, the drillpipe eccentricity, i.e., the drillpipe lying on the lower side of the borehole, and the rheological properties of the mud force the high-velocity fluid flow on the high-side of the wellbore. On the other hand, due to the shear-thinning behavior and the yield stress characteristics of the drilling mud, the flow velocity on the low-side of the borehole is significantly reduced. Therefore, drillpipe rotation is essential to agitate the cuttings from the bed into the flow stream on the high-side of the hole. Moreover, the cuttings that are already in the flow stream experience multiple forces, including gravity, which can result in them falling and settling on the low-side of the borehole after traversing a certain distance. This distance traveled is a function of factors such as flowrate, rotational speed, fluid rheology, cuttings size, cuttings distribution, etc. (Kenny et al., 1996; Ozbayoglu et al., 2008; Sanchez et al., 1997).

Sanchez et al. (1997) performed over 600 experiments to study the effects of rotary speed, hole inclination, mud rheology, cuttings size, and flowrate on hole cleaning in directional wells. The authors discovered a strong correlation between drill pipe rotation speed and cuttings transport. Sifferman and Becker (1992) performed a detailed experimental study to understand the effects of ten different variables on hole cleaning and find the variables that affect it the most. The variables considered were mud density, annular mud velocity, mud type, mud rheology, rate of penetration, cuttings size, inclination angle, drillpipe dimensions, drillpipe eccentricity, and drillstring RPM. The authors concluded that the height of the cuttings bed was most influenced by annular mud velocity, mud density, inclination angle, and drillstring RPM. Walker and Li (2001, 2000) performed experiments to study the effects of different cuttings particle sizes, fluid rheology, and pipe eccentricity on solids transport for coil tubing operations. Over 700 tests were performed with three different cutting sizes, for various gas and liquid concentrations, at different inclination angles and for two different eccentricities. Power et al. (2000) discussed the advantages of using weighted sweeps rather than high viscous sweeps to enable more efficient cuttings removal from deviated boreholes. Saasen and Løklingholm (2002) and Kjøsnes et al. (2003) discussed the effect of rheological properties of drilling fluids such as gel strength, viscosity, and yield point on their ability to remove cuttings by minimizing the cuttings bed consolidation.

Based on mass and momentum conservation equations, multiple models have been developed to determine the adequacy of hole cleaning by calculating parameters such as cuttings bed height in the well at different depths, cuttings concentration in suspension, the total weight of cuttings in the well, etc. These models can primarily be categorized as two-layer models or three-layer models. The main difference between the two types is the settling condition for cuttings in the drilling fluid. Two-layer models consider a cuttings bed layer and a suspension layer, while the three-layer models consider a suspension layer, a stationary cuttings bed layer, and moving cuttings bed layer.

Gavignet and Sobey (1989) developed a two-layer model to estimate the cuttings bed height and cuttings concentration. Martins and Santana (1992) developed a two-layer model with the presence of cuttings in the suspension layer. The authors calculated the stress at the interface between the two layers by using a friction factor, which includes the effect of cuttings. Iyoho and Takahashi (1993) developed a model for describing unstable cuttings transport at low velocities in horizontal wells. The model discusses the flow characteristics at low velocities, such as dunes formation, coupled with pressure variations. Kamp and Rivero (1999) discussed the development of a two-layer model that predicts cuttings build up during drilling. The suspension layer is assumed to be heterogeneous with both drilling mud and cuttings. Larsen (1990) developed a two-layer cuttings transport model to predict the required critical transport fluid velocity to keep the cuttings moving, and the cuttings concentration in the borehole for any velocity lower than this critical velocity. Larsen's model was later supplemented by the work of Jalukar (1993) and Bassal (1995), to include the effects of the hole size and drillpipe rotation, respectively, on the critical velocity. Nguyen and Rahman (1998) developed a three-layer cuttings transport model. This model relates the various flow patterns such as sliding bed, saltation of cuttings, etc., to variables such as flow rate, cuttings size, mud rheology, and annulus geometry. Similarly, Zou et al. (2000) and Cho et al. (2000) developed three-layer cuttings transport models for estimating cuttings bed height and cuttings concentration in deviated and horizontal wells as functions of parameters such as wellbore geometry, mud rheology, cuttings characteristics etc.

The paper by Nazari et al. (2010) compared multiple hole cleaning approaches from previous models and performed a classification of the different drilling parameters as inputs, outputs, and internal states. The goal of this classification is to treat hole cleaning during drilling as an internal state, relate it to input and output variables, and be able to check for its observability and controllability. Cayeux et al. (2014) have developed a more comprehensive model for estimating real-time cuttings transport by accounting for downhole transient conditions. The developed model considers the coupled effects of both drillstring mechanics and fluid transport. More recently, Erge and van Oort (2020) developed a model where the localized annular velocity profile is used to determine the cuttings bed height. This model considers the effects of eccentricity, pipe rotation, and annular blockage on the annular velocity.

2.1.2 Hydraulics modeling

The goal with hydraulics modeling is to accurately estimate the value of Equivalent Circulation Density (ECD) in the annulus. ECD at a depth is the gradient of the sum of the hydrostatic head exerted by the drilling mud (which is a function of the true vertical depth (TVD) of the well) and the total circulating frictional pressure loss in the annulus between the drillstring and the wellbore (which is a function of the measured depth (MD) along the annular space) (Mitchell & Miska, 2011). The circulating frictional pressure loss in the annulus is affected by factors such as wall roughness and friction, drillstring RPM, presence of cuttings beds, annular restrictions, or any tight annular clearances, drillpipe eccentricity in the annulus, etc. The hydrostatic head primarily depends on the total vertical depth and the density of the mud, which itself is a function of temperature and pressure, barite sag, and any cuttings suspended in the mud. Equation (1) shows the formula for estimating ECD at a measured depth of D.

$$ECD = \frac{P_{hydrostatic\_D_{TVD}} + P_{frictional\_pressure\_loss\_D_{MD}}}{D_{TVD}.\,g} \tag{1}$$

An accurate estimation of ECD is essential to manage the downhole pressure gradient and keep it within the drilling margin, i.e., between fracture gradient and pore pressure (or the minimum mud weight to maintain wellbore stability, whichever is higher), as shown in **Figure 5**. Pore pressure is exerted on the borehole by the fluids (hydrocarbons or brine) present in the pore spaces of the formation rocks. If the ECD falls below this lower limit (referred to as stability limit (SL) in this research), it can cause wellbore instability and, in some cases, an unwanted influx of formation fluids into the borehole (which is called a 'kick'). Exceeding the upper limit (which is the fracture gradient (FG)) can fracture the formation and lead to mud loss, which is referred to as a lost circulation event (Bourgoyne, 1986).

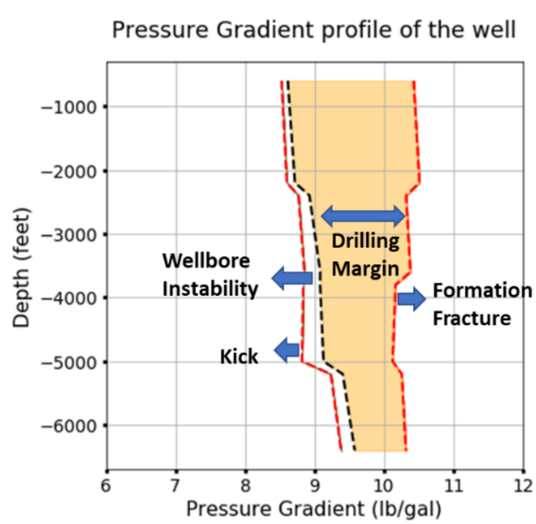

Figure 5 Representation of the drilling safety margin.

Multiple models in literature try to quantify the effects of different parameters on ECD. In the paper by Erge et al. (2016), the authors investigated the impact of drillpipe eccentricity in horizontal wells while circulating non-Newtonian fluids. Hemphill (2015), Erge et al. (2014) and, Ahmed and Miska (2008) are some of the researchers that have tried to quantify the effect of drillpipe rotation on annular frictional pressure drop.

Hemphill (2015) proposed a model to calculate this frictional pressure drop by including the effects of drillpipe geometry and eccentricity. Shahri et al. (2018) discussed the development of a hydraulics model by considering the impact of drillpipe eccentricity and pipe rotation for real-time drilling operations.

Other factors that need to be considered during tripping operations are the surge and the swab effects. Sudden and fast movement of drillstring, either in or out of the hole, can result in high-pressure spikes in the annulus. When running a drillstring in the hole, a piston effect causes a surge pressure that adds to the hydrostatic head of the mud. Similarly, while pulling the drillstring out of the hole, a suction effect results in a swab pressure that results in a temporary reduction of the hydrostatic head of the mud. These pressure spikes can result in the ECD going out of the drilling margin, thereby causing well control issues. The factors that have a significant effect on the surge and swab pressures are tripping velocity, drilling mud properties, BHA length, and annular space (Al-Abduljabbar et al., 2018). Therefore, it is important to consider these effects and control the drillstring velocity to keep the total ECD within the drilling margin. There have been many studies to model these effects, starting from a simple, conservative approach by Burkhardt (1961) to model surge pressures caused by pipe movement in a mud-filled borehole by considering a clinging factor which is a function of the ratio of pipe and hole diameters. Since then, there have been many other models such as the one by Mitchell (1988), which considered the effects of two regions: pipe to annulus and pipe to bottom hole, on the frictional pressure drop. The pressure drops in the two regions were calculated by simultaneously solving mass and momentum balance equations. In the study by Srivastav et al. (2012), the authors performed experimental investigations to study the effect of drillpipe eccentricity on surge and swab pressures and concluded that eccentricity could result in a significant reduction of surge and swab pressures, of the order of 40 percent.

2.1.3 Torque and drag modeling

Drag is the axial contact force between the drillstring and the casing or the formation, and it acts in the direction opposite to the direction of drillstring motion. Torque is the rotational force acting between the drillstring and the casing or the formation. These forces are primarily caused by a combination of the side forces and frictional forces acting on the drillstring. Side forces are experienced in the drillstring due to its weight, tension due to bending (or dog-leg severity), buckling, and the string's stiffness. The friction forces occur due to any motion of the drillstring, axial or rotational. Therefore, during rotary drilling, the drillstring experiences rotational friction; during tripping or slide drilling, it experiences axial friction, and operations such as reaming or back reaming result in a combination of the two friction forces acting on the drillstring. As the depth of the well increases, or the quality of the borehole worsens, or some issues are encountered downhole, the torque and drag values can increase to the point that drilling further can become challenging. Therefore, it is crucial to model and monitor these values (Mitchell & Miska, 2011).

In literature, there are many torque and drag models based on either stiff-string or soft-string approximation (Mirhaj et al., 2016). The difference between them being that in soft-string models, the bending moments and shearing forces are considered to have a negligible contribution to friction. Most of the models, however, are based on the early work done by Johancsik et al. (1984) and Sheppard et al. (1987). Since then, the basic concept of torque and drag modeling and prediction has not changed much. With the advancements in computational technology, finite element modeling, etc. several numerical models have been created, such as by Lesage et al. (1988) and Menand et al. (2006). Also, analytical models such as by Mitchell (2007, 2008), Aadnoy et al. (2010), and Mason and Chen (2007) have been widely used. There also have been attempts to implement real-time torque and drag models to aid in the decision-making process, such as by Brown et al. (2014) and Shahri et al. (2018).

2.2 Digital Twinning in the Well Construction Domain

Well construction is a highly involved multi-step process where each step has multiple co-occurring sub-processes and various systems interacting with each other. This level of complexity has the potential to lead to operational inefficiencies at best, and safety issues at worst. Over the past few decades, much research has been conducted to manage this complexity. For instance, process modeling (Cayeux et al., 2014b; Erge et al., 2014; Gu et al., 2019) and advanced data analytics (Al-Ghunaim et al., 2017; Coley, 2019; Gul & van Oort, 2020; Isemin et al., 2019; Okoli et al., 2019; Saini et al., 2018) have assisted in the monitoring of well construction operations for improving its efficiency and safety. **Figure 6** depicts the general idea behind digital twinning for well construction operations.

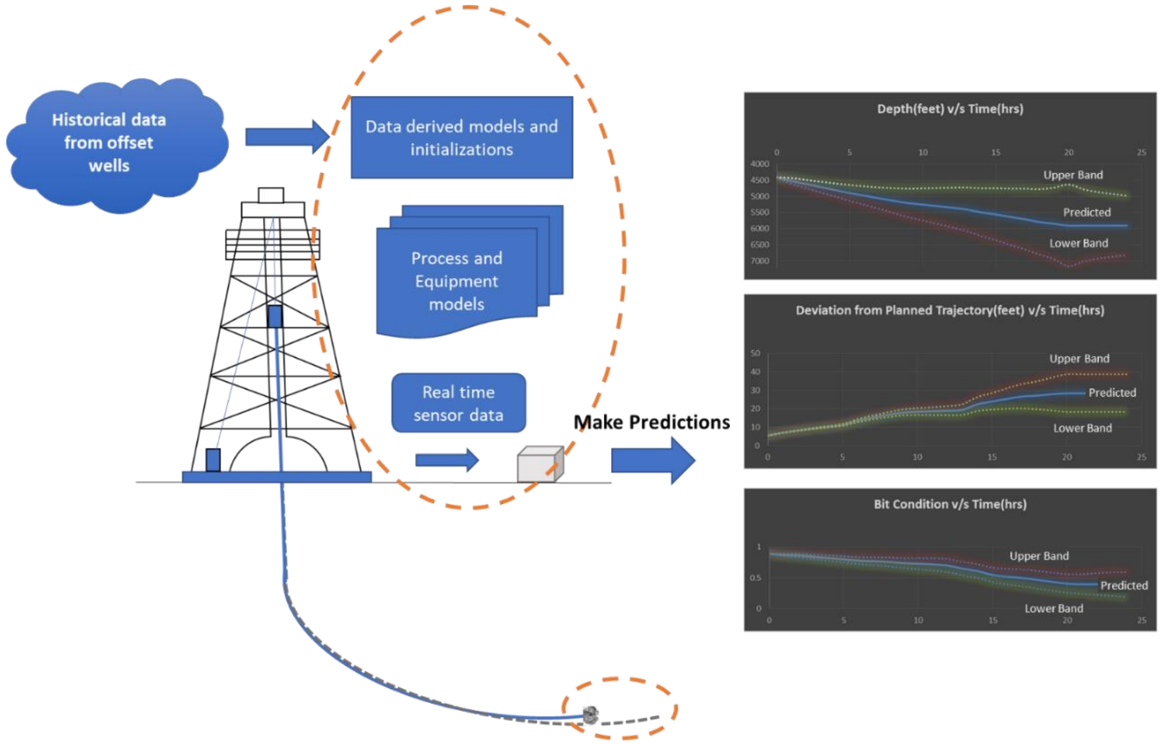

Figure 6 Utilizing multiple datasets, process models and advanced analytics techniques to make predictions (digital twinning).

Applications of setting up digital twins can be categorized into the following main groups:

- Non-productive time (NPT) identification and prevention
- Prognostics for equipment failure and detection
- Invisible lost time (ILT) evaluation and mitigation
- Logistics and planning
- Training and development

2.2.1 NPT identification (diagnostics) and prevention

NPT or non-productive time refers to the time lost due to events that cause any well construction operation to pause or stop. Incidents such as stuck pipe, loss of well control due to kicks or lost circulation events, time spent 'fishing' for lost drillstring components downhole, or time lost due to equipment or tool failures can contribute to a well's NPT. NPT identification and prevention is an essential consideration for oil and gas companies since NPT accounts for over 30 percent of upstream production costs, and thus can significantly affect a project's profitability (Forshaw et al., 2020). Some current and potential applications of digital twinning for NPT diagnostics and prevention include:

- Mitigation of well control issues (such as kicks and losses) (Isemin et al., 2019; Mao & Zhang, 2019; Pournazari et al., 2015)
- Drilling dysfunction identification and mitigation (Jeong et al., 2020; Zhao et al., 2019)
- Wellbore quality degradation identification and mitigation (Hutchinson et al., 2019; Mayani et al., 2020a; Rommetveit et al., 2019)
- Hole cleaning and stuck pipe prevention (Forshaw et al., 2020; Hindi et al., 2018)

Even though the above applications have helped move the industry towards an overall improvement in safety and drilling efficiency, there is additional potential for improvement using digital twins.

2.2.2 Prognostics for equipment failure and detection

Due to the advancements in data-driven modeling and learning techniques, and the ability to instantaneously stream big data, models have become more sophisticated and can accurately replicate the performance of different drilling equipment. These advancements have allowed for performance and condition management of various drilling equipment, thereby improving overall operational efficiency. Condition Based Maintenance (CBM) or prognostics of an equipment refers to calculating its degradation, estimating its remaining useful life, and predicting its failure. CBM allows for optimizing equipment usage by operating it within an optimal window, as well as for proactively scheduling maintenance to reduce cost and downtime associated with repairs. Some current and potential applications of digital twinning for prognostics, and equipment failure detection and prevention are:

- CBM of subsea Blowout Preventer (BOP) pipe rams (Mutlu et al., 2018)
- CBM and remaining useful life determination of downhole components such as MLWD tools, mud motors, and drill pipes (Carter-Journet et al., 2014; Lines et al., 2014; Reckmann et al., 2010; You et al., 2020)
- CBM of surface equipment such as top drive, mud pumps, drawworks, and pipe handling equipment (Johnson & Rao, 2020; Kyllingstad & Nessjøen, 2011; Pournazari et al., 2016)
- CBM for artificial lift systems for the prediction of failures in submersible pumps (Guo et al., 2015; Y. Liu et al., 2010)
- Identifying and optimizing drilling tool performances within their operating windows

2.2.3 ILT evaluation and mitigation

ILT refers to the inefficiencies and, consequently, time lost when an operation or a part of the operation is not performed at its maximum efficiency (Mittal et al., 2020). ILT occurs due to either suboptimal operational performance, or non-optimized usage of equipment. Suboptimal operational performance can be related to human inefficiencies, or inefficient standard operating procedures. Non-optimized usage of equipment could be due to either not using the right equipment for the operation, or performance degradation of the equipment. As per statistics presented by Damski (2019), NPT and ILT taken together are around 40 to 50 percent of the total well construction time. Some current and potential applications of ILT evaluation by digital twinning include:

- Rig crew performance monitoring and improvement (Contreras et al., 2020; El Afifi et al., 2015; Ouahrani et al., 2018)
- Defining and monitoring key performance indicators (KPIs) for quantifying rig's operational performance for various auxiliary tasks (De Oliveira et al., 2016; Lakhanpal & Samuel, 2017; Mittal et al., 2020)
- Efficiency gains in auxiliary operations, such as for making connections, tripping, cementing, and running casing

To summarize, small amounts of ILT accrued across different activities can add up and result in being a significant fraction of the total operational time. Therefore, utilizing digital twins constructed for ILT identification and mitigation would result in overall increased efficiency.

2.2.4 Logistics and planning

Multifaceted oilfield development requires multidisciplinary collaboration. This necessitates the definition of overarching field development objectives that encompass individual well objectives. Currently, in the industry, many approaches exist for well planning and oilfield development, including machine learning (Kumar, 2019), systems planning (Brechan et al., 2018; Ciccarelli et al., 2018; McManus et al., 2012), and using various risk mitigation strategies (Birnie et al., 2019; Rowatt et al., 2020). Another planning method that has recently gained traction is by using digital twins (Brechan & Sangesland, 2019; Pivano et al., 2019). Some current and potential applications that exploit the repetitive nature of the well construction operations to build digital twins include:

- Predicting bit degradation and RT downhole drilling fluid properties, and utilizing this information for optimizing drilling parameters (Liu et al., 2018; Millan & Ringer, 2018; Shirangi et al., 2020)
- Replication of well construction operations such as drilling, casing, tripping and cementing (short- and long-term operational planning) (Hutchinson et al., 2019; Nadhan et al., 2018)
- Prediction of times to end of different operations, for instance, time to drill to a well's planned total depth, or time till the end of the casing and cementing operations

Digital twins built by combining multiple well delivery tasks can be utilized as dynamic planning and scheduling tools for the current well or extend to entire drilling programs.

2.2.5 Training and development

Drilling environments can be unpredictable, potentially hazardous, and may require rig crews to make high impact decisions under stress. Therefore, it is of utmost importance for the rig personnel to be adequately trained and be situationally aware at all times. This requires training them on realistic system replicas, or drilling simulators (Hodgson & Hassard, 2006). Since digital twins can replicate equipment and processes, an essential application of theirs is in the development of drilling simulators. Some applications these simulators for aiding in training and development are:

- Industrial and academic drilling simulators to replicate surface drilling operations (and equipment) and downhole process behavior (Crichton et al., 2017; Shirkavand et al., 2010; Chan et al., 2020)

- Developing and testing drilling programs and operation manuals (Höhn et al., 2019; Howell et al., 2019)
- Testing and improving processes and software to iron out any issues before rolling them out to the field (Kelessidis et al., 2015)

To summarize, the application of digital twinning of processes and equipment has resulted in considerable value addition to the oil and gas industry. More value addition, however, can still be achieved by applications of digital twinning for drilling optimization and advisory, as well as planning and decision-making systems.

Table 1 summarizes the many areas within the well construction domain where progress has been made. While all of these approaches use models (physics or data-based), none of them have a framework for scenario analysis, which is an essential component of digital twinning (as shown in the example on race strategy planning in Chapter 1).

Table 1 Summary of the current applications for improving operational efficiency and safety and in well construction.

Application Type	**Value Addition**	**Potential Applications**
NPT identification (diagnostics) and prevention	• Real-time process monitoring and diagnostics • Improved and faster decision making • Event detection • Drilling optimization	• Mitigating well control issues (e.g., kicks and losses) • Drilling dysfunction identification and mitigation • Wellbore quality degradation identification and mitigation • Hole cleaning and stuck pipe prevention
Prognostics for equipment failure and detection	• Reduce downtime associated with operational failures • Early diagnosis of failures • Condition-based maintenance (CBM) of drilling tools and equipment • Optimizing drilling tool performances within their operating windows	• CBM of subsea Blowout Preventer (BOP) pipe rams • Estimating the remaining useful life of downhole components (MLWD tools, mud motors, and drill pipes) • CBM of surface equipment such as top drive, mud pumps, drawworks, and pipe handling equipment • CBM of artificial lift systems
ILT evaluation and mitigation	• Improve operational efficiency for various processes • Key performance indicator (KPI) monitoring and tracking • Identification of performance gaps in different processes	• Rig crew performance monitoring and improvement • Defining KPIs for quantifying rig's operational performance for various auxiliary tasks
Logistics and planning	• Forecasting and planning • Ability to run what-if scenarios on multiple processes • Delivery of safe, cost-effective wells • Improved well planning and more efficient oilfield development	• Predicting bit degradation and RT downhole drilling fluid properties for optimizing drilling parameters • Replication of well construction operations such as drilling, casing, tripping, and cementing (short- and long-term operational planning)
Training and development	• Training drilling crew on specific technology • Preparing college students • Testing new technology in a safe environment	• Replicating surface drilling operations (and equipment) and downhole process behavior • Developing and testing drilling programs and operation manuals • Beta-testing software before rolling them out to the field

2.2.6 Scenario analysis

An application of digital twins for decision-making across many other industries is for performing scenario analysis. The primary goal of scenario development is not only to make predictions but understand the different driving factors and how they might influence the system behavior. Scenarios deal with steps or different tasks that will result in a certain state of the system by considering uncertainties across different variables and processes (Minchev & Shalamanov, 2010). The scenarios can be developmental or situational. In developmental scenarios, starting from a point in time, a cause-effect relationship can be built based on different values taken on by different parameters. Situational scenarios, on the other hand, are snapshots of the future states at some given point in time, and the goal is to analyze the situation itself rather than the process of arriving at that state (NATO, 2007). In other domains, the use of sophisticated decision-making systems performing scenario analysis has resulted in an overall improvement in safety and operational efficiency. Such systems, coupled with digital twins of operations or equipment, have been utilized in areas such as manufacturing (Kunath & Winkler, 2018), autonomous vehicles (Kiran et al., 2020; Schwarting et al., 2018), and smart grid management (Kang et al., 2009; Blech et al., 2017).

There are also numerous applications of scenario analysis in defense planning and renewable energy forecasting and planning. For instance, Kamjoo et al. (2016) solve a multi-objective optimization problem to optimally design a renewable energy system for economics (cost) and reliability (probability of failure) by considering wind turbines, solar photovoltaic panels as a part of the power grid, and the associated uncertainties in wind speed and solar irradiance. In the field of defense planning, one application of scenario analysis is resource planning under a time constraint, and Abbass et al. (2009) discuss the underlying methodology by solving a problem to optimize the number and types of required field vehicles by 2025, by generating and solving for different scenarios.

2.3 Sequential Decision-Making and Action Planning

Planning is the process of generating an action sequence from an initial system state to some goal state to satisfy some high-level objective function. Setting up a planning system requires explicitly stating the problem objectives and constraints, defining the state- and action-space, and identifying goal states (LaValle, 2006). The various state-action transitions can either be fully specified in advance or be incrementally discovered (by utilizing models) as the planning proceeds. The solution of a planning problem is a policy or a strategy that suggests the sequence of actions for every successive decision-making step (called a decision epoch). The following sections discuss the necessary components for setting up planning systems and examine the different planning algorithms.

2.3.1 Setting up planning systems

All planning problems have the following essential components (LaValle, 2006):

- **Objective function**, stating the initial and the desired (goal) states, and constraints that can influence decision-making;
- **Decision epochs**, or the times at which decisions need to be made. Epochs can either be explicitly represented as time intervals, or implicitly represent a sequence of actions in succession;
- **State-space,** to describe all possible situations or scenarios (states) the system can be in, at any given decision epoch;

- **Action-space**, to quantify all possible decisions or actions that can be utilized to manipulate states;
- **Plan**, or strategy which represents the sequence of actions taken at every successive decision epoch.

In effect, planning problems are sequential decision-making problems that can be solved by reinforcement learning (RL) techniques. In RL, a goal-directed learning agent interacts with an uncertain environment (either physically or virtually) based on specific policies or action plans. Every interaction is associated with immediate feedback or reward. The goal of this agent is to maximize the long-term reward. To accomplish this, the agent needs to exploit what it has already experienced and also try new actions to learn from unexplored trajectories (Gelly & Silver, 2011; Silver et al., 2012; Sutton & Barto, 2018). **Figure 7** shows a schematic of this agent-environment interaction, where an action a_t by the agent in the environment (observed by the agent to be in the state s_t) results in an immediate reward r_t and a new observed state s_{t+1}.

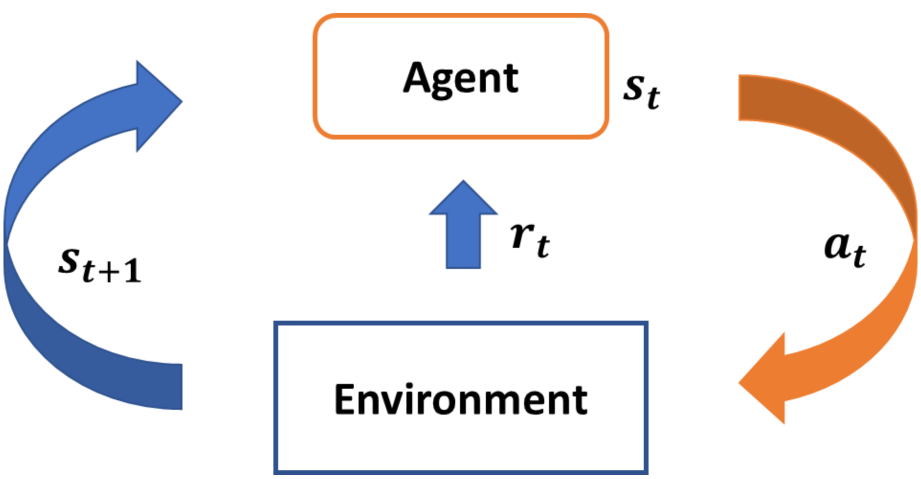

Figure 7 Agent-environment interaction in RL (modified from Sutton & Barto, 2018).

Such interactions between a decision-making agent and a fully observable environment to achieve some long-term objective can be formalized in a Markov decision process (MDP) framework. A process is said to be Markovian if it follows the Markovian property, i.e., any future outcomes depend only on the current system state and the immediate action. An MDP is defined by a tuple ({S,A,P,R}) and a policy (π) (Puterman, 1994).

S is the state-space, where s_t ($s_t \in S$) represents the state of the system, as perceived by the agent, at time t. A state is defined by a set of parameters to quantify the condition of the environment completely (fully observable). A is the action-space, where a_t ($a_t \in A$) is an individual action taken by the agent at time t to manipulate the system in the state s_t. An action is a combination of different control variables that can influence the environment. Depending on the process, and the state and action representation, the state-space and action-space may be continuous or discrete.

P is the transition function representing the state-action transition probabilities. $P_{ss'}^{a}$ is the probability that a system in state s, at time t transitions to state s' at time $t+1$ on taking an action a. These transitions can be learned from actual agent-environment interactions or calculated from process models or be derived by a combination of both.

$$P_{ss'}^{a} = \Pr(S_{t+1} = s' | S_t = s, A_t = a) \tag{2}$$

R is the reward function to quantify the immediate feedback associated with a state-action transition. Reward may depend either only on the final state, or the final state and the action. $R_{ss'}^{a}$ is the expected reward when an action a transitions the system from state s at time t to s' at time $t+1$.

$$R_{ss'}^{a} = E(R_{t+1} | S_t = s, S_{t+1} = s', A_t = a) \tag{3}$$

The accumulation of rewards over multiple time steps or decision epochs is the system's return. The time horizon for accumulating these rewards may be finite (fixed number of steps) or infinite, and may include a discount factor $\gamma(\leq 1)$ in the case of infinite time horizon problems. The purpose of discounting later rewards is to vary the importance of future feedback in the present total return.

$$G_t = R_{t+1} + \gamma . R_{t+2} + \gamma^2 . R_{t+3} + \gamma^3 . R_{t+4} + \cdots = \sum_{i=1}^{\infty} \gamma^{i-1} . R_{t+i} \tag{4}$$

$$G_t = R_{t+1} + R_{t+2} + R_{t+3} + \cdots R_T = \sum_{i=1}^{T-t} R_{t+i} \tag{5}$$

The policy π is the logic or set of rules used by an agent to select an action from a given state, and it may be stochastic or deterministic. $\pi(a|s)$ is the probability of selecting a specific action a given the system is in state s (as shown in equation (6)), or for a deterministic policy, a is the action that is selected for the system is in state s (as shown in equation (7)**)**.

$$\pi(a|s) = \Pr(A_t = a|S_t = s) \tag{6}$$

$$\pi(s) = a \tag{7}$$

Associated with a policy is its value function, which can either be state-based value function or a state-action pair based value function. State value function V^{π} is the agent's expected return from the state s when following the policy π. The state-action value function Q^{π} is the agent's expected return after taking an action a from state s and subsequently following the policy π.

$$V^{\pi}(s) = E[G_t|S_t = s] = E[R_{t+1} + \gamma . v(s_{t+1})|S_t = s] \tag{8}$$

$$Q^{\pi}(s, a) = [G_t|S_t = s, A_t = s]$$
$$= E[R_{t+1} + \gamma . q(s_{t+1}, a_{t+1})|S_t = s, A_t = s] \tag{9}$$

The goal of an agent is to find a policy that allows it to maximize its total return. There is always at least one optimal policy for an MDP that helps extract the maximum return from the system (Feinberg, 2011). Another crucial step in MDP formulation is reward shaping, or engineering the reward function to get more frequent feedback on appropriate system behaviors (Wiewiora, 2017). Thus, reward shaping influences the total return, thereby affecting the system's policy.

2.3.2 Planning algorithms

Planning algorithms can be compared based on a multitude of factors, such as the search-space traversal methodology, requirement of a heuristic, ability to plan in a limited amount of time, memory requirement for storing intermediate results, computational complexity, etc. (LaValle, 2006). A straightforward approach to solving planning problems, however, is the **exhaustive tree search**, wherein all possible actions from all states are evaluated until either a goal state is reached, or the available evaluation time is exhausted. Although this method ensures finding an optimal plan, for large systems (with large state and action spaces), the associated time complexity renders this method impractical. Some other classifications of algorithms based on different search-space traversal methodologies are breadth-first search (BFS), depth-first search (DFS), and best-first search (BestFS).

BFS is a first-in, first-out (FIFO) algorithm that searches equally in all directions, i.e., all actions from a given state are evaluated first before the evaluation of the next state's actions can begin. The algorithm stops and outputs the shortest path as soon as a goal state is reached (LaValle, 2006; Poole & Mackworth, 2017). **DFS** is a more aggressive strategy, wherein, from any state, actions are chosen at random to traverse the system, until either a goal state or a dead-end state is reached. If a dead-end state is reached, the algorithm backtracks one step, then simulates any action not yet explored, i.e., this algorithm works in a last-in, first-out (LIFO) manner. The priority of such algorithms is to search deeper than to expand the search-space. A potential issue with this method is the search becoming stuck in a repetitive loop (Bennett, 2019; Poole &

Mackworth, 2017). Neither the DFS nor the BFS utilizes an evaluation function or a heuristic to direct the search, i.e., costs associated with all actions taken from all the states are the same. Also, both methods require keeping track of the visited, unvisited, and dead-end states. Therefore, these algorithms run into issues when dealing with large state- or action-space systems due to high computation-time and memory requirements, with BFS more so than DFS due to its more exhaustive nature (LaValle, 2006; Mussmann & See, 2017).

The BFS algorithm can be enhanced by using some form of evaluation functions or heuristics or both. **Dijkstra's** algorithm utilizes an evaluation function to quantify the path traversed to reach a given state after starting from the initial state. It, like the BFS, will find an optimal path (if one exists) between the initial and the goal state, but suffers from the same computational and memory issues associated with larger systems (Alija, 2015; Reddy, 2013). If a heuristic is defined to quantify the approximate cost of a state relative to its position from the goal state, this results in a **greedy BestFS** algorithm. The next action is chosen greedily based on this heuristic. Although greedy BestFS is usually faster than Dijkstra's algorithm, a drawback of this algorithm is the lack of exploration and backtracking, i.e., once an action is selected, it is not re-evaluated based on any new information (Bhaumik et al., 2019; LaValle, 2006). This search strategy is therefore not guaranteed to find an optimal path. Dijkstra's algorithm supplemented by the greedy BestFS heuristic results in the **A* search** algorithm (Cui & Shi, 2011; LaValle, 2006). A* search is a BFS algorithm for which both an evaluation function and an admissible heuristic are defined. A* search will find an optimal path (if one exists) faster than BFS or the Dijkstra's algorithm, but it is memory-intensive since it requires storing all the visited states and keeping track of all possible and tried actions from all possible states.

Another issue with A* search is the necessity for a well-defined admissible heuristic (Klein, 2015).

Iterative deepening search (IDS) is a variant of the DFS, especially useful in systems with high branching factors. For IDS, the DFS algorithm is continually run with increasing depth bounds until a goal state or a dead-end state is reached. During each iteration, every state encountered in the path is expanded in a BFS manner. IDS is faster than the BFS and is guaranteed to find an optimal path if one exists (Li et al., 2014). The **iterative deepening A*** (IDA*) algorithm utilizes the search technique of the IDS in conjunction with a heuristic to quantify the cost of any state relative to the goal state. IDA* is guaranteed to find the optimal solution if the heuristic is admissible (LaValle, 2006; Poole & Mackworth, 2017). The main advantage of iterative search algorithms (IDA and IDA*) is that they do not require much memory, since only the current path is stored. **Evolutionary algorithms** such as the genetic algorithm evaluate and rank multiple action sequences simultaneously using an expert-designed fitness function. The quality of the population of these action sequences is successively improved using selection, crossover, and mutation operations, until some stopping criterion is met. The intrinsic randomness in crossover and mutation steps ensures a balance between exploration and exploitation of the search space. These algorithms are the most effective if the search space is sufficiently small, or if time is not a constraint for search. Additionally, the performance of these algorithms is highly dependent on the design of the fitness function, and the crossover and mutation strategies (Korkmaz & Durdu, 2018; Sutton & Barto, 2018).

For systems with a vast state- and action-space, lack of an admissible heuristic or minimal dependency on some evaluation function, memory constraints, and limited computation time availability, **simulation-based search** (SBS) methods are the best suited. SBS, a decision-time planning algorithm, is a type of model-based RL method suited for online action planning, starting from a given state (Sutton & Barto, 2018). Here, a goal-directed agent interacts (virtually) with an uncertain environment (models representing the underlying processes) based on specific policies or action plans which evolve with time. These policies are designed to balance exploration and exploitation of the search space, and every state action transition has an associated reward. These algorithms build an 'asymmetric' search tree starting from an initial or root node using a sequential BestFS strategy, as shown in **Figure 8**. Multiple episodes of experience (starting from the root or the current state, s_t) are simulated until either the goal state or a fixed depth bound is reached. After every episode, one or more nodes (representing a state-action transition) are added to the tree, and the values of the already present nodes are updated. SBS algorithms do not require a heuristic (i.e., they are 'aheuristic'); however, a well-defined heuristic can considerably improve the convergence time. Another useful feature of these algorithms is their 'anytime' property, i.e., the algorithm can be stopped at any time to return the best plan thus far (Silver, 2009).

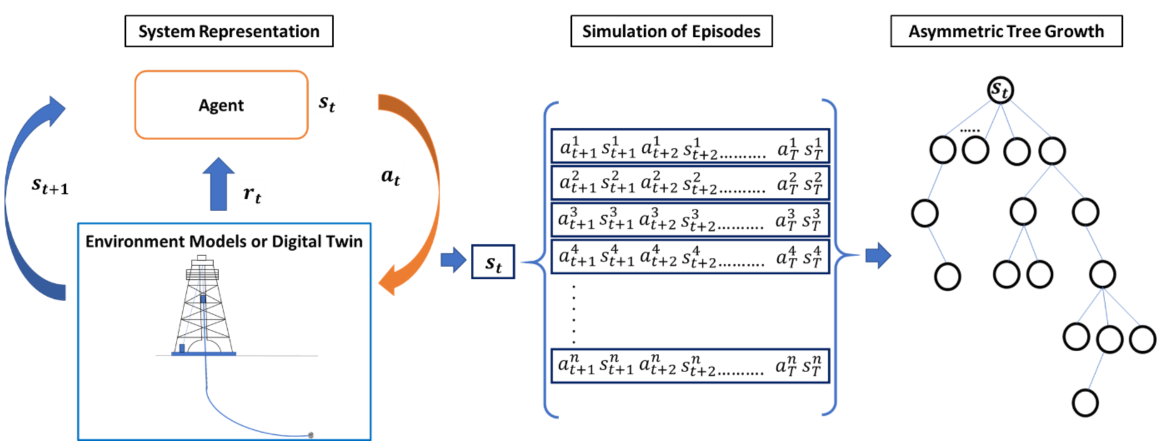

Figure 8 Asymmetric tree growth using simulation-based search algorithms. An action a_t by the agent in the environment (observed by the agent to be in a state s_t) results in an immediate reward r_t and a new observed state s_{t+1}.

Essentially, the anytime, asymmetric, and aheuristic nature of the SBS algorithms makes them a preferred candidate for large systems with memory and computational constraints, as is the case in well construction.

2.5 SUMMARY

The concept of utilizing digital twins for performing scenario analysis or for building intelligent action planning systems is still in its infancy in the well construction domain. Such systems, however, have actively been utilized in many other industries to either outperform the competition (e.g., in race strategy planning) or to help improve operational safety and efficiency (e.g., in manufacturing, asset management or energy dispatch problems) or to achieve super-human levels of performance (e.g., in complex RT strategy or adversarial games). There are, however, numerous avenues for development and application of such intelligent decision-making and action planning systems in the well construction domain; hole cleaning advisory for stuck pipe prevention being one such critical application.

The rest of the dissertation is dedicated to defining a generalized framework for building such intelligent systems for well construction operations, with hole cleaning advisory demonstrated as an application.

Chapter 3: A Framework for Developing Digital Twinning Systems for Real-Time Scenario Analysis

While there are approaches and tools to monitor the well construction operations, there are none that evaluate potential action sequences and scenarios, and select the best possible sequence of actions. This chapter outlines a generalized iterative methodology for setting up digital twinning systems to address this shortcoming. The goal here is to advance state of the art in digital twinning of well construction operations by formulating a step by step process for building digital twins, that are also capable of real-time scenario analysis. The proposed methodology is then demonstrated by developing an integrated multi-model twin to replicate hole cleaning operations for stuck-pipe prevention. This twin is also used to simulate multiple future scenarios to quantify the effects of different actions on eventual outcomes.

3.1 Digital Twinning Methodology

The proposed methodology to develop digital twinning systems for any well construction operation consists of the following steps:

1. The first step is to determine the objectives of the system being twinned. For instance, the goal of a 'Real-time (RT) drilling dysfunction mitigation twin' would be to detect signatures of dysfunctions (such as vibrations, bit balling, stick-slip), and suggest drilling parameters (such as RPM, WOB, torque, flowrate) to optimize the rate of penetration (ROP) while minimizing dysfunctions.
2. The next step is to set up the twinning system, which is itself a cyclic process and requires a compromise between the desired and the practical outputs. This compromise depends on the system's objectives, the available data, and the

computation capacity for model implementation. The following three steps are iterated over:

- Based on the twin's objectives, the metrics or outputs required to quantify the state of the system are identified. For the dysfunction mitigation twin, parameters such as mechanical specific energy, depth of cut, and stick-slip index would be required to quantify the drilling performance and dysfunctions.
- Once these metrics are recognized, the next step is identification and implementation of the different models (data- or physics-based or combination of both) to calculate them, i.e., building the digital twin. The selection of these models depends on the application type and the associated temporal and computational constraints. For instance, since online action planning applications require balancing accuracy with runtime speed, analytical model implementations may be acceptable. On the other hand, for offline planning or more detailed post-job analysis, where computation time or capacity may not be a constraint, numerical models may be used.
- Subsequently, based on the input requirements of the various models (twin), the necessary data streams are identified and aggregated; the data is filtered and processed (data wrangling) and integrated with the twin. If the available data stream does not support the calculation of a desired output component, the required system outputs or the underlying models are tweaked accordingly.

3. The twinning system thus set up is then used for performance tracking and scenario analysis. The goal of scenario analysis is to make predictions about

future system states, understand the different driving factors, and how they might influence the system behavior.

Figure 9 illustrates the different steps and the cyclical relationships between them.

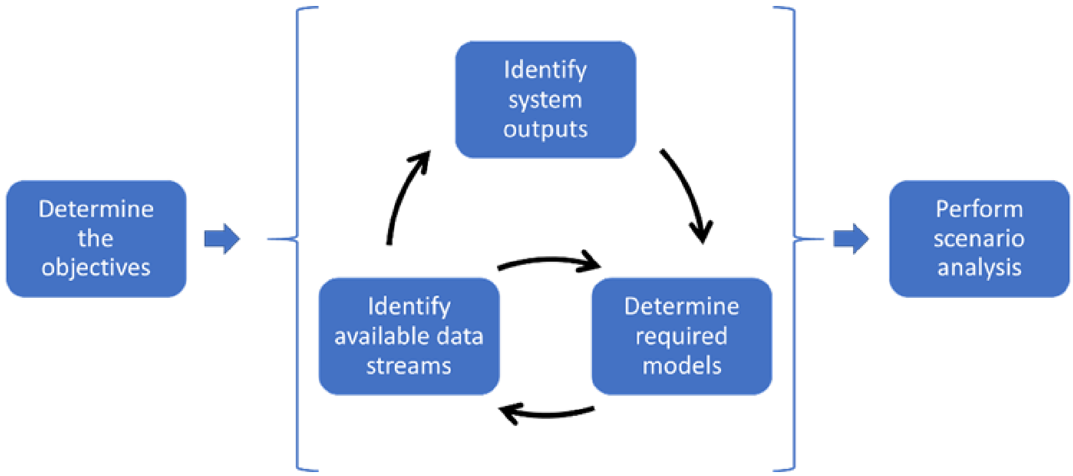

Figure 9 The digital twinning methodology.

3.2 Development of a Digital Twin for Hole Cleaning Advisory

As discussed in the previous chapters, inadequate or poor hole cleaning can lead to a series of costly drilling issues such as stuck pipe, formation damage, reduction in drilling speed, difficulty tripping out of the hole, or issues while running casing. Therefore, it is of value to digitally twin the hole cleaning system to understand the progression of the borehole condition in real-time and track the outcomes of different actions. The primary objective of hole cleaning is to remove solids (including cuttings, caving, or cement) from the borehole to ensure the safe and efficient performance of the various well construction operations. The following sections discuss the creation and application of such a twin.

3.2.1 Building the digital twin

Since a well can be many thousands of feet in depth, hole cleaning measures directed towards one interval of the well may not necessarily result in effective hole cleaning in another interval. Thus, it is essential to quantify and monitor the condition of the borehole in real-time for the entire well. These quantifications are based on either real-time data, or a combination of real-time data with models such as cuttings transport, hydraulics and, torque and drag.

3.2.1.1 Identification of system outputs

The purpose of modeling cuttings transport is to understand the process of removal of solids from the borehole. The solids in the borehole can be quantified using a combination of the cuttings bed height and the concentration of cuttings in the flow. Also, not maintaining the ECD within the drilling margin can result in wellbore instability issues such as kicks or lost circulation events. Therefore, the following metrics may be used to describe the state of the borehole for a hole cleaning system:

- Height of the cuttings bed at different depths along the wellbore;
- Concentration of cuttings in suspension along the wellbore;
- ECD along the length of the wellbore;
- The average friction factor of the wellbore.

3.2.1.2 Determining the required models

The next step is to identify the models required to calculate these metrics. Analytical implementations, to balance accuracy and runtime speed, of the following models need to be adapted, integrated, and implemented to build the twin:

- Hydraulics model to calculate the frictional pressure losses and ECD throughout the well;

- Torque and drag model to evaluate the friction factor of the well, using rotary, slack-off and pick-up weights;
- Cuttings transport model to estimate cuttings bed height and cuttings concentration in the flow throughout the well.

Implementing analytical models is of importance since the ability to run thousands of simulations in a few minutes provides the capability to evaluate multiple actions and action sequences in near real-time.

3.2.1.2.1 Hydraulics model

The implemented hydraulics model was adapted from the narrow slot approximation based analytical hydraulics model for Yield power law (YPL) fluids discussed by Erge et al. (2015). Some modifications were made to the model to include the effects of cuttings bed height and cuttings concentration in the flow on the density of the drilling fluid. The effects of temperature on the mud rheology were also included based on the work of Karstad and Aadnoy (1997). At this stage of the development, the mud was assumed to be incompressible, but compressibility can be added without too many challenges to the modeling approach. The model also accounted for the drillstring eccentricity by modeling it as a linear function of the inclination.

ECD calculation at any given hole depth D_{MD} and corresponding total vertical depth D_{TVD} is performed using equations (10), (11) and (12). It is important to note that the density of mud in different control volumes may not be the same, since it is a function of cuttings concentration, temperature, and pressure.

$$ECD = \frac{P_{hydrostatic\_D_{TVD}} + P_{frictional\_pressure\_loss\_D_{MD}}}{D_{TVD}.\, g} \qquad (10)$$

$$P_{hydrostatic\_D_{TVD}} = \int_0^{D_{TVD}} \rho_{mud}(z).g.dz \tag{11}$$

$$P_{frictional\_pressure\_loss\_D_{MD}} = \int_0^{D_{MD}} dP\,.dx \tag{12}$$

In these equations, dz and dx are the changes in a control volume element's total vertical depth and measured depth, respectively, as shown in **Figure 10**, and g is the acceleration due to gravity. dP is the frictional pressure drop in a control volume element. The eccentricity of the drillstring element in the borehole can be calculated using equation (13).

$$ecc = \frac{2.d_{cc}}{D_o - D_i} \tag{13}$$

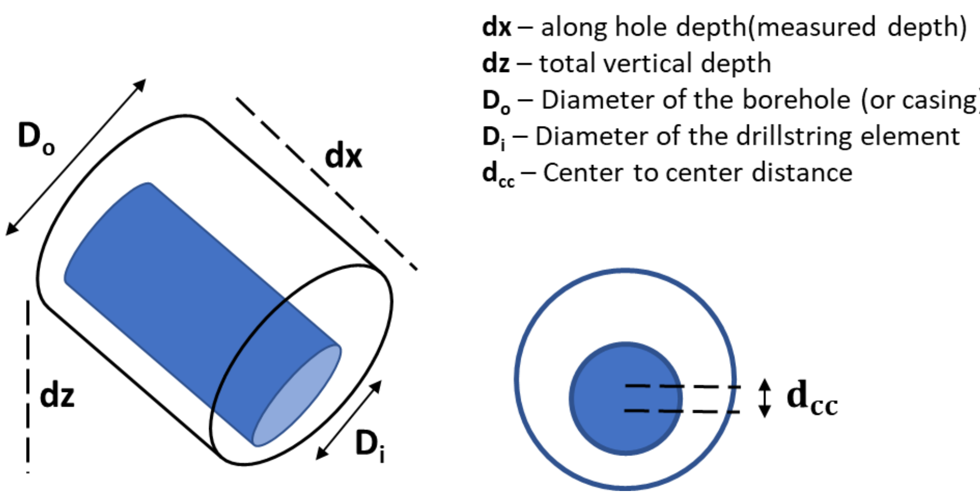

Figure 10 Eccentric placement of the drillstring in a control volume.

Frictional pressure drop calculations are performed individually for every control volume segment using equations (14) and (15).

$$dP = \int 2\frac{f_f.\rho_{mud}(x).v_{axial}^2}{D_o - D_i}.dx \tag{14}$$

$$v_{axial} = \frac{Q}{A_{flow}} \tag{15}$$

In these equations, Q is the flowrate (of drilling mud) and A_{flow} is the annular flow area available to the drilling mud. The annular flow area depends on borehole geometry, cuttings bed height, and drillstring eccentricity in the given control volume element. Associated with the flow of fluid in drillstring and annulus is the friction factor, f_f, and its calculation depends on the fluid flow regime. The flow regime can be either laminar or turbulent or transitional between the two. The friction factor also depends on mud density and rheology, pipe roughness, the eccentricity of the drillstring, drillstring RPM, and axial mud velocity (Bourgoyne, 1986; Mitchell & Miska, 2011).

The output of this model is a plot of ECD versus measured depth. **Figure 11** demonstrates the effect of relative changes in different input variables (flowrate, cuttings bed height, and drillstring RPM, respectively) on ECD values versus measured depth. The original mud weight for simulation was 10 pounds per gallon (ppg). As the flowrate increases, so does the axial flow velocity, which results in a higher frictional pressure drop in the annulus, thus an increased ECD. Similarly, a higher cuttings bed results in increased axial flow velocity (due to reduced A_{flow}), which also results in a higher frictional pressure drop in the annulus, thereby increasing the ECD. Finally, an increase in the drillstring rotation speed also results in an increased annular frictional pressure loss.

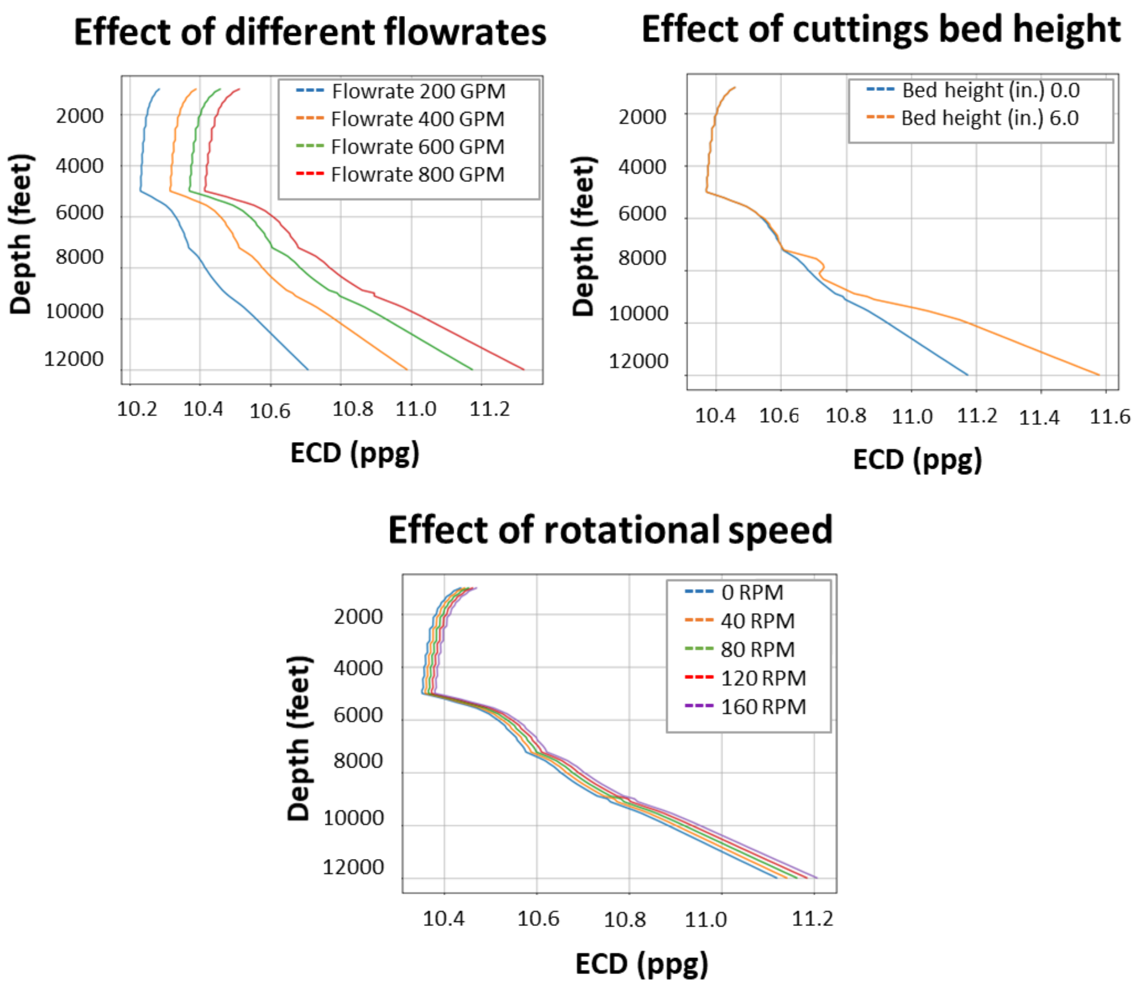

Figure 11 Effects of relative changes in different input variables (flowrate, cuttings bed height, and drillstring RPM, respectively) on the ECD along the depth of the well.

The model was also tested and validated against multiple real drilling datasets with different wellbore geometries, various BHA designs, and different open hole section sizes.

3.2.1.2.2 Torque and drag model

For this digital twin, an analytical soft string model was implemented based on Aadnoy et al.'s work (Aadnoy et al., 2010; Fazaelizadeh, 2013). The model treats the well as having a 3-D profile, as opposed to being restricted to a plane. Furthermore, the well is segmented into straight and curved sections by calculating the dog-leg severity (DLS) of the different control volume segments. Dog-leg angle α measures the absolute change in direction, while DLS measures the rate of change of the dog-leg angle over 100 feet (or 30 m) intervals. In straight sections of the well, drillstring weight dominates the tension, while in the curved sections, tension is the major contributor to the normal contact force. As shown in **Figure 12(a)**, the force at the top of a segment (F_2) is calculated using the equations (16) and (17) for straight sections and curved sections, respectively. The calculated force F_2 then serves as F_1 for the next section above it. Since friction acts in the direction opposite to the motion, the positive and negative signs indicate hoisting (or pick-up) and lowering (or slack-off) of the drillstring, respectively.

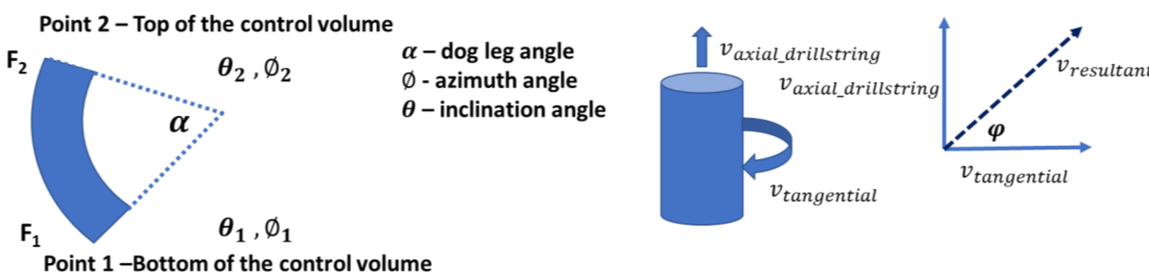

Figure 12 a) Forces acting on a control volume segment, (b) Axial and tangential components of drillstring velocity.

$$F_2 = F_1 + \beta .\ w_{unit} .\Delta L. cos\theta \pm \mu.\beta.w_{unit}.\Delta L. sin\theta. sin\varphi \tag{16}$$

$$F_2 = F_1 + F_{1.}\left(e^{\pm\mu.|\alpha_2 - \alpha_1|} - 1\right). sin\varphi + \beta.w_{unit}.\Delta L.\left(\frac{sin\theta_2 - sin\theta_1}{\theta_2 - \theta_1}\right) \tag{17}$$

In these equations, β is the buoyancy factor and is calculated using equation (18). It accounts for the reduction in the effective weight of a drillstring element due to its immersion in the drilling mud. As shown in **Figure 12(b)**, φ is the angle between the resultant and the tangential drillstring velocities and is calculated using equation (19).

Axial drillstring velocity is the speed at the drillpipe is hoisted or lowered, and tangential velocity is a function of the drillstring RPM.

$$\beta = 1 - \frac{\rho_{mud}}{\rho_{steel}} \tag{18}$$

$$\varphi = tan^{-1}\left(\frac{v_{axial\_drillstring}}{v_{tangential}}\right) \tag{19}$$

Similarly, equations (20) and (21) are used for calculating the torque for the straight and curved sections, respectively. In these equations $r_{element}$ is the radius of the drillstring element.

$$\tau = \mu . r_{element} . \beta . w_{unit} . \Delta L . sin\theta . cos\varphi \tag{20}$$

$$\tau = \mu . r_{element} . F_1 |\alpha_2 - \alpha_1| . cos\varphi \tag{21}$$

The output of this model is a broomstick chart with individual lines representing pick-up and slack-off weights for the various friction factors, as demonstrated on one dataset in **Figure 13**. For the given well profile with a 6.75-inch diameter production section, the friction factor (as indicated by the blue dots) is around 0.25. The model was also tested and validated against real drilling data for multiple wells, for 8.5-inch and 6.75-inch open hole sections, with different BHA designs and casing setting points.

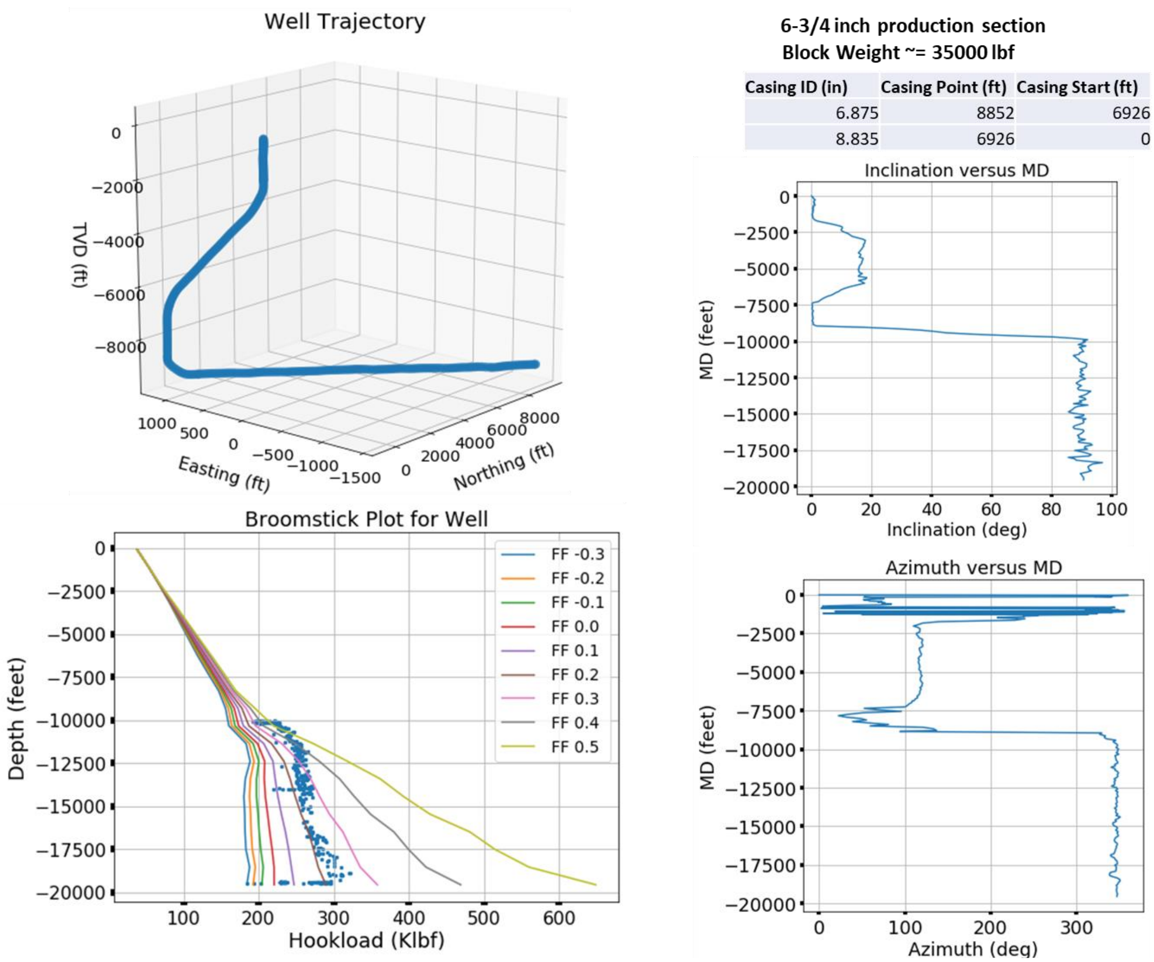

Casing ID (in)	Casing Point (ft)	Casing Start (ft)
6.875	8852	6926
8.835	6926	0

Figure 13 Torque and drag model implementation.

3.2.1.2.3 Cuttings transport model

A quasi-transient analytical cuttings transport model was derived and implemented based on a combination of concepts from the cuttings transport work by Larsen et al. (1990; 1997), Jalukar (1993), Bassal (1995), Duan and Miska (2009), Rubiandini (1999), and Naganawa et al. (2006), along with further modifications to account for mass conservation and physics of fluid flow. The model operates in near real-time and tracks the evolution of the wellbore over time. In every 5-minute (or 10-minute) interval, RT data is collected, and the well is segmented into appropriate control volumes based on the most recent information about well trajectory and profile. For every control volume segment, the critical transport fluid velocity (CTFV) and the axial fluid flow velocity are calculated, compared, and subsequently used for further state calculations. CTFV is the minimum fluid velocity required to prevent a cuttings bed from developing. CTFV is influenced by factors such as cuttings size and weight, wellbore inclination and geometry, mud density and rheology, and drillstring RPM. The following metrics are generated as the output of the model to quantify the state of the system:

- Height of the cuttings bed versus the hole depth for sections with inclination angles greater than 30 degrees;
- Concentration of cuttings in the flow versus hole depth for the entire well;
- Total concentration of cuttings in the annulus versus hole depth for the entire well.

Calculation of these metrics depends on factors such as differences in CTFV and axial flow velocity, the control volume geometry, mud rheology, and the volume of cuttings in suspension. Furthermore, the analytical methods to calculate CTFV are functions of the average inclination angle for a control volume segment, i.e., if the average inclination of a segment is 85 degrees (lateral), it would be evaluated differently as compared to a segment with average inclination 25 degrees (near vertical). CTFV for vertical (inclination < 30 degrees) and near-lateral sections (inclination > 60 degrees) is calculated using equations (22) and (23), respectively. To ensure a smooth transition in the inclinations between 30 and 60 degrees, the CTFV is calculated using a linear weighted combination of the two equations.

$$v_{critical} = v_{cutt} + v_{slip}.C_{vertical} \tag{22}$$

$$v_{critical} = v_{cutt} + v_{slip}.C_{rpm}.C_{ang}.C_{size}.C_{MW}.C_{geo\_d}.C_{geo\_pv}.C_{geo\_inc} \tag{23}$$

In equations (22) and (23), v_{cutt} or the velocity of the cuttings particles is derived based on mass balance, and can be estimated using equation (24). Mass of cuttings generated by drilling at a rate ROP should be equal to the mass of cuttings flowing in the available annular space, given no cuttings deposit to form a bed. c_{cutt}, the concentration of cuttings in the annulus, is a function of the ROP and has been derived experimentally by Larsen (1990). $C_{rpm}, C_{ang}, C_{size}, C_{MW}, C_{geo\_d}, C_{geo\_pv}$ and C_{geo_inc} are the correction factors derived based on the calculations of Larsen et al. (1990; 1997), Jalukar (1993), and Bassal (1995). $C_{vertical}$ is the correction factor for vertical borehole sections based on the work by Rubiandini (1999).

$$v_{cutt} = \frac{A_{bit}.ROP}{A_{flow}.c_{cutt}} \quad (24)$$

Since the model also has a quasi-transient or time-based component to it, the underlying algorithm can be summarized as follows (and supported by the schematic in **Figure 14**):

- The well is segmented into N control volumes based on the most recent trajectory information (obtained from the survey data) and any wellbore geometry changes.
- For a given evaluation time interval $t_{evaluation}$ (5 or 10-minute), the total volume of cuttings generated while drilling, starting at segment N, is calculated using equation (25). A_{bit} is the surface area of the drill bit, and the factor $\frac{12}{3600}$ is used for calculating the volume in cubic inches.

$$vol_{cuttings} = \frac{12}{3600} ROP.A_{bit}.t_{evaluation} \quad (25)$$

- The maximum distance traversed (up-hole) by these newly generated cuttings is calculated (and the segment up to which they can travel is labeled as M). This calculation requires estimating the velocity of the cuttings through each segment, and then calculating the time taken to cross that segment.

- The well is then solved by dividing it into two parts: one form surface to segment M, and the other from segment $M + 1$ to N.

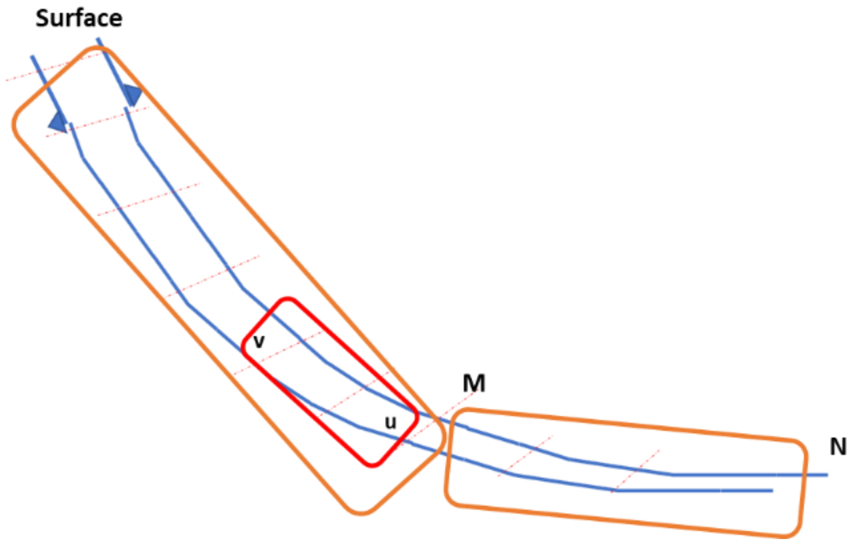

Figure 14 Schematic for the control volumes underlying the cuttings transport model algorithm.

- The calculations for segments $M + 1$ to N proceed as follows (supported by **Figure 15**):
    - For every segment, the CTFV and the fluid flow velocity are calculated.
    - Traversal of cuttings up-hole is modeled in a segment-by-segment manner, starting from the bottom segment N. In every segment along the way, the volume of cuttings not yet deposited is used in combination with the CTFV and the fluid flow velocity to calculate deposition and re-suspension of cuttings.

- Thus, cuttings bed height, concentration of cuttings in the flow, and concentration of cuttings in the annulus are re-calculated for every segment.

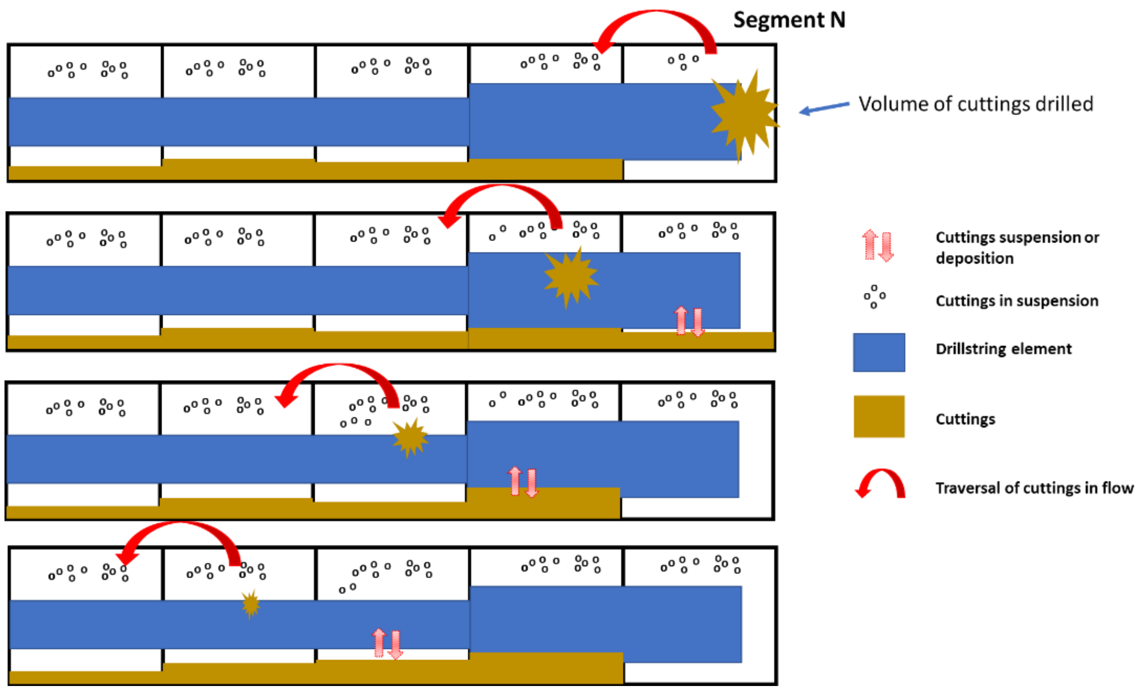

Figure 15 Algorithm for cuttings traversal from segments N to M+1.

- For control volume segments from *M* to the surface, the method for solution can be summarized as follows (**Figure 16**):
    - For every segment, the CTFV and the fluid flow velocity are calculated.
    - These velocities, the volume of undeposited cuttings already in suspension (calculated from the previous iteration), and the volume of cuttings in concentration are then used to solve for deposition and re-suspension of cuttings.

- The maximum distance which cuttings re-suspended from for some segment u (as shown in **Figure 14**) can traverse up-hole in the evaluation interval (5- or 10-minute) is then is estimated (and labeled as segment v).
- Finally, looping from the surface to segment M, cuttings starting from every individual segment u, are traversed up-hole (to at most its corresponding segment v), and in every segment deposition and re-suspension calculations are performed.
- Thus, cuttings bed height, concentration of cuttings in the flow, and concentration of cuttings in the annulus are re-calculated. Also, the volume of undeposited cuttings in the segment is then used for subsequent iterations.

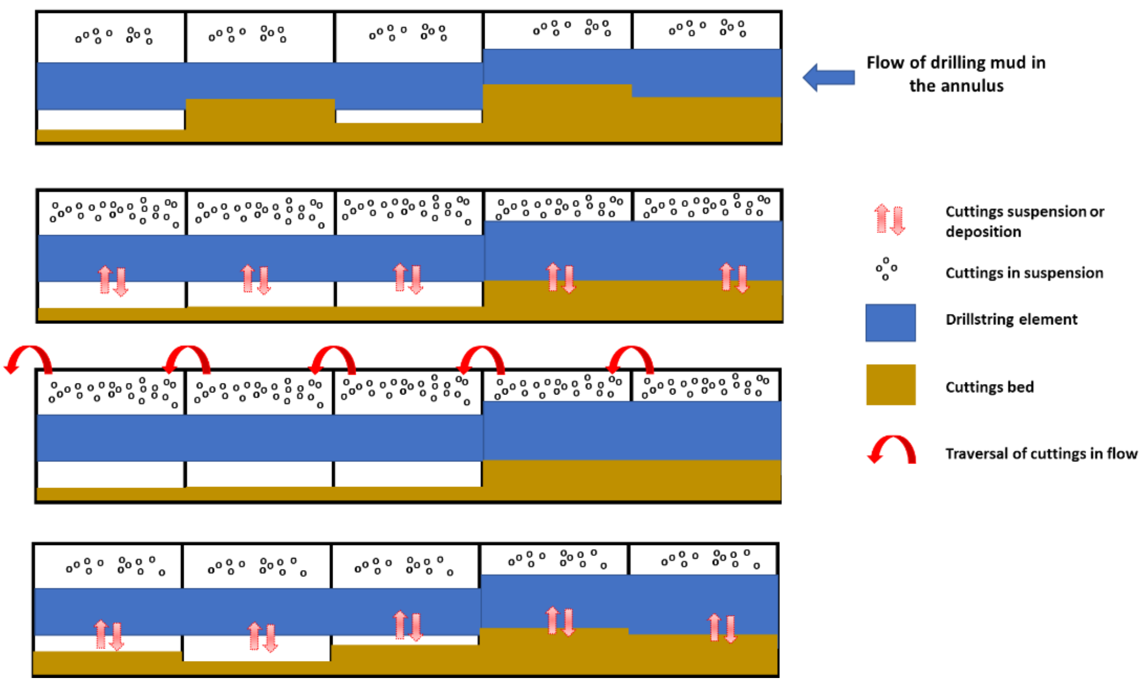

Figure 16 Algorithm for cuttings traversal from segment M to the surface.

The model runs in near real-time. For every 5- or 10-minute interval (which is the evaluation time interval), it accumulates the data, performs calculations, and returns an estimate of the state of the system versus the hole depth.

The model was tested and validated by comparing the simulation results against the data available from the extensive experimental work performed at the University of Tulsa by Larsen (1990), Jalukar (1993), and Bassal (1995). The test data comprised measured cuttings bed heights from multiple experiments performed by varying the well geometry (by changing the inner pipe diameter and the flow loop inclinations), mud rheology and density, cutting injection velocity (to simulate different ROP values), flowrates, drill pipe rotation speeds and cuttings properties (diameters and densities). The difference between the simulations with the developed cuttings transport model and the experimental results averaged around 5 percent and remained within +/- 10 percent for all the cases. A possible cause of this discrepancy in the results could be the analytical nature of the underlying models, which were originally derived by performing regression analysis on the data.

3.2.1.2.4 Rig state detection engine

Rig states are mutually exclusive operational states that are used to classify the operations being performed on the rig site. This classification is based on the data collected from the surface and (or) downhole sensors. For this research, a rule-based rig state detection engine was implemented to classify the following rig states in real-time based on the surface sensor data:

- Rotary drilling
- Slide drilling
- Making or breaking a connection

- Tripping the drillstring in or out of the borehole
- Circulation while on or off the bottom (of the borehole)
- Reaming (simultaneous rotation and axial movement of the drillstring) in or out of the borehole
- Survey identification

Assigning rig states to the different data points allows for a more accurate understanding and interpretation of the drilling process.

3.2.2.3 Identification of the data

The next step is the identification and aggregation of the required data streams to implement the above models. This data can be grouped into the following categories:

- Information about the **well profile**, obtained from pre-drill well plans and near real-time directional survey data;
- **Details about the BHA** such as geometry and unit weights of the individual components, obtained from pre-drill well plans;
- **Casing information** such as geometry and casing setting depths for different casing strings and liners, obtained from well's operational data and pre-drill well plans;
- **Real-time drilling data** collected from surface and downhole sensors, such as drillstring RPM, surface torque, drilling ROP, flowrate, hookload, tripping velocity, mud rheology, downhole near-bit sensor data, and downhole pressure data.

3.2.3 The developed digital twin

Figure 17 summarizes the structure of the proposed digital twin for the hole cleaning system. Initially, well profile and well geometry information are utilized for segmenting the well into smaller discrete control volumes. These segments represent any changes in well dimensions (changes in inner or outer diameter) or different survey intervals. Solving each control volume with time and depth outputs an estimate of the state of the system (hole condition quantification metrics for the well). The actual state of the system is determined by utilizing downhole tools such as, pressure while drilling (PWD) tool for calculating ECD, and near-bit MLWD tools for estimating friction factor. The differences between the actual and the predicted state values can then be used to update the system models.

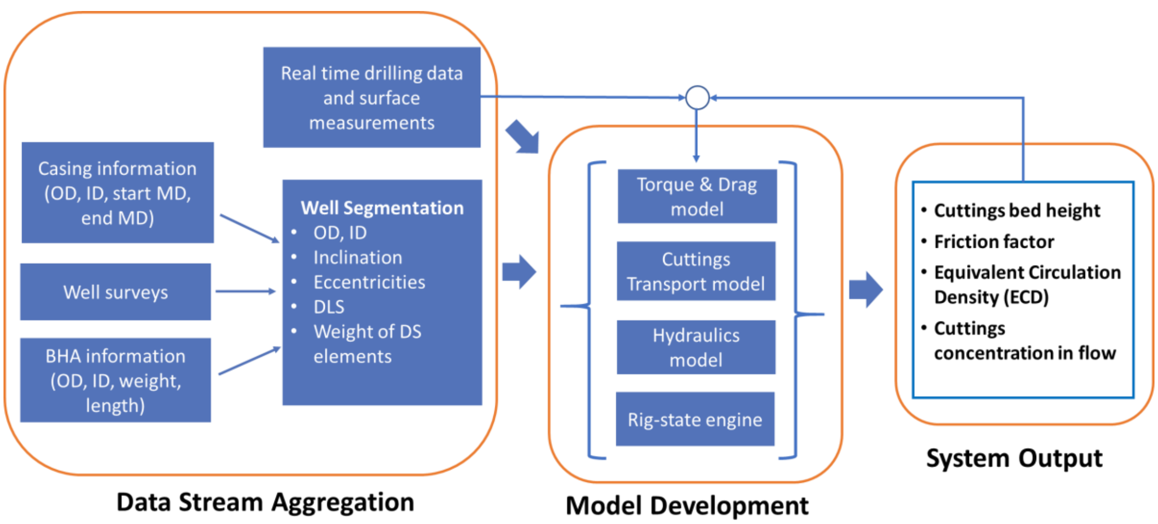

Figure 17 Structure of the proposed digital twin for the hole cleaning system.

3.3 Application of the Digital Twin for Performance Tracking and Scenario Analysis

The methodology was applied on a set of wells to develop a variant of the proposed hole cleaning digital twin, as shown in **Figure 18**. The data stream did not include tripping information such as tripping rig states or tripping velocities; therefore, the twin's desired output was adjusted not to incorporate the friction factor (indicative of the cyclical nature of the methodology). Also, since the available data streams did not include downhole tool data (no PWD or near-bit MLWD data), no immediate feedback about the actual system state was possible. This resulted in a digital twin with only the cuttings bed height, ECD, and cuttings concentration in the flow as the outputs. The developed twin was used as a tool for performance tracking by continuously evaluating the state of the wellbore. This twin also offers the capability to perform scenario analysis and action planning.

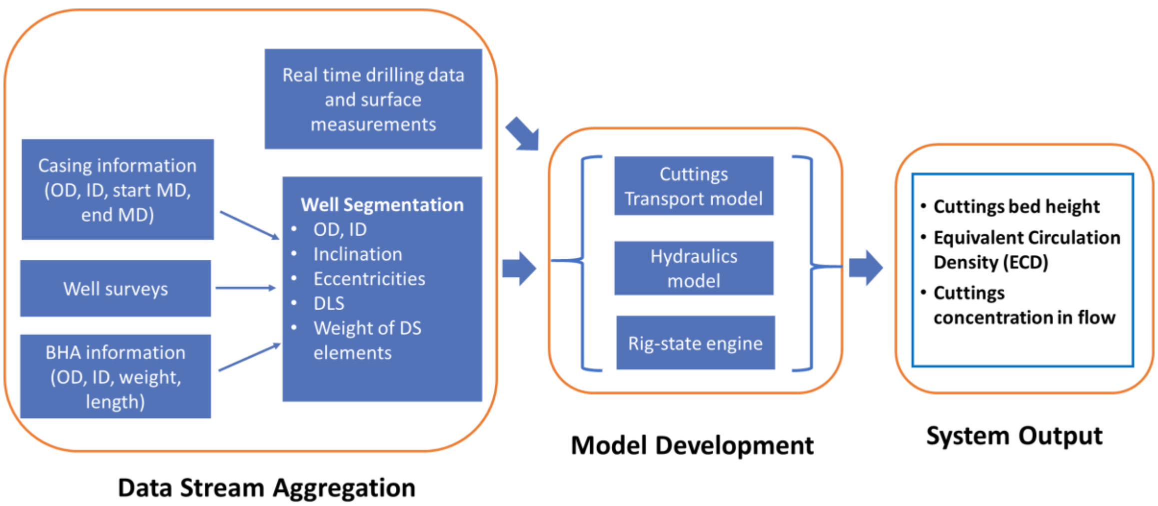

Figure 18 The developed variant of the digital twin for the hole cleaning system.

3.3.1 Performance tracking

The digital twin was deployed to replicate the hole cleaning performance of multiple wells. For one well, **Figure 19** represents the state of the borehole after tracking its evolution from the surface in 10-minute intervals. In this case, the well has been drilled to a hole depth of 10,000 feet. In the prior 10-minute interval, the system was slide drilling at an ROP of 93 feet per hour, with an average surface rotational speed of 14 RPM (slide drilling mode), and a flowrate of 598 gallons per minute (GPM). Properties of the drilling mud for this system are stated in the figure. For this system, the table (inset **Figure 19**) shows some of the required initializations regarding cuttings properties, thermal properties, and thermal gradients. The state of the well defined by the plots of ECD, cuttings concentration in the flow, and cuttings bed height versus hole depth are displayed in the figure. In the horizontal section at depths greater than 7500 feet, there exist cuttings bed approximately 3 to 4 inches high (in a 7.875-inch open hole). The ECD at 10,000 feet is around 13.1 ppg for drilling mud with a surface density of 12.5 ppg. The cuttings concentration in the flow for most of the well is under 5 percent. A relatively high cuttings concentration near the bit is due to the recently drilled cuttings that have not yet been deposited.

Evaluation Hole Depth **10000 feet**

The operation in the previous 10-minute interval was:

- **RPM = 14**
- **ROP = 93 ft/hr**
- **Flowrate = 598 GPM**
- **Mud density: 12.5 ppg**
- **Mud Rheology: PV = 40 cP, YP = 25 lb/100ft2 , Tau_y = 4.1Pa**

Hole section (inches)	**7.875**
Surface Temp (deg C)	**20**
Surface Pressure (Pa)	**101325**
Density of cuttings (ppg)	**20**
Diameter of cuttings (inches)	**0.25**
Annulus heat transfer coeff. (W/(m^2 degC))	**15**
Drillpipe heat transfer coeff. (W/(m^2 degC))	**55**
Sonic velocity (m/sec)	**1500**
Thermal coefficient (1/degC)	**1.50E-04**
Thermal gradient (degC/m)	**0.0275**
Mud heat capacity (J/Kg.degC)	**3200**

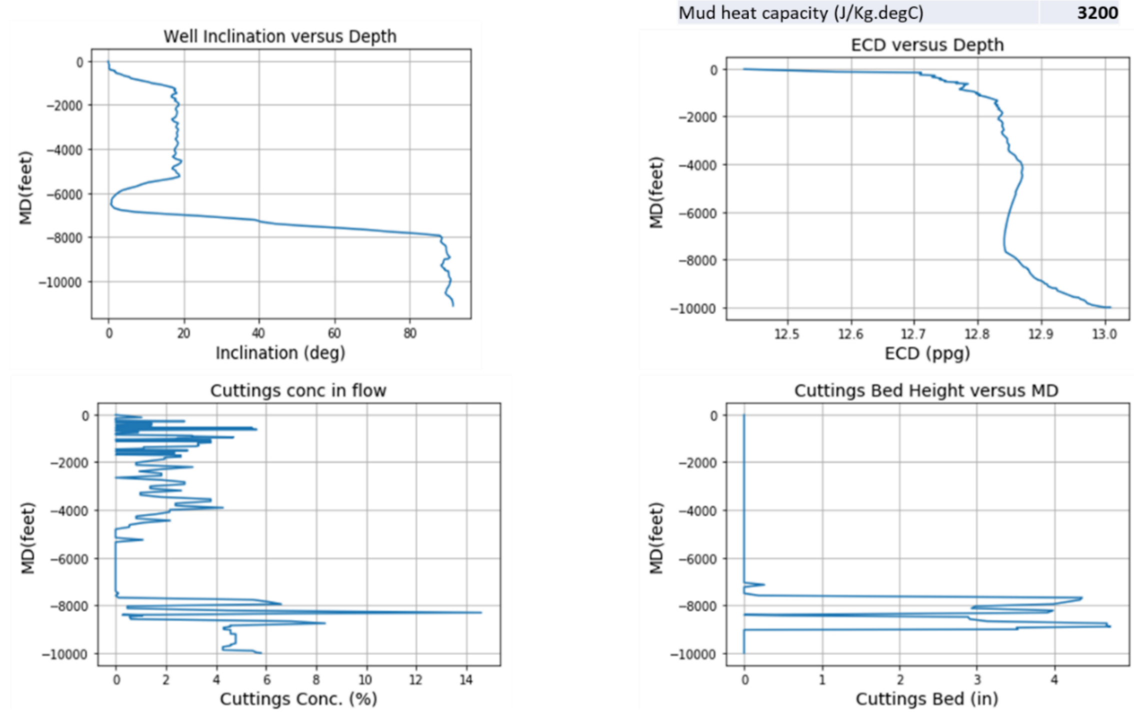

Figure 19 State of the system at 10000 feet hole depth after tracking its evolution from the surface.

3.3.2 Scenario analysis

The system from its current state (**Figure 19**) was used to simulate multiple scenarios or actions (a combination of changes in action variables such a flowrate, RPM, and ROP) to evaluate the outcomes of each. **Figure 20** describes the different actions and their predicted consequences on the hole cleaning system state. For the system at 10,000 feet, its state is represented by cuttings concentration, cuttings bed height, and ECD. Then, five different actions over the next 10-minute interval were simulated using the digital twin. As expected, different actions lead to different future system states, some more desirable than the others. Some actions lead to minimal improvement in hole condition; actions 1 and 2 result in only a slight reduction in the cutting bed height and the ECD. Some actions (such as actions 3 and 4) lead to improved hole condition by reducing the bed height, while minimally affecting the ECD. On the other hand, more aggressive actions (such as action 5) result in a significantly reduced bed height, but simultaneously result in a high ECD value. Although such actions assist with cuttings removal, an increase in the ECD to the fracture gradient can result in wellbore instability issues.

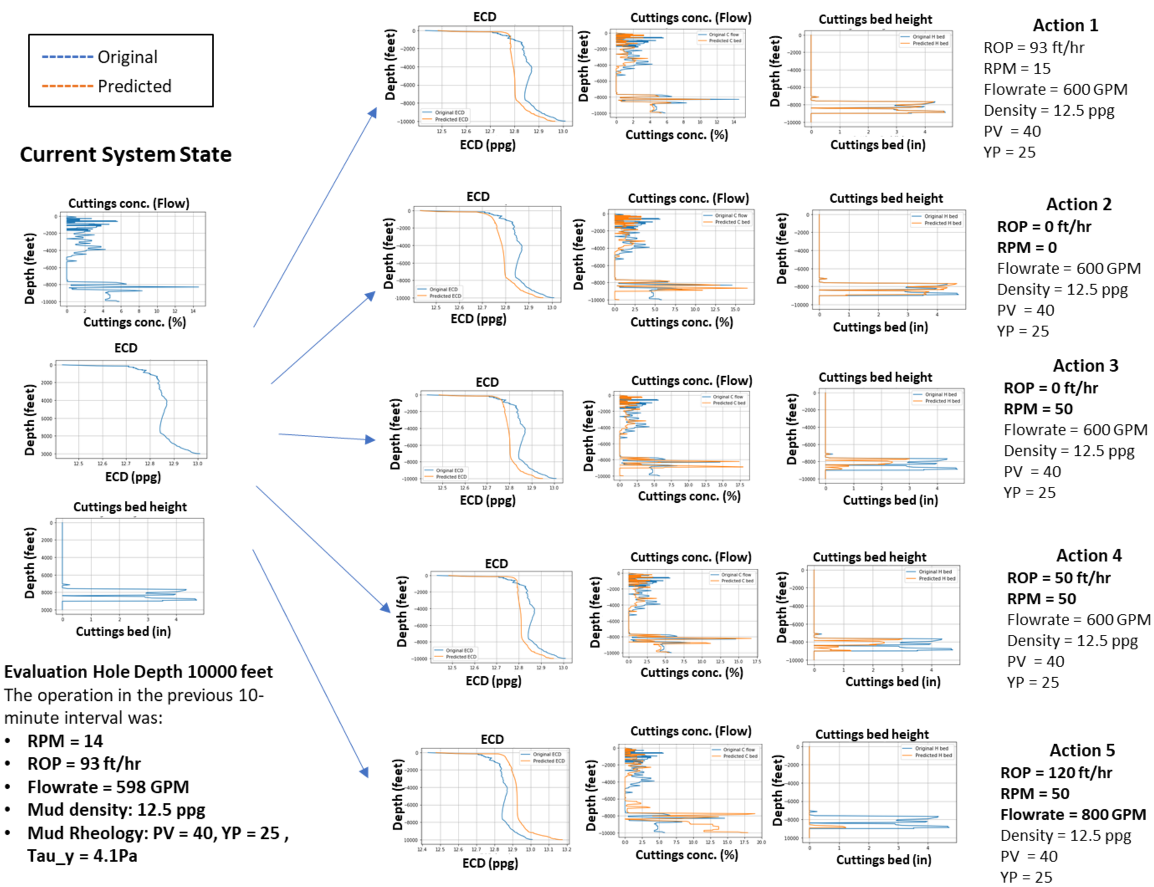

Figure 20 Scenario analysis for predictive action planning.

This concept of a single-step scenario analysis can easily be expanded to multi-step analysis, as shown in **Figure 21**. This digital twin, therefore, can be used to evaluate multiple action sequences over several time steps (evaluation intervals) to find the optimal way of traversing through the system, i.e., coming up with an optimal plan (action planning). Such short- and long-term scenario analysis is only possible with a predictive model and is a prime requirement for any twin.

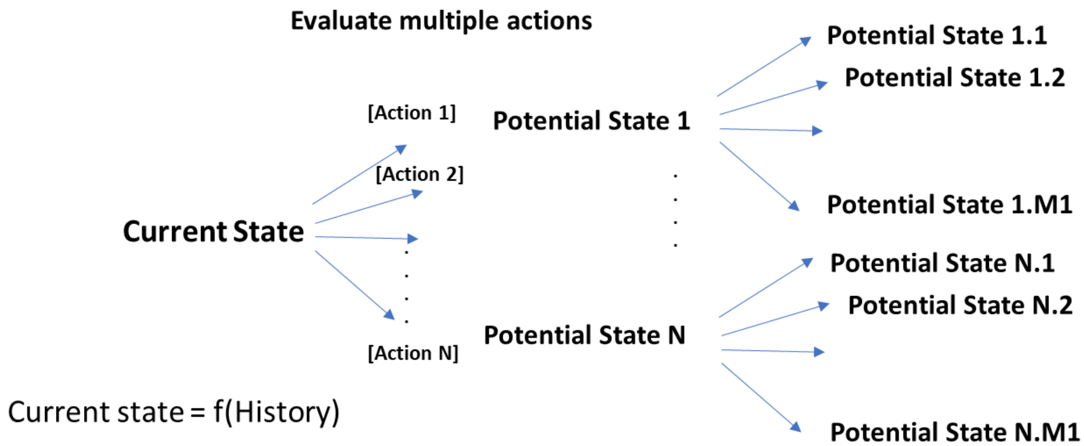

Figure 21 Simulating multiple action sequences.

3.4 SUMMARY

There are many models available in the drilling literature to address drilling efficiency and safety issues; however, to the best of our knowledge, none of provide a framework for analyzing scenarios or action planning. In this chapter, a robust cyclic methodology to build and use twinning systems for single-step scenario analysis was detailed. This methodology addresses the following aspects of digital twinning in the well construction domain:

- The cyclic process of development of the digital twin ensures that the final built twin is a compromise between the application type, the available data, and the memory and computational constraints.
- The integrated multi-model nature of the twin results in more realistic constraints around the permitted action values; for instance, as shown for the hole cleaning system, an aggressive increase in the flowrate would result in faster cuttings removal, but lead to increased ECD, which could be detrimental to the wellbore quality.
- Scenario design and selection is highly dependent on the twin and the available computation time. Thus, domain-knowledge can be employed to intelligently structure scenarios and build action sequences.

Due to their short- and long-term decision-making capability, digital twins serve as baselines for developing intelligent decision-making systems, which is discussed in the following chapters.

Chapter 4: Structuring Finite Horizon Sequential Decision-Making Systems

This chapter details the steps in structuring unbiased purpose-built sequential decision-making systems for well construction operations. Setting up such systems entails representing the operation as a Markov decision process (MDP). This requires explicitly defining states and action values, defining goal states, building a digital twin to model the process, and appropriately shaping reward functions to measure feedback. The digital twin, in conjunction with the reward function, is utilized for simulating and quantifying the different action sequences. A finite-horizon sequential decision-making system, with discrete state- and action-space, is then set up for hole cleaning advisory during well construction. A non-sparse normalized reward structure is formulated as a function of the state and action values. Hydraulics, cuttings transport, and rig-state detection models are integrated to build the hole cleaning digital twin, the development which is detailed in Chapter 3. This system is then used for performance-tracking and scenario simulations (with each scenario defined as a finite-horizon action sequence) on real-world oil wells. The different scenarios are compared by monitoring state-action transitions and the evolution of the reward with actions. The predicted output of the algorithm for the multiple operational scenarios is validated by comparing it with actions that a hole cleaning/ extended reach drilling (ERD) expert would have taken when given similar scenarios.

4.1 Setting Well Construction Sub-Processes as MDPs

Well construction is a multi-step process that requires planning and decision-making at every step of its various sub-processes. Planning necessitates identifying objectives, constraints, and required data associated with the individual sub-processes. A crucial step in developing such planning systems is setting them up properly, which requires the following elements:

- Formulating an MDP for the operation, which includes appropriately defining state-and action-space
- Defining a goal or a desired state
- Efficient shaping of the reward function
- Setting up an integrated-multi model system replicating the process (environment), i.e., building its digital twin

4.1.1 MDP formulation

Formulating an MDP for any process requires the following (Puterman, 1994):

- The process should satisfy the Markovian property
- Any state defined for the process should be fully observable
- State-space should be finite or countably infinite, with states defined by exhaustively incorporating all relevant parameters
- There is an explicit definition of the action-space with appropriately identified control variables

For most well construction processes, the condition (state) of the wellbore at any time is a culmination of all the previous operations (actions), past conditions (past states), and state transitions. In other words, the current state is a representation of the well's operational past, and any subsequent transition depends only on this state and the immediate action. The assumption that well construction operations follow the Markovian property is, therefore, valid. The state of the system needs to be represented by all relevant parameters required to describe the process under consideration fully. The state is also continually refined based on the data received from the surface or downhole sensors (at frequencies 1 Hz or higher). This results in the state being a complete representation of the environment as perceived by the agent, i.e., the state is assumed to be fully observable. The operations or variables that can be actively controlled to bring about state transitions constitute the action.

The state-and action-spaces could be either discrete or continuous; however, for the work presented here, both are defined as discrete sets. **Figure 22** illustrates the proposed method for discretizing the state-space based on wellbore inclinations A directional well can be analyzed by dividing it into three distinct sections based on the inclination angles: near-vertical section, build or curve section, and horizontal section. The segment of the well with inclination angles between 0 and 30 degrees is the near-vertical section, while regions of the well with inclination angles greater than 60 degrees constitute the near-lateral horizontal section. The intermediate inclination angle segments comprise the build or the curve section of a well. This method for discretizing the state-space is proposed since the state variables' response to different actions depends to a high degree on the inclination of the well segment. As discussed in Chapter 2, wellbore inclination significantly influences the cuttings transport mechanisms, which are different for near-vertical, intermediate, and lateral sections. Consequently, this affects the hole cleaning requirements.

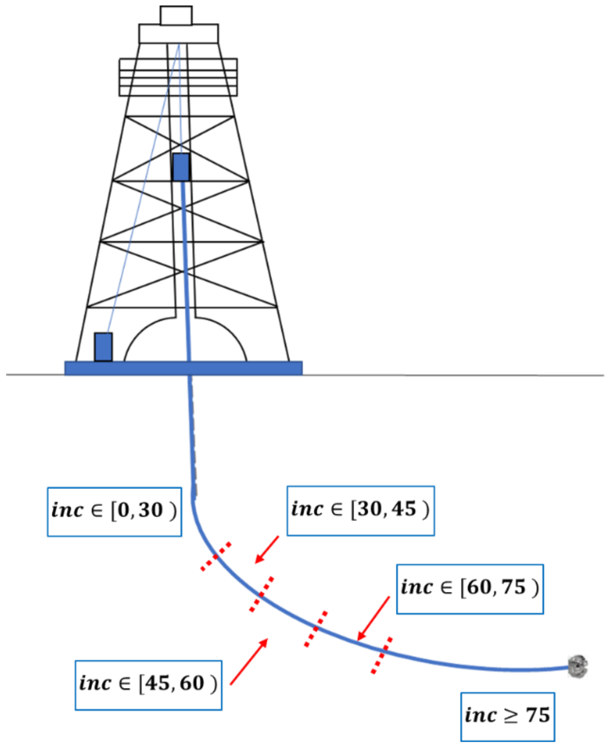

Figure 22 The proposed strategy for defining discrete state-space based on wellbore inclination angles.

Equation (26) represents the state vector, where 'p_1' through 'p_n' are the exhaustive set of parameters required to define the system state completely. The state of the system here consists of some functional value of these parameters over the appropriate inclination intervals $\{[0,30),[30,45),[45,60),[60,75),[75+)\}$. Another point to note is that these inclination interval definitions can be adjusted depending on the requirements of the underlying process.

$$s_t = \begin{Bmatrix} p_{1\_0-30} \\ p_{1\_30-45} \\ p_{1\_45-60} \\ p_{1\_60-75} \\ p_{1\_75+} \\ \cdot \\ p_{n\_0-30} \\ \cdot \\ p_{n\_75+} \end{Bmatrix} \tag{26}$$

Similarly, the action-space is constructed by different combinations of possible values of the identified control variables. For drilling operations, some such control variables are the surface drillstring rotation speed (RPM), weight on bit (WOB), drilling mud properties, flowrate, and drillstring tripping speeds. These variables can take on discrete values between specified minimum and maximum thresholds. These thresholds are dictated by safety constraints, process and equipment limitations, and operational economics.

4.1.2 Goal state

The goal or desired state, as the name suggests, refers to the subset of the state-space which the drilling agent aims to achieve. The goal state is used as the reference to direct the agent's search. The desired functional values of individual goal state components are used for the construction of the overall goal state, as shown in equation (27).

$$s_{goal} = \left\{ \begin{matrix} {p^g}_{1\_0-30} \\ {p^g}_{1\_30-45} \\ {p^g}_{1\_45-60} \\ {p^g}_{1\_60-75} \\ {p^g}_{1\_75+} \\ \cdot \\ {p^g}_{n\_0-30} \\ \cdot \\ {p^g}_{n\_75+} \end{matrix} \right\} \tag{27}$$

4.1.3 Reward shaping

Shaping the reward function allows for rewarding or penalizing a drilling agent's behavior more frequently, instead of at sparse intervals or at the end of an episode. Frequent rewards, in turn, help with more directed and faster learning. A possible strategy for reward shaping is to provide the agent with regular feedback based on its position relative to the goal state. Another factor to consider is the contribution to the reward of the relative changes in different action control variables. For instance, if a state transition from s to s' can be achieved by two completely different actions a and a', the reward function needs to be able to recognize and quantify this difference. This is especially important, for instance, in cases where the agent suggests changing drilling RPM and flowrate with an alternative action being a change to mud rheological parameters (which may be economically and temporally more expensive).

4.1.4 Digital twin of the environment

For action planning, a comprehensive model or digital twin of the process needs to be constructed. This twin is then used for replicating the environment, thereby simulating multiple episodes or trajectories of experience (Jones et al., 2020; Kunath & Winkler, 2018; Saini et al., 2020). Model-free RL techniques can then be applied to these episodes to improve the return value and, subsequently, to determine an optimal policy. **Figure 23** details these steps.

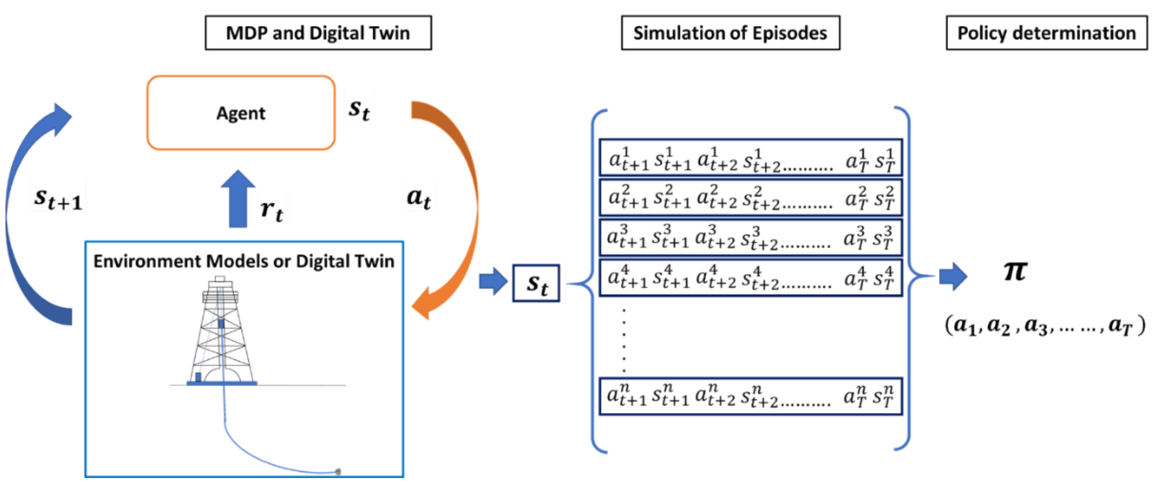

Figure 23 Application of MDP and digital twins for simulating episodes to determine the optimal policy.

4.2 Setting up the Hole Cleaning Decision-Making System

Here, we demonstrate step-by-step how to set up a decision-making and planning system for the hole cleaning operation.

4.2.1 Formulating the MDP for the hole cleaning system

The objective of hole cleaning operations is to manage:

- Height of the cuttings bed (that settles on the low-side of the borehole) to low enough values to prevent issues during any subsequent stage of well construction (**Figure 24)**

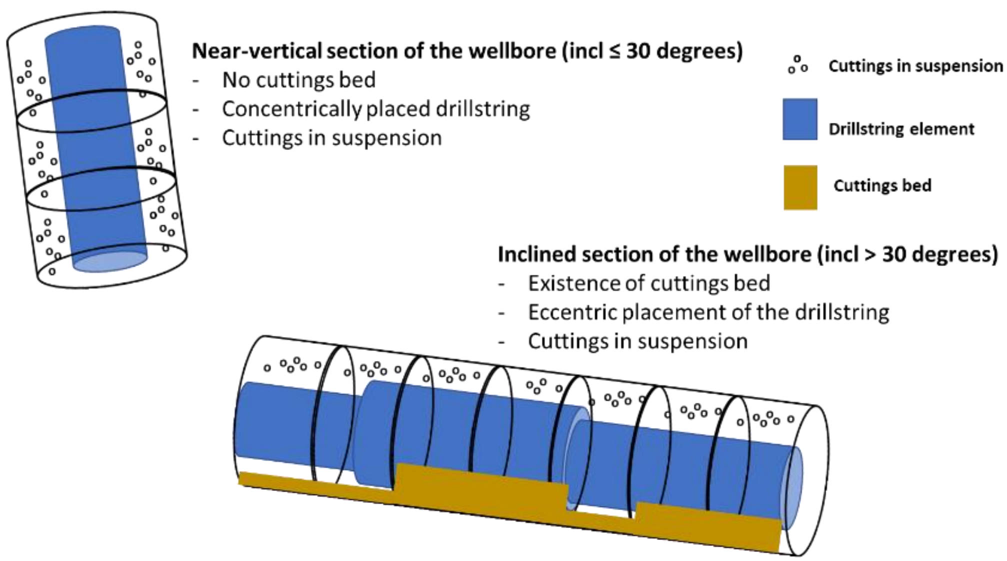

Figure 24 Segmentation of the well into different control volumes and cuttings transport mechanisms in different sections of the well.

- Downhole ECD values to remain within a given drilling margin (**Figure 25**)

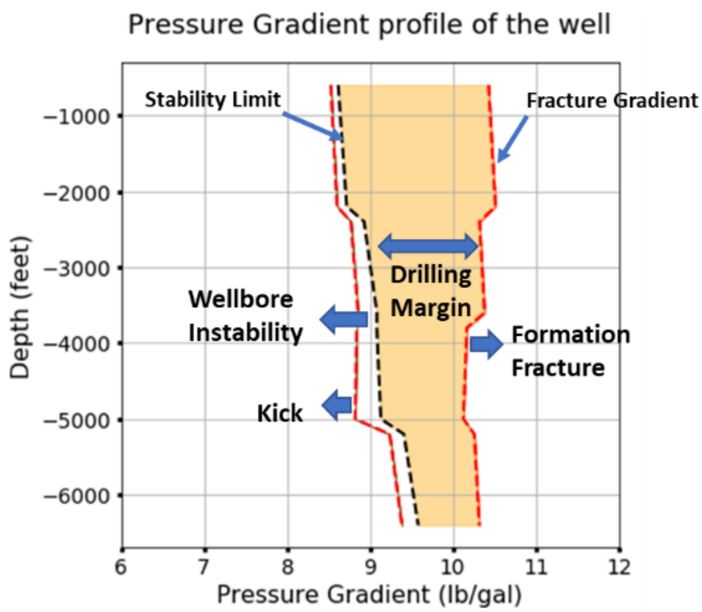

Figure 25 Drilling safety margin.

4.2.1.1 State-space

For building such hole cleaning systems, the following parameters are required to quantify the condition of the borehole from the perspective of hole cleaning (Baldino et al., 2015; Eric Cayeux et al., 2014b):

- Height of the cuttings bed in the curve and the lateral sections of the wellbore;
- ECD along the entire length of the wellbore.

The well can be treated as a series of interconnected control volumes, segmented based on any changes in well dimensions (e.g., changes in inner or outer diameters) or based on different survey intervals (as shown in **Figure 24**). Each control volume's condition can be independently represented by absolute values of ECD and cuttings bed height. However, with the well being segmented into multiple inclination intervals (based on the strategy discussed in **Figure 22**), every inclination interval usually consists of many such control volumes. A functional value derived from the absolute value is calculated for each of these parameters in every control volume. These values are then averaged over the different inclination segments to obtain a single value per inclination interval for every parameter. Converting to a functional value normalizes the absolute value to specific operational thresholds, and assists in reward shaping, as discussed in later sections.

4.2.1.1.1 Cuttings bed height

The absolute value of the cuttings bed height for every control volume is normalized to its outer diameter (**Figure 26**). These values are then used to calculate the average normalized cuttings bed height H for every inclination segment of the well, as shown by equation (28).

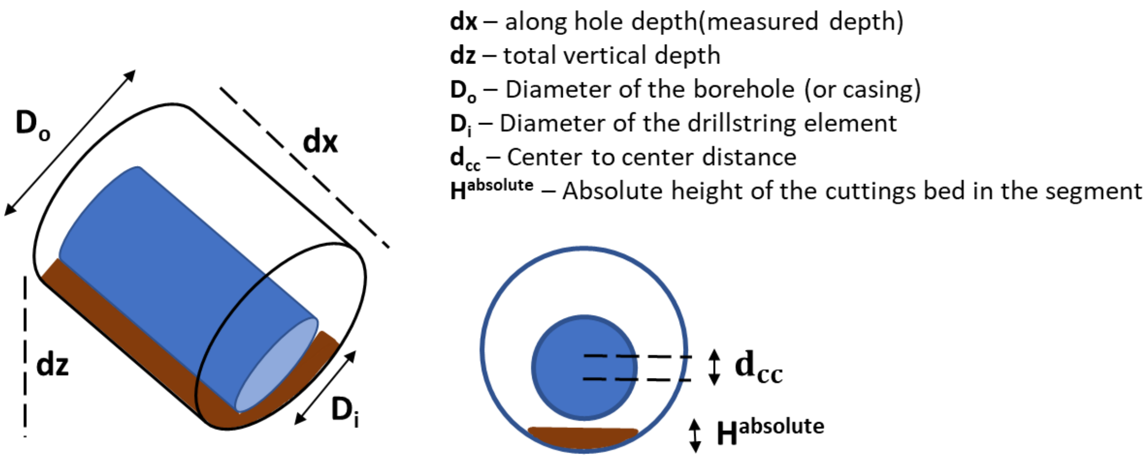

Figure 26 Absolute cuttings bed height for a single control volume element.

$$H_k^{norm} = \frac{H_k^{absolute}}{D_{o\_k}} \quad , \; H = \frac{\sum_{k=1}^{N_{seg}} H_k^{norm}}{N_{seg}} \tag{28}$$

The functional value $H_{inc.}$ is then derived from H using equation (29), as visualized in **Figure 27**.

$$H_{inc.} = \begin{cases} 0 & \boldsymbol{H} \leq 0.20 \\ 1 & 0.20 < \boldsymbol{H} \leq 0.40 \\ 2 & 0.40 < \boldsymbol{H} \leq 0.60 \\ 3 & 0.60 < \boldsymbol{H} \leq 0.80 \\ 4 & \boldsymbol{H} > 0.80 \end{cases} \quad (29)$$

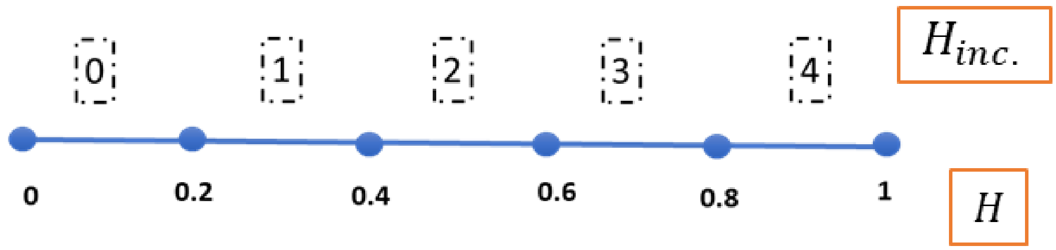

Figure 27 Functional value assignment for the cuttings bed height parameter.

The parameter $H_{inc.}$ is evaluated for all non-vertical sections because no cuttings bed will form in the $[0, 30)$ degree inclination interval. Thus, the bed height components of the state vector are $\{H_{30-45}, H_{45-60}, H_{60-75}, H_{75+}\}$.

4.2.1.1.2 ECD

As previously discussed, ECD needs to be managed within the drilling margin. There is, however, some degree of uncertainty associated with its limits, which is accounted for by considering an uncertainty factor $DF(\leq 0.25)$. ECD_{avg}, the average ECD for an inclination interval, is calculated by averaging absolute ECD values over all the control volume segments in that interval (equation (30)). Since the SL and FG values vary with depth, ECD_{avg} is calculated independently for the different intervals.

$$ECD_{avg} = \frac{\sum_{k=1}^{N_{seg}} ECD_k^{absolute}}{N_{seg}} \quad (30)$$

Using ECD_{avg}, the functional value of ECD, $ECD_{inc.}$ is calculated using equation (31), and is discussed in **Figure 28**.

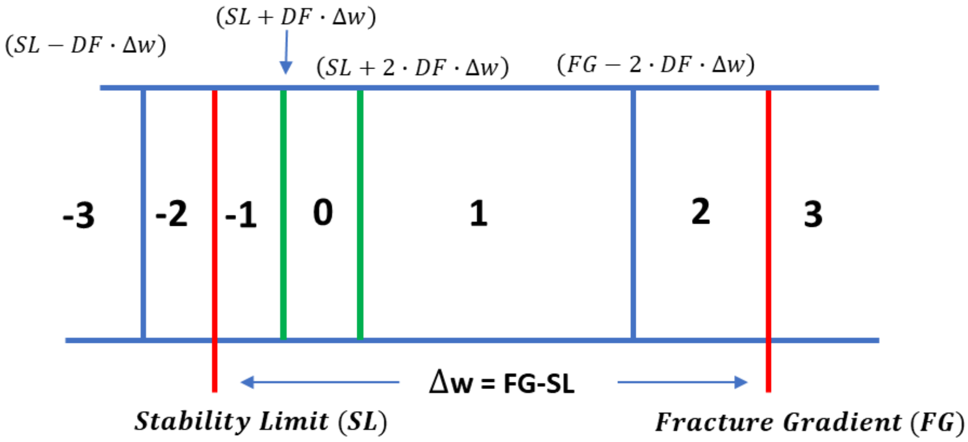

Figure 28 Functional value assignment for the ECD parameter.

$$ECD_{inc.} = \begin{cases} -3 & \boldsymbol{ECD_{av}} \leq SL - DF \cdot \Delta w \\ -2 & SL - DF \cdot \Delta w < \boldsymbol{ECD_{av}} \leq SL \\ -1 & SL < \boldsymbol{ECD_{av}} \leq SL + DF \cdot \Delta w \\ 0 & SL + DF \cdot \Delta w < \boldsymbol{ECD_{av}} \leq SL + 2 \cdot DF \cdot \Delta w \\ 1 & SL + 2 \cdot DF \cdot \Delta w < \boldsymbol{ECD_{av}} \leq FG - 2 \cdot DF \cdot \Delta w \\ 2 & FG - 2 \cdot DF \cdot \Delta w < \boldsymbol{ECD_{av}} \leq FG \\ 3 & \boldsymbol{ECD_{av}} > FG \end{cases} \tag{31}$$

$$where \qquad \Delta w = FG - SL$$

Since keeping ECD within the drilling margin is essential throughout the well, the state components related to the ECD parameter, $\{ECD_{0-30}, ECD_{30-45}, ECD_{45-60}, ECD_{60-75}, ECD_{75+}\}$ are calculated for all intervals.

Equation (32) represents the complete hole cleaning state of the wellbore. In this form, every component of the state vector is represented by its functional value at every decision epoch.

$$s = \left\{ \begin{matrix} H_{30-45} \\ H_{45-60} \\ H_{60-75} \\ H_{75+} \\ ECD_{0-30} \\ ECD_{30-45} \\ ECD_{45-60} \\ ECD_{60-75} \\ ECD_{75+} \end{matrix} \right\} \tag{32}$$

This representation of state is Markovian, since it fully represents the condition of the hole cleaning system and encompasses all the information about the system's history. Any subsequent state transition depends only on the state and the action taken.

4.2.1.2 Goal state

The goal for any decision-making system is to first search the state- and action-space and then move towards the desired state. The functional values for all state variable components are defined such that 0 represents the desired state for each; therefore, the target goal state for the system is as shown in equation (33).

$$s_{goal} = \left\{ \begin{matrix} 0 \\ 0 \\ 0 \\ 0 \\ 0 \\ 0 \\ 0 \\ 0 \\ 0 \end{matrix} \right\} \tag{33}$$

4.2.1.3 Action-space

Hole cleaning, while managing the ECD within the drilling margin, is a function of (see, e.g., Erge et al., 2015; Gul et al., 2020; Saasen & Løklingholm, 2002):

- Drilling mud properties (particularly density and viscosity);
- Cuttings properties (size and density);

- Drilling parameters such as drilling RPM and flowrate;
- Drillstring geometry and its eccentricity in the borehole;
- Rate of cuttings generation (which depends on the drilling rate);
- Borehole geometry (diameters of the open or cased hole sections along the well) and inclination angle;
- Hole cleaning pills or sweeps, i.e., limited volumes of fluid with altered density and/or viscosity to aid in cuttings evacuation from the hole (mostly effective in vertical hole rather than deviated hole).

Some of these control variables affect the condition of the borehole to a greater extent than others. Also, some variables can be controlled more readily than others. **Figure 29** illustrates a chart comparing the different control variables, plotted for their relative influence on hole cleaning against their ability to be actively controlled in real-time.

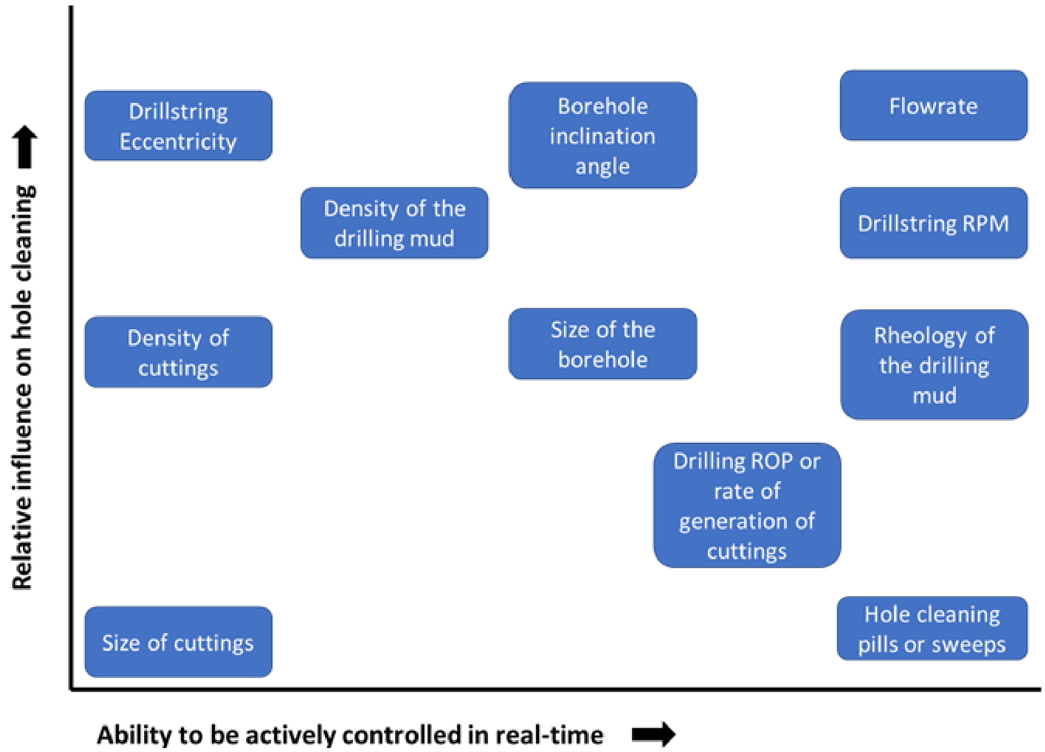

Figure 29 Variables contributing to the hole cleaning performance in a deviated hole (modified from Nazari et al., 2010).

Thus, the key parameters that have a significant influence on the hole cleaning performance, and can be actively controlled in the field, are flowrate, RPM, mud properties (rheological parameters), and the WOB to control the rate of penetration (ROP). In the following, we will assume that the fluid behavior is that of a Bingham Plastic fluid, in which case its rheology is quantified by its plastic viscosity (PV) and yield point (YP). Another critical parameter that influences the ECD is the mud density. A combination of these variables at every decision epoch constitutes an action, which is represented by equation (34). Each control variable can take on a finite number of values between some minimum and maximum thresholds that are determined by safety constraints, operational economics, and equipment and process limitations. For instance, if the flowrate has ten values in the [0, 1800] interval, its equally spaced values, in gallons per minute (GPM), are {0, 200, 400, 600, 800, 1000, 1200, 1400, 1600, 1800}.

$$a_t = \begin{Bmatrix} Flowrate \\ ROP \\ RPM \\ Mud\ density \\ Mud\ PV \\ Mud\ YP \end{Bmatrix} \tag{34}$$

4.2.2 Digital twin of the environment

A digital twin of the hole cleaning operations, development of which is detailed in Chapter 2, was built by integrating multiple data streams with analytical implementations of the cuttings transport, hydraulics, and rig-state detection models (Saini et al., 2020). The cuttings transport and hydraulics models estimate the height of the cuttings bed and the ECD along the well, respectively. The rig-state detection engine outputs the current operational state (such as rotary or slide drilling, tripping in or out the borehole, etc.)(De Oliveira et al., 2016). The purpose of this twin is twofold: first, for performance tracking by simulating different hole cleaning actions, and second, as a forward simulation model for assisting with action planning. **Figure 30** illustrates the application of the twin as a forward-simulation model, where an action a_t transitions the system state from s_t, to s_{t+1}, at decision epoch t. The epoch is the smallest time step of the planning problem for which an action is determined. The digital twin was designed to plan either every 5-minute interval into the future, or whenever there is a change in the well operations.

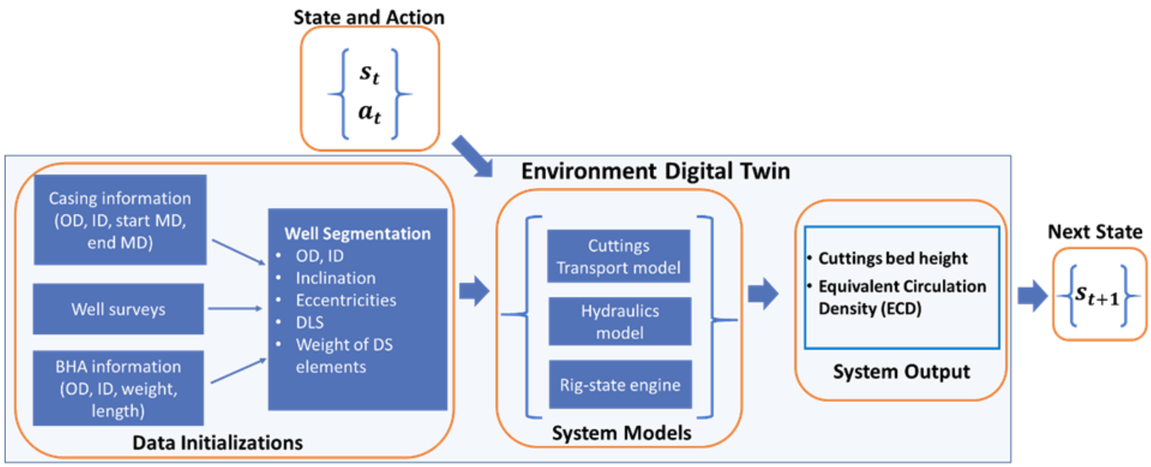

Figure 30 Digital twin of the hole cleaning system's environment.

4.2.3 Reward function

To quantify the immediate feedback associated with state-action transitions, a reward function is defined for the hole cleaning system, which has three distinct components:

- The reward associated with state transition;
- The penalty associated with action transition;
- The reward associated with action value.

4.2.3.1 Reward associated with state transition

Since the objective of the system is to reach the goal state, every component of the state vector tries to achieve a functional value of 0. This was used as a reference to calculate normalized reward values associated with every state vector component in the $[-1,1]$ range.

Table 2 details the functions used for these calculations.

Table 2 Reward function associated with state vector components.

Component	Reward Function	Values
H_{30-45}	$R_{H30-45} = \frac{2 - H_{30-45}}{2}$	$\{\mathbf{1},\ \mathbf{0.33},\ -\mathbf{0.33},\ -\mathbf{1}\}$
H_{45-60}	$R_{H45-60} = \frac{2 - H_{45-60}}{2}$	$\{\mathbf{1},\ \mathbf{0.33},\ -\mathbf{0.33},\ -\mathbf{1}\}$
H_{60-75}	$R_{H60-75} = \frac{2 - H_{60-75}}{2}$	$\{\mathbf{1},\ \mathbf{0.33},\ -\mathbf{0.33},\ -\mathbf{1}\}$
H_{75+}	$R_{H75+} = \frac{2 - H_{75+}}{2}$	$\{\mathbf{1},\ \mathbf{0.33},\ -\mathbf{0.33},\ -\mathbf{1}\}$
ECD_{0-30}	$R_{ECD0-30} = 1 - \frac{2}{3}.\lvert E_{0-30}\rvert$	$\{-\mathbf{1}, -\mathbf{0.33},\ \mathbf{0.33},\ \mathbf{1},\ \mathbf{0.33}, -\mathbf{0.33}, -\mathbf{1}\}$
ECD_{30-45}	$R_{ECD30-45} = 1 - \frac{2}{3}.\lvert E_{30-45}\rvert$	$\{-\mathbf{1}, -\mathbf{0.33},\ \mathbf{0.33},\ \mathbf{1},\ \mathbf{0.33}, -\mathbf{0.33}, -\mathbf{1}\}$
ECD_{45-60}	$R_{ECD45-60} = 1 - \frac{2}{3}.\lvert E_{45-60}\rvert$	$\{-\mathbf{1}, -\mathbf{0.33},\ \mathbf{0.33},\ \mathbf{1},\ \mathbf{0.33}, -\mathbf{0.33}, -\mathbf{1}\}$
ECD_{60-75}	$R_{ECD60-75} = 1 - \frac{2}{3}.\lvert E_{60-75}\rvert$	$\{-\mathbf{1}, -\mathbf{0.33},\ \mathbf{0.33},\ \mathbf{1},\ \mathbf{0.33}, -\mathbf{0.33}, -\mathbf{1}\}$
ECD_{75+}	$R_{ECD75+} = 1 - \frac{2}{3}.\lvert E_{75+}\rvert$	$\{-\mathbf{1}, -\mathbf{0.33},\ \mathbf{0.33},\ \mathbf{1},\ \mathbf{0.33}, -\mathbf{0.33}, -\mathbf{1}\}$

Thus, the reward function contribution of state transition is represented by the set given in equation (35).

$$\boldsymbol{R_S} = \{R_{H30-45}, R_{H45-60}, R_{H60-75}, R_{H75+}, R_{ECD0-30}, R_{ECD30-45}, R_{ECD45-60}, R_{ECD60-75,} R_{ECD75+}\} \tag{35}$$

4.2.3.2 Penalty associated with action transition

Table 3 details the calculation of the penalty (negative reward) related to changes in action values. The purpose of these definitions is twofold:

- To discourage the system from making extreme changes in actions, unless the reward associated with state transition offsets this penalty;
- Select the least penalizing action in case multiple actions result in the same state transition.

Table 3 Reward function associated with action transition.

Component	No. of Intervals	Reward Function	Values
$Flowrate$	$n_{flowrate}$	$R_{flowrate} = -\frac{\lvert \Delta N_{flowrate} \rvert}{n_{flowrate}}$	$[-\mathbf{1},\ \mathbf{0}]$
$Drilling\ ROP$	n_{ROP}	$R_{ROP} = -\frac{\lvert \Delta N_{ROP} \rvert}{n_{ROP}}$	$[-\mathbf{1},\ \mathbf{0}]$
$Drillstring\ RPM$	n_{RPM}	$R_{RPM} = -\frac{\lvert \Delta N_{RPM} \rvert}{n_{RPM}}$	$[-\mathbf{1},\ \mathbf{0}]$
$Mud\ density$	$n_{density}$	$R_{density} = -\frac{\lvert \Delta N_{density} \rvert}{n_{density}}$	$[-\mathbf{1},\ \mathbf{0}]$
$Mud\ PV$	n_{PV}	$R_{PV} = -\frac{\lvert \Delta N_{PV} \rvert}{n_{PV}}$	$[-\mathbf{1},\ \mathbf{0}]$
$Mud\ YP$	n_{YP}	$R_{YP} = -\frac{\lvert \Delta N_{YP} \rvert}{n_{YP}}$	$[-\mathbf{1},\ \mathbf{0}]$

The terms $\Delta N_{variable}$ and $n_{variable}$ respectively are the number of interval changes between consecutive actions and the number of discrete values possible for a given control variable. Their use to calculate a penalty value is illustrated in **Figure 31**. The action transition based penalty set is expressed in equation (36).

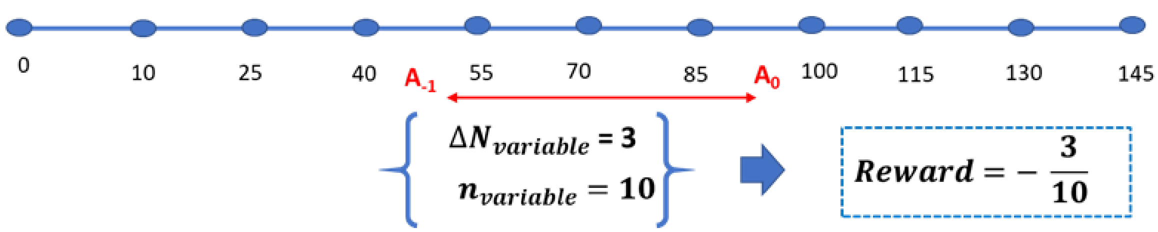

Figure 31 Example calculation of an action transition based penalty.

$$\boldsymbol{R_{ap}} = \{R_{flowrate}\ , R_{ROP}, R_{RPM}, R_{density}, R_{PV}\ , R_{YP}\} \tag{36}$$

4.2.3.3 Reward associated with action value

In the planning phase of drilling operations, the hole cleaning requirement of the system would push the ROP to zero simply because no cuttings are generated at zero ROP leading to zero bed height and optimum ECD. However, because a critical objective of drilling is to drill a well as fast as reasonably possible (within given limits), there needs to be a positive feedback or reward associated with the ROP. Equation (37) represents this reward, which is calculated using equation (38) as a ratio of the discrete interval number for a given ROP value to the total number of ROP intervals. This reward component is in the range [0,1].

$$\boldsymbol{R_{ar}} = \{0, R_{ROP}, 0,0,0,0\} \tag{37}$$

$$R_{ROP} = \frac{n_{interval}}{n_{ROP}} \tag{38}$$

4.2.3.4 Calculating the net reward

Reward value quantifies the 'goodness' of taking some action from a given system state. Thus, the next step for the hole cleaning system is to combine the individual reward components to output a single reward value in the [0,1] range. This is accomplished by assigning different relative weights to the various components. This ability to assign different weights provides a way to prioritize different objectives. This would be advantageous in drilling wells where there, for instance, is a high risk of well control issues. In these wells, the objective of keeping the ECD within the drilling margin becomes a higher priority than completely removing the cuttings bed. Similarly, reducing the penalty associated with taking drastic actions will not be as important for certain wells as reaching the desired state quickly. Managing these objectives can be accomplished by assigning different relative weights to the individual state or action reward components.

The sets W_s, W_{ap} and W_{ar} respectively are the weights associated with sets for state transition reward, action transition penalty, and the action reward. Equations (39), (40) and (41) represent the method to combine these weights and their associated reward sets. The final values of the R_{S_net}, R_{ap_net} and R_{ar_net} are in the ranges $[-1,1]$, $[-1,0]$ and $[0,1]$, respectively.

$$R_{S\_net} = \frac{\sum_i W_{si}\, R_{si}}{\sum_i W_{si}} \tag{39}$$

$$R_{ap\_net} = \frac{\sum_i W_{api}\, R_{api}}{\sum_i W_{api}} \tag{40}$$

$$R_{ar\_net} = \frac{\sum_i W_{ari}\, R_{ari}}{\sum_i W_{ari}} \tag{41}$$

Before further combining these three components, they are first normalized to the $[0,1]$ range, using the method presented in equations (42), (43) and (44).

$$R_{s\_norm} = \frac{R_{S\_net} + 1}{2} \tag{42}$$

$$R_{ap\_norm} = R_{ap\_net} + 1 \tag{43}$$

$$R_{ar\_norm} = R_{ar\_net} \tag{44}$$

Finally, the individual normalized rewards R_{s_norm}, R_{ap_norm} and R_{ar_norm} are combined based on the weights W_{s_norm}, W_{ap_norm} and W_{ar_norm} as per equation (45). These weights define the relative importance of the individual normalized rewards and can also be tuned in real-time.

$$R_{net} = \frac{W_{s\_norm}R_{s\_norm} + W_{ap\_norm}R_{ap\_norm} + W_{ar\_norm}R_{ar\_norm}}{W_{s\_norm} + W_{ap\_norm} + W_{as\_norm}} \tag{45}$$

The above definition of the reward function ensures immediate feedback after every action, as opposed to the agent having to wait until the end of an episode (as is the case for sparse reward functions).

4.3 Implementing the System as an MDP

Here, we demonstrate the developed hole cleaning decision-making system for performance tracking and action planning using a specific example. The dataset used is from an actual oil well that exhibited issues due to insufficient hole cleaning during tripping, casing, and cementing operations. The dataset for the well included information such as:

- **well trajectory**, represented by directional surveys (inclination and azimuth versus the hole depth);
- **well profile**, represented by the BHA, casing and bit details;
- **one-second surface sensor data**, for directly and indirectly measuring the drilling parameters;
- **mud-checks**, to determine mud density and rheology among other drilling mud properties.

A digital twin of the well was developed by integrating physics-based models (cuttings transport and hydraulics with an incorporated thermal model), data-based models (rig-state detection engine), and relevant raw data sources (as detailed in **Figure 30**).

4.3.1 Well profile

The well had a short vertical section and a shallow kick-off point (where the well starts building inclination from the vertical) around 300 feet MD. After kick-off, the inclination angle was continuously built until the well became horizontal at about 1250 feet MD. After this, the well stayed near-horizontal until it reached its total depth (TD) of 2500 feet MD. The well profile and trajectory are shown in **Figure 32**.

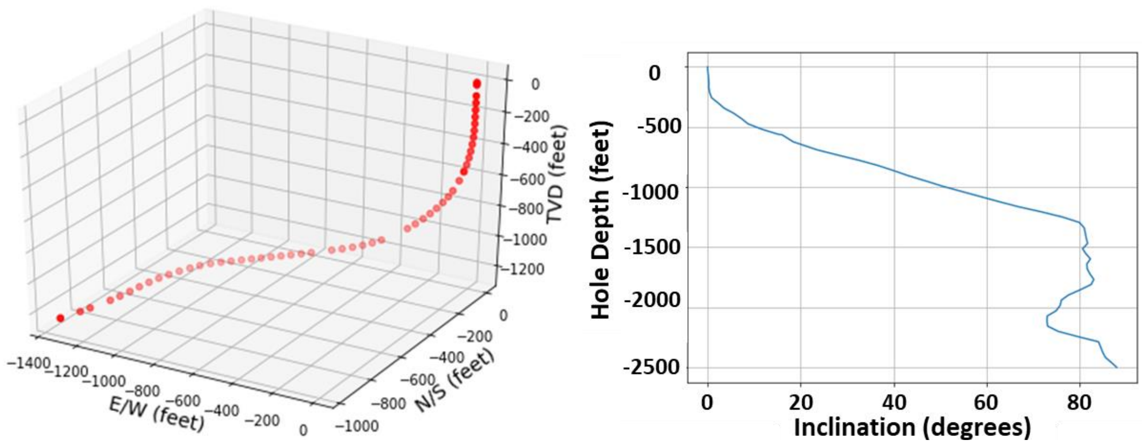

Figure 32 Well trajectory and inclination profile (negative sign indicates downward depth into the sub-surface).

This well was completed in two 'BHA runs' where each run comprised of drilling to a predetermined hole depth and subsequently, casing and cementing the hole. After the first BHA run, a surface casing of internal diameter 13.375-inch was set at a depth of 623 feet MD. Following this, in the second BHA run, a 12.25-inch hole section was drilled to well TD. Upon reaching TD, a 50-minute on-bottom circulation cycle (at a flowrate of around 910 GPM and 60 RPM) was performed for hole cleaning purposes. The drillstring was then tripped out of the hole with intermittent back-reaming (at 900 GPM and 60 RPM), and finally, a 9.625-inch casing was run to TD and cemented. The drilling and tripping operations for the well are summarized in **Figure 33**. Poor hole cleaning negatively affected the last trip out of the hole with the drilling BHA, the run into the hole with the casing, and, ultimately, the casing cementing operation.

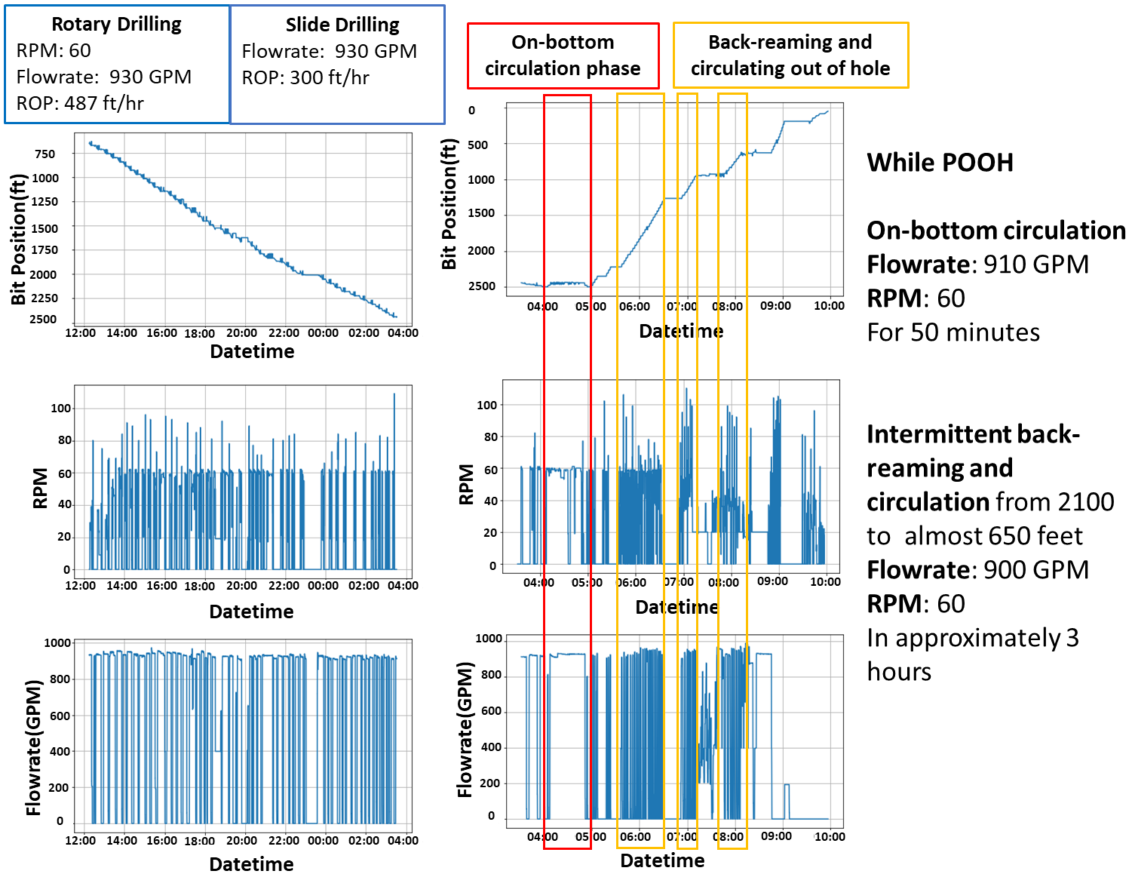

Figure 33 Operational summary for the well.

Calculations show that for running a 9.625-inch casing in a 12.25-inch borehole, the maximum theoretical cuttings bed height (on pulling the drillstring out of hole) should not exceed approximately 5-inches (**Figure 34**). This 5-inch bed height corresponds to 45.1 in^2 of cuttings in the cross-section.

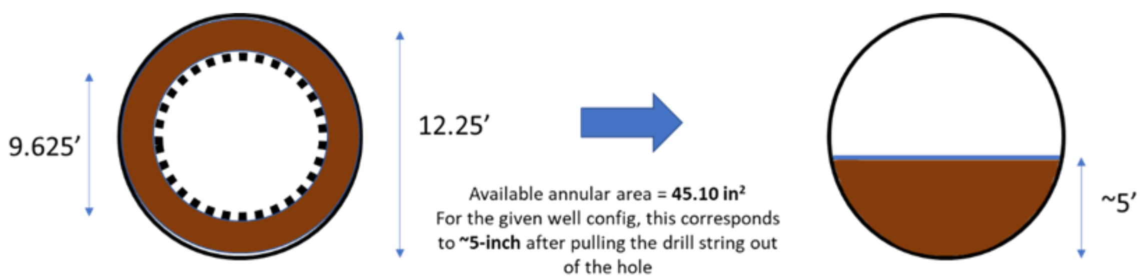

Figure 34 The theoretical limit of allowed cuttings bed height for the given well profile.

This cross-section of cuttings was then translated to an equivalent bed height by assuming the drillstring to be in the hole with the drill bit at TD. For the given well profile and trajectory (based on changes in outer diameters and eccentric placements of different drillstring components), this limit is represented by the red line in **Figure 35(a)**. The red shaded region corresponds to unsafe levels of cuttings bed height, while the green zone represents the goal state. Similarly, **Figure 35(b)** depicts the ECD profile (drilling window) for the well, bounded by SL and FG, with ten percent uncertainty in their values. As in **Figure 35(a)**, the green shaded zone corresponds to the goal state, while the red zones represent regions with the potential for well control issues. The yellow zones for both profiles are safe but suboptimal states.

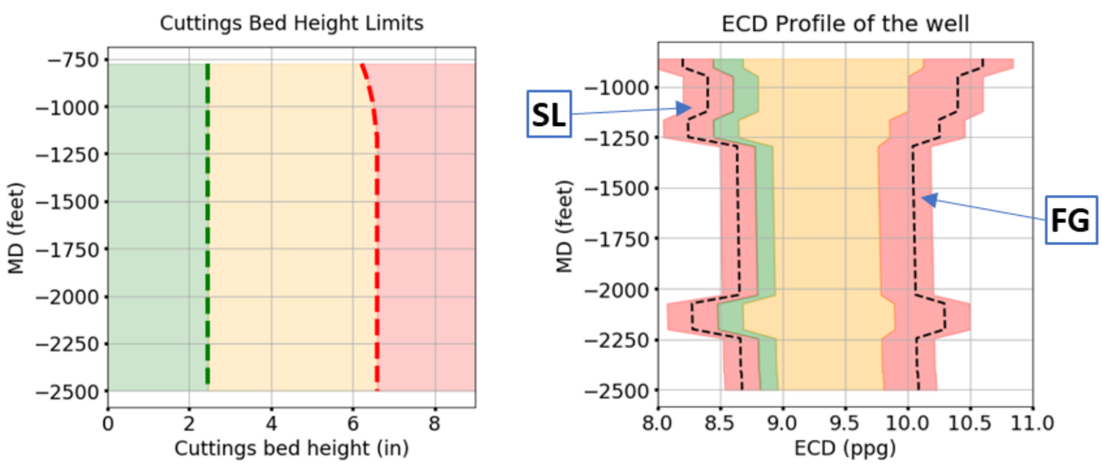

Figure 35 (a) Equivalent bed height limits for the given well profile (b) ECD limits for the well considering a ten percent uncertainty in the SL and FG values (negative sign indicates downward depth into the sub-surface).

The SL and FG values to define the drilling margins for the different sections of the well are shown in **Table 4**. For the near-vertical section, the SL and FG were assigned non-limiting values of 6 ppg and 18 ppg, respectively, because this interval was entirely cased while drilling the 12.25-inch section during the second BHA run.

Table 4 The SL and FG values to define drilling margin for the different inclination intervals.

Inclination Interval	**Stability Limit (ppg)**	**Fracture Gradient (ppg)**
[0,30)- in casing	6	18
[30, 45)	8.2	10.6
[45,60)	8.4	10.4
[60, 75)	8.2	10.2
[75+)	8.6	10.0

4.3.2 Performance tracking of the system and summary of issues

State transitions were monitored, and associated rewards were calculated to track the performance of the system during drilling operations. State-space was defined by dividing the well into five inclination-based segments, with the procedure as discussed in the previous section. The reward function was shaped based on state and action values and transitions. Determining the action-space required the specification of the discrete values of the different control variables. **Table 5** shows the number and range of values for the different variables.

Table 5 Value discretization of control variables.

Control Variable	**Number of Discrete Values**	**Range of Values**
Flowrate (GPM)	10	[0, 1500]
Drilling ROP (ft/hr.)	10	[0, 900]
Drillstring RPM (rev/min)	10	[0, 150]
Mud Density (ppg)	5	[8.5, 9.7]
Mud Plastic Viscosity (cP)	5	[7, 42]
Mud Yield Point (lb./100ft^2)	5	[7, 42]

The weights assigned to the different reward function components are shown in **Table 6.** Equal weights for all the state transitions components (W_s) assumes equal relative importance of the different state components. Similarly, the relative penalties associated with changing the different action components (W_{ap}) are also assumed to be the same. As discussed in the previous section, these weights can be tuned by the rigsite engineer to prioritize different objectives. However, for the following example, the weights for combining the normalized reward components (weights associated with R_{s_norm}, $R_{ap_norm}$and R_{ar_norm}) are assigned such that being in or near the goal states is prioritized over the penalty associated with changes in action variables, or the rewards due to an increased ROP. Similarly, while drilling, the weight of the reward associated with a higher ROP is more than the weight of the penalty associated with the changes in action variables. The weight of the normalized action reward component (W_{ar_norm}) has two values depending on the operation being tracked. A weight of zero is assigned to circulation operations because no new hole is being drilled (i.e., ROP is zero).

Table 6 Weight assignments for reward function shaping.

$W_s = [1,1,1,1,1,1,1,1,1]$	
$W_{ap} = [1,1,1,1,1,1]$	
$W_{ar} = [0,1,0,0,0,0]$	
$W_{s\_norm} = 0.50$	
$W_{ap\_norm} = 0.20$	
Drilling	**Circulation**
$W_{ar\_norm} = 0.30$	$W_{ar\_norm} = 0.00$

Figure 36 overlays the different normalized reward components calculated for decision-epoch intervals of 5-minutes. For this system, the net-reward tracks the state reward, since W_{s_norm} is significantly higher than the other weights. The reward value at the end of the drilling operation stabilizes to around 0.46. An increase in reward value to 0.68 at the end of the circulation cycle shows an improvement in the hole condition. This improvement is also reflected in the state reward value, which increases from 0.51 to 0.59.

Figure 36 Normalized reward components versus decision epochs for the well.

Figure 37 shows the state of the system at the end of the drilling operation (12.25-inch hole section), which can be represented by equation (46). The mud properties for drilling the last section of the well were: mud density of 9.06 ppg, PV of 11 cP, and YP of 36.5 lbf/100 ft^2. The final bed height was around 9-inch, which needed to be significantly reduced.

$$s_{TD} = \begin{Bmatrix} 0 \\ 3 \\ 4 \\ 4 \\ 1 \\ 1 \\ 1 \\ 1 \\ 1 \end{Bmatrix} \quad (46)$$

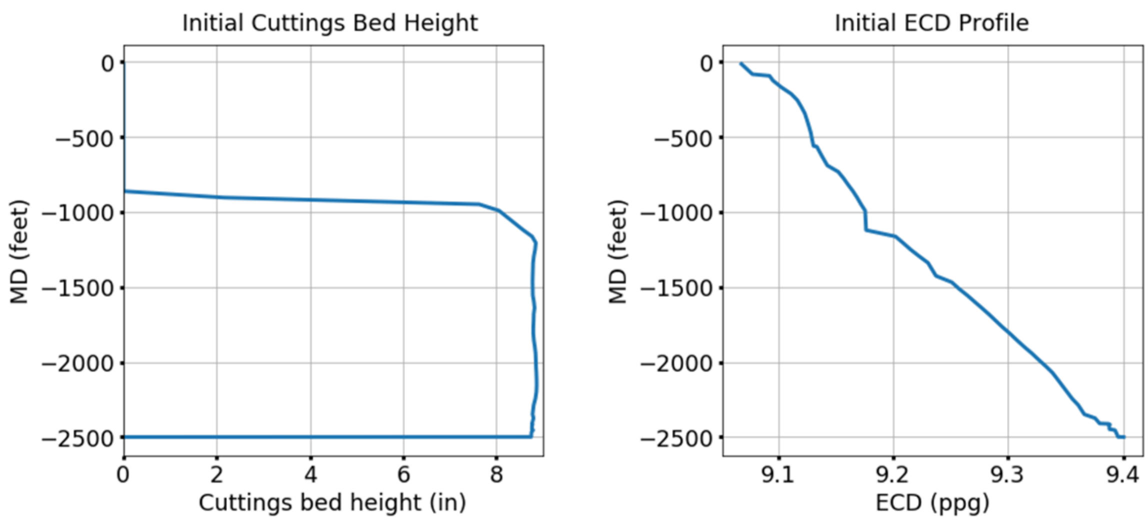

Figure 37 State of the borehole at the end of the drilling operation.

- Thus, a 50-minute circulation cycle to remove cuttings followed. Removal of cuttings is essential to ensure safe tripping operations without getting stuck, as well as to prepare the well for casing and cementing operations. The resulting state of the system is represented by equation (47) and is shown in **Figure 38**. As can be seen, the cuttings bed height was very close to the allowed limit, and therefore still non-optimal, leading to issues while running casing and subsequently cementing.

$$s_{TD\_circ} = \begin{Bmatrix} 0 \\ 2 \\ 3 \\ 3 \\ 1 \\ 1 \\ 1 \\ 1 \\ 1 \end{Bmatrix} \tag{47}$$

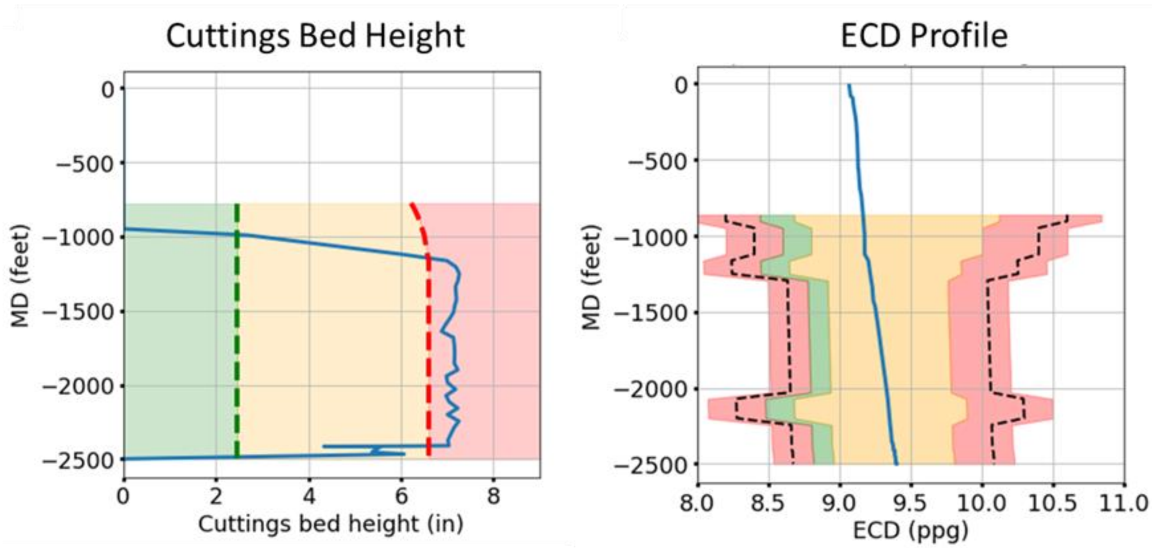

Figure 38 State of the borehole at the end of the circulation cycle.

Therefore, to summarize, the primary operational issue leading to the observed problems and NPT is insufficient hole cleaning. This claim can be supported based on the following findings by the hole cleaning digital twin:

- Throughout the drilling operations in the lateral section, the cuttings bed height was approximately 5-inches during rotary drilling and approximately 9-inch during slide drilling
- Even after the clean-up circulation cycle, a high cuttings bed remained
- Back-reaming while POOH does not assist significantly with hole cleaning

- High friction factor while drilling, erratic torque while back-reaming, presence of softball-sized clay chunks while circulating, casing getting stuck and issues with cementing support the presence of a high cuttings bed

4.3.3 Basic action planning

Here, we discuss the utilization of the hole cleaning planning system to simulate various state-action transition options. Multiple action sequences were simulated for a 50-minute (10 decision epochs) circulation interval starting from the state of well at the end of the drilling operation, s_{TD} (represented by equation (46)). The purpose of these simulations was to understand and quantify the effects of different action sequences on the hole condition, and in identifying a viable course of action. A viable action sequence would result in an improved wellbore condition, without compromising wellbore stability **Table 7** details some of the simulated action sequences, where each action is structured in the form of equation (34).

Table 7 Simulated action sequences.

Sequence #	Action Sequence (10 actions)
1	$\begin{Bmatrix}1000\\0\\83\\9.1\\21\\21\end{Bmatrix},\begin{Bmatrix}1000\\0\\83\\9.1\\21\\21\end{Bmatrix},\begin{Bmatrix}1000\\0\\100\\9.1\\21\\21\end{Bmatrix},\begin{Bmatrix}1000\\0\\100\\9.1\\21\\21\end{Bmatrix},\begin{Bmatrix}1000\\0\\117\\9.1\\21\\21\end{Bmatrix},\begin{Bmatrix}1000\\0\\117\\9.1\\21\\21\end{Bmatrix},\begin{Bmatrix}1000\\0\\133\\9.1\\21\\21\end{Bmatrix},\begin{Bmatrix}1000\\0\\133\\9.1\\21\\21\end{Bmatrix},\begin{Bmatrix}1000\\0\\150\\9.1\\21\\21\end{Bmatrix},\begin{Bmatrix}1000\\0\\150\\9.1\\21\\21\end{Bmatrix}$
2	$\begin{Bmatrix}833\\0\\83\\9.4\\21\\21\end{Bmatrix},\begin{Bmatrix}833\\0\\83\\9.4\\21\\21\end{Bmatrix},\begin{Bmatrix}1000\\0\\83\\9.4\\21\\21\end{Bmatrix},\begin{Bmatrix}1000\\0\\83\\9.4\\21\\21\end{Bmatrix},\begin{Bmatrix}1167\\0\\83\\9.4\\21\\21\end{Bmatrix},\begin{Bmatrix}1167\\0\\83\\9.4\\21\\21\end{Bmatrix},\begin{Bmatrix}1334\\0\\83\\9.4\\21\\21\end{Bmatrix},\begin{Bmatrix}1334\\0\\83\\9.4\\21\\21\end{Bmatrix},\begin{Bmatrix}1500\\0\\83\\9.4\\21\\21\end{Bmatrix},\begin{Bmatrix}1500\\0\\83\\9.4\\21\\21\end{Bmatrix}$
3	$\begin{Bmatrix}833\\0\\83\\8.8\\21\\21\end{Bmatrix},\begin{Bmatrix}833\\0\\83\\8.8\\21\\21\end{Bmatrix},\begin{Bmatrix}1000\\0\\100\\8.8\\21\\21\end{Bmatrix},\begin{Bmatrix}1000\\0\\100\\8.8\\21\\21\end{Bmatrix},\begin{Bmatrix}1167\\0\\117\\8.8\\21\\21\end{Bmatrix},\begin{Bmatrix}1167\\0\\117\\8.8\\21\\21\end{Bmatrix},\begin{Bmatrix}1334\\0\\133\\8.8\\21\\21\end{Bmatrix},\begin{Bmatrix}1334\\0\\133\\8.8\\21\\21\end{Bmatrix},\begin{Bmatrix}1500\\0\\150\\8.8\\21\\21\end{Bmatrix},\begin{Bmatrix}1500\\0\\150\\8.8\\21\\21\end{Bmatrix}$
4	$\begin{Bmatrix}833\\0\\83\\8.8\\21\\21\end{Bmatrix},\begin{Bmatrix}833\\0\\83\\8.8\\21\\21\end{Bmatrix},\begin{Bmatrix}1000\\0\\83\\8.8\\21\\21\end{Bmatrix},\begin{Bmatrix}1167\\0\\83\\8.8\\21\\21\end{Bmatrix},\begin{Bmatrix}1334\\0\\83\\8.8\\21\\21\end{Bmatrix},\begin{Bmatrix}1500\\0\\83\\8.8\\21\\21\end{Bmatrix},\begin{Bmatrix}1500\\0\\100\\8.8\\21\\21\end{Bmatrix},\begin{Bmatrix}1500\\0\\117\\8.8\\21\\21\end{Bmatrix},\begin{Bmatrix}1500\\0\\134\\8.8\\21\\21\end{Bmatrix},\begin{Bmatrix}1500\\0\\150\\8.8\\21\\21\end{Bmatrix}$
5	$\begin{Bmatrix}833\\0\\83\\8.8\\28\\14\end{Bmatrix},\begin{Bmatrix}833\\0\\83\\8.8\\28\\14\end{Bmatrix},\begin{Bmatrix}1000\\0\\83\\8.8\\28\\14\end{Bmatrix},\begin{Bmatrix}1167\\0\\83\\8.8\\28\\14\end{Bmatrix},\begin{Bmatrix}1334\\0\\83\\8.8\\28\\14\end{Bmatrix},\begin{Bmatrix}1500\\0\\83\\8.8\\28\\14\end{Bmatrix},\begin{Bmatrix}1500\\0\\100\\8.8\\28\\14\end{Bmatrix},\begin{Bmatrix}1500\\0\\117\\8.8\\28\\14\end{Bmatrix},\begin{Bmatrix}1500\\0\\134\\8.8\\28\\14\end{Bmatrix},\begin{Bmatrix}1500\\0\\150\\8.8\\28\\14\end{Bmatrix}$
6	$\begin{Bmatrix}833\\0\\83\\8.8\\21\\14\end{Bmatrix},\begin{Bmatrix}1000\\0\\100\\8.8\\21\\14\end{Bmatrix},\begin{Bmatrix}1167\\0\\117\\8.8\\21\\14\end{Bmatrix},\begin{Bmatrix}1334\\0\\134\\8.8\\21\\14\end{Bmatrix},\begin{Bmatrix}1500\\0\\150\\8.8\\21\\14\end{Bmatrix},\begin{Bmatrix}1500\\0\\150\\8.8\\21\\14\end{Bmatrix},\begin{Bmatrix}1500\\0\\150\\8.8\\21\\14\end{Bmatrix},\begin{Bmatrix}1500\\0\\150\\8.8\\21\\14\end{Bmatrix},\begin{Bmatrix}1500\\0\\150\\8.8\\21\\14\end{Bmatrix},\begin{Bmatrix}1500\\0\\150\\8.8\\21\\14\end{Bmatrix}$

Changing the mud properties (density and rheology) is a time-consuming process; therefore, it is highly impractical to change them in the middle of the circulation cycle, they are changed at the beginning of the action sequences. For the first four action sequences, PV value is increased to 21 cP, while the YP value is reduced to 21 lbf/100 ft^2. For the fifth action sequence, the PV and YP are changed to 28 cP and 14 lbf/100 ft^2, respectively. Finally, for the sixth sequence, PV and YP values are adjusted to 21 cP and 14 lbf/100 ft^2, respectively. For the first action sequence, the mud density is unaltered (at 9.1 ppg); for the second sequence, the density is increased to 9.4 ppg. For the remaining four action sequences, the mud density is reduced to 8.8 ppg.

Implementing action sequence number one would have resulted in a slightly better hole condition than for the actual hole after circulation, as shown in **Figure 39**. Note that drillstring RPM was the only parameter that was changed (from 83 to 150 RPM) in this case. The reward obtained by the system would have stabilized at around 0.76, compared with 0.68 after the circulation cycle. Also, the normalized state reward would have been 0.67, as compared to 0.59 after the circulation cycle (which can be seen in **Figure 36**).

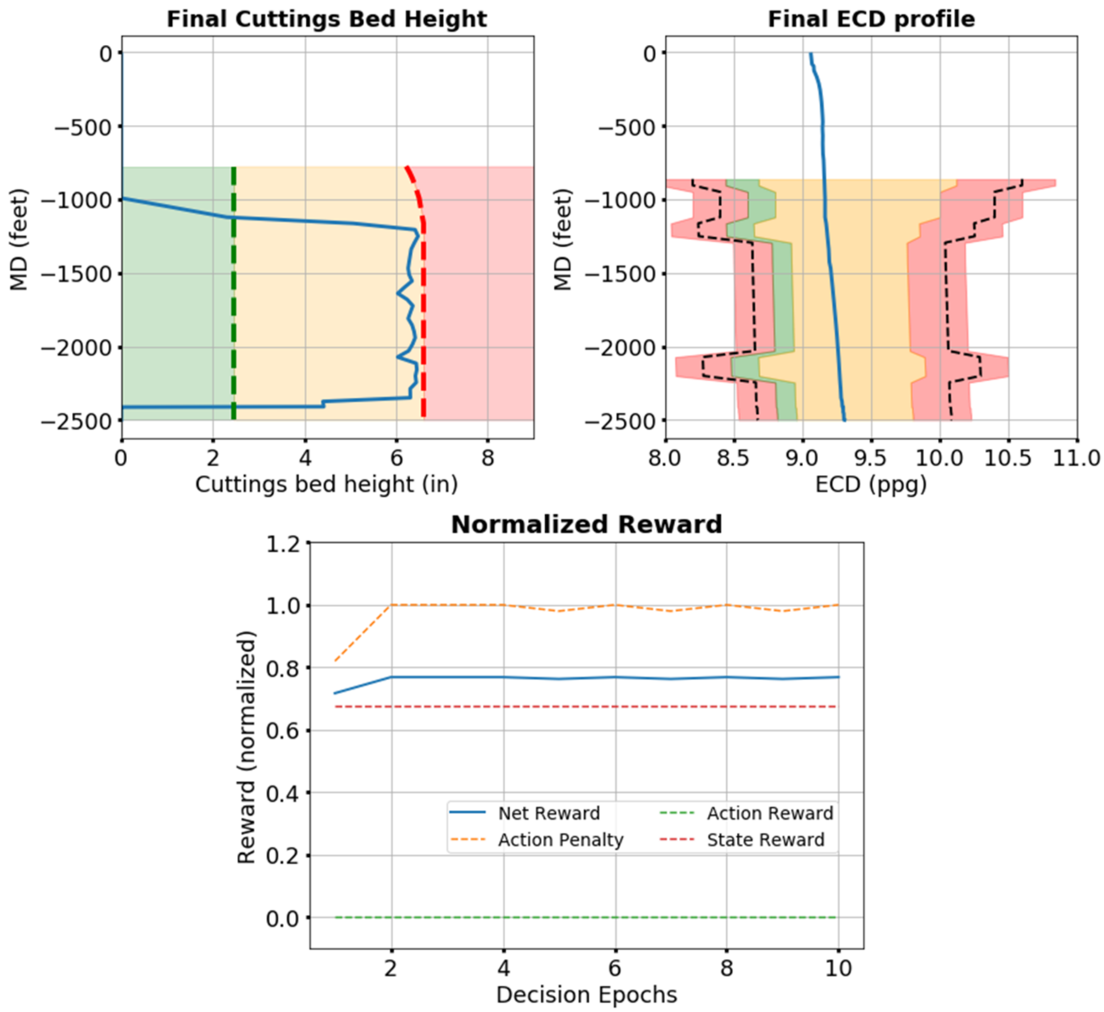

Figure 39 Predicted final system state and rewards after implementing action sequence one.

Action sequence two would have resulted in an even lower bed height; however, the predicted ECD value at greater depths nears the upper instability region, as shown in **Figure 40**. In this case, only the flowrate parameter is changed (from 833 to 1500 GPM) during the operation. The expected net reward for this case would have approached 0.77, and the state reward would have stabilized around 0.69.

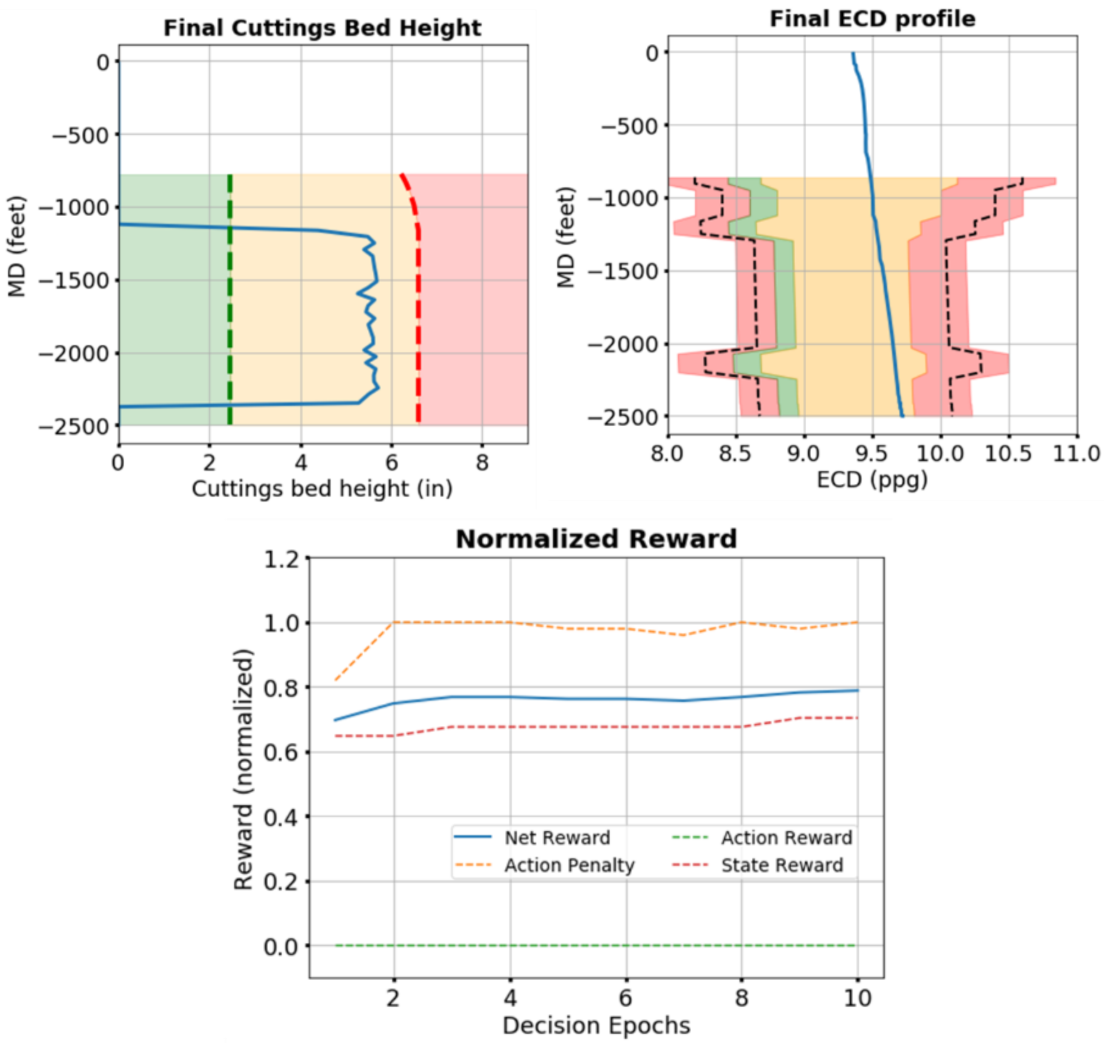

Figure 40 Predicted final system state and rewards after implementing action sequence two.

Figure 41 shows the predicted state after simulating action sequence number three. There would have been a significant reduction in the bed height (to approximately 4.5-inch), and the ECD value would be very close to the desired region. Both flowrate and drillstring RPM are changed during the operation; the flowrate varies from 833 to 1500 GPM, and the drillstring RPM from 83 to 150. The net and the state reward for this case would have been around 0.79 and 0.70, respectively.

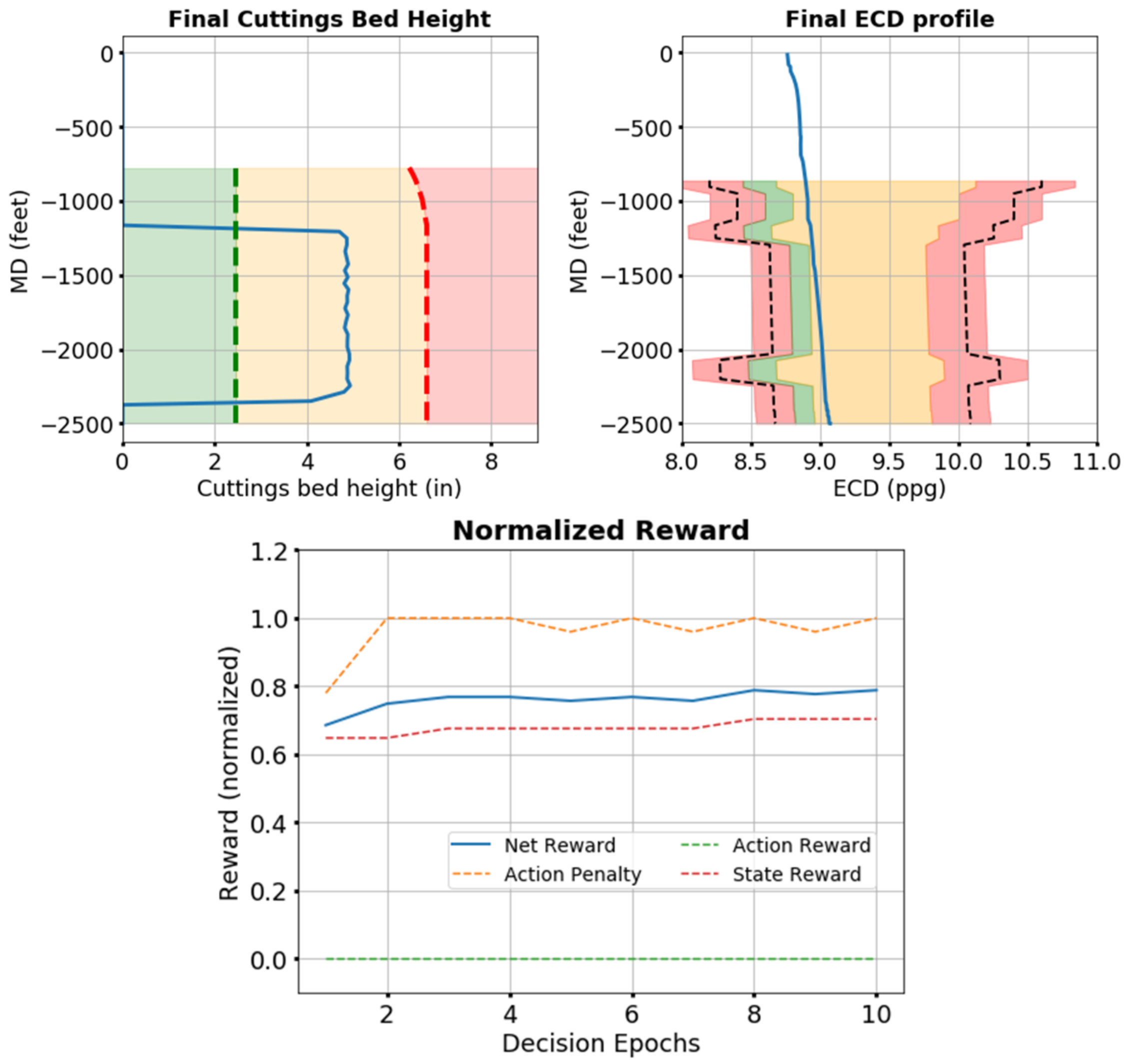

Figure 41 Predicted final system state and rewards after implementing action sequence three.

Figure 42 shows the final state of the system after simulating action sequence four. The expected net and the state reward for this case would also have been around 0.79 and 0.70, respectively. Like action sequence three, both the flowrate and the drillstring RPM are increased during the operation. The primary difference between the two sequences is the order in which the changes are suggested.

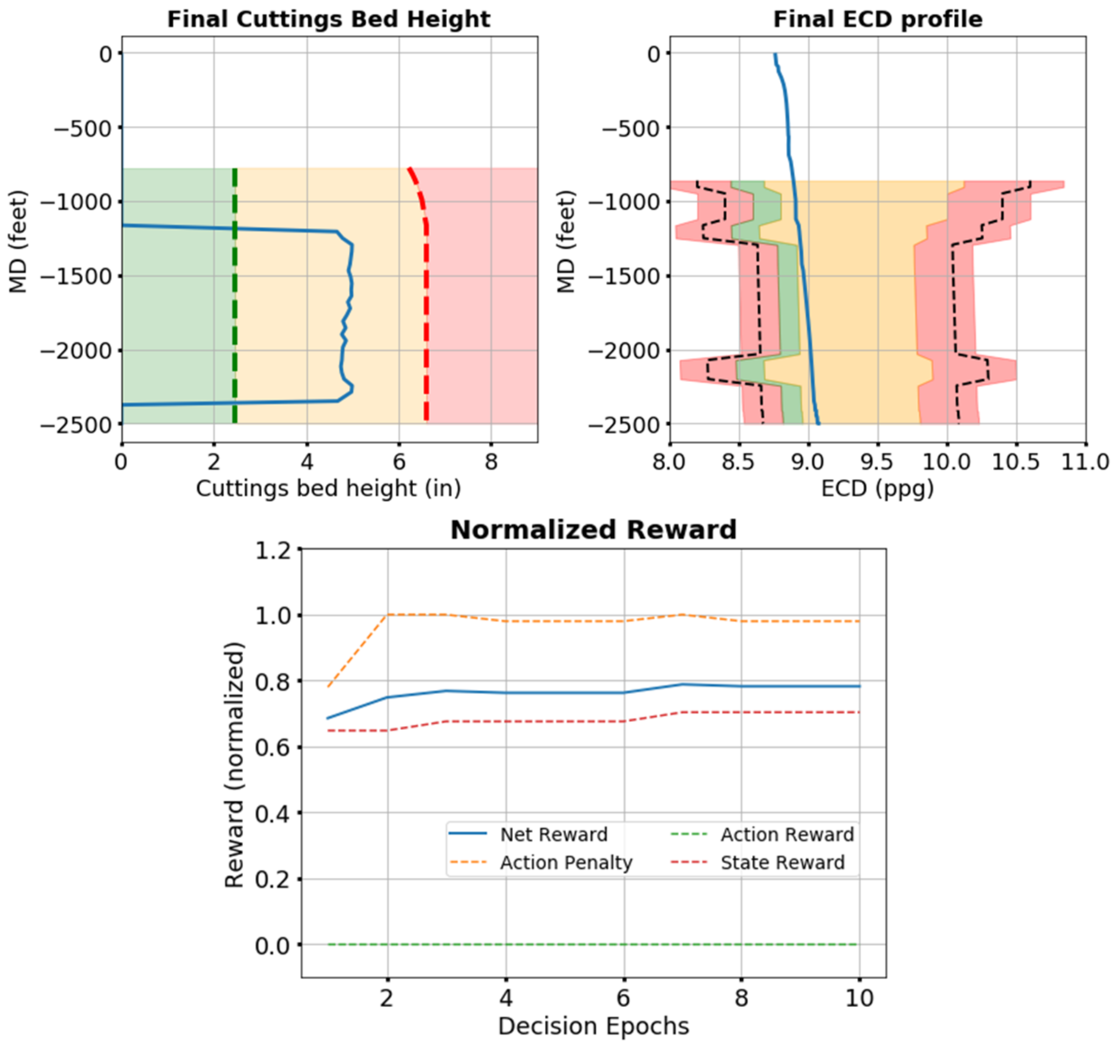

Figure 42 Predicted final system state and rewards after implementing action sequence four.

The output of the execution of action sequence five is depicted in **Figure 43**. This sequence would result in a substantially reduced bed height (under 3.5-inch) and an ECD value very close to the desired region. The net and the state reward values for this case are 0.82 and 0.76, respectively. In this case, both the flowrate and the RPM are increased from 833 to 1500 GPM and 83 to 150 RPM, respectively.

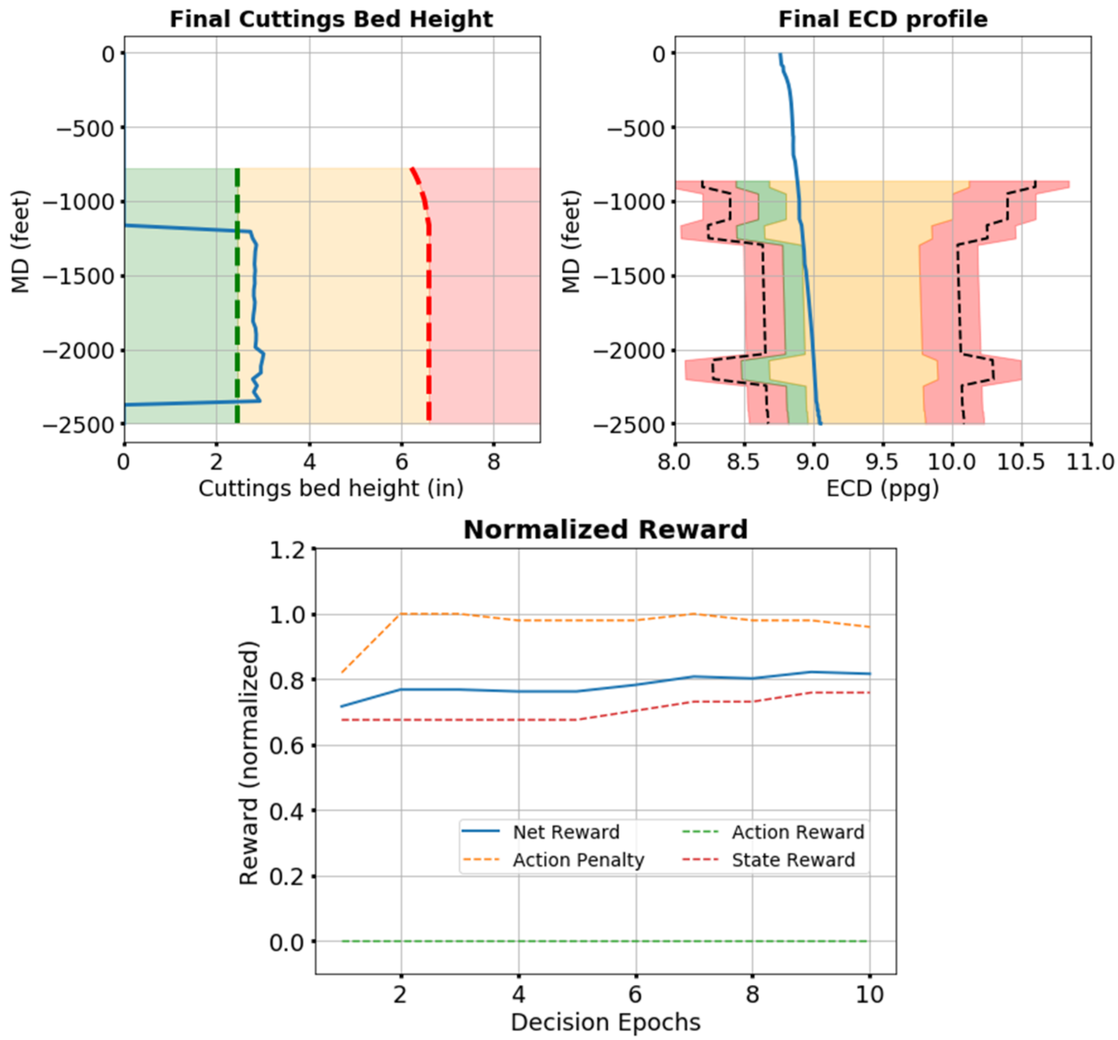

Figure 43 Predicted final system state and rewards after implementing action sequence five.

Figure 44 shows the expected output of implementing action sequence six. This sequence would also result in a substantially reduced bed height (under 2.5-inch) and an ECD value very close to the desired region. The expected net and state rewards would be 0.86 and 0.81, respectively, highest among all previous simulated trajectories. In this case, both the flowrate and the RPM are increased from 833 to 1500 GPM and 83 to 150 RPM, respectively.

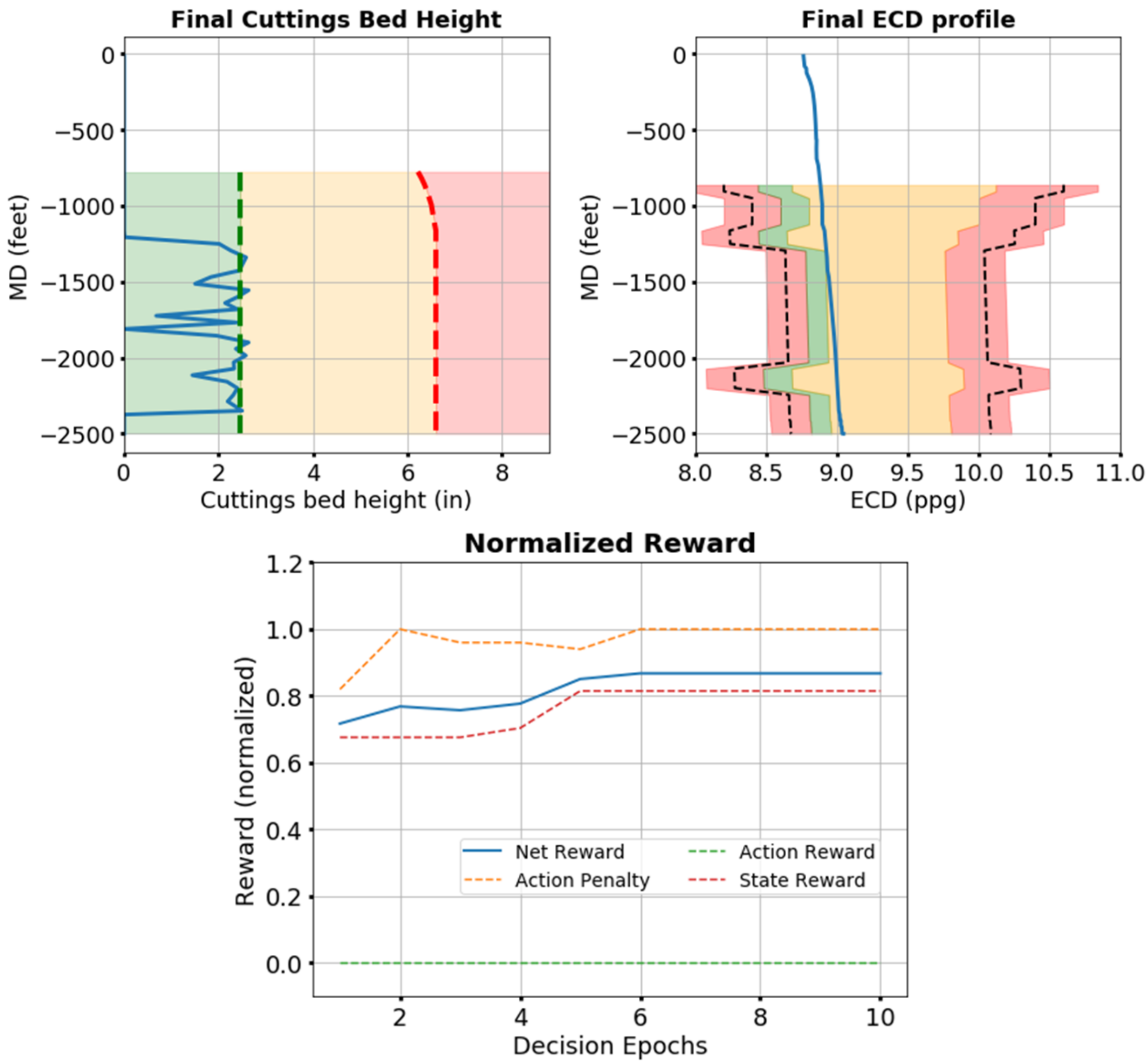

Figure 44 Predicted final system state and rewards after implementing action sequence six.

This example shown on field data, clearly illustrates the potential for such a decision-making approach. Explicitly classifying the hole condition (state) and quantifying state -action transitions allows evaluation and comparison of the different action sequences, which is a vital component in building an intelligent hole cleaning advisory system.

Table 8 summarizes the net and the state rewards associated with the different action sequences. Here, action sequence number 6 performs the best (as quantified by the highest final state reward) and has the highest net reward (which depends on both the final state and the state-action transitions).

Table 8 Summary of the rewards associated with the different action sequences.

Action Sequence #	Net Reward	Final State Reward
0 (Original)	0.68	0.59
1	0.76	0.68
2	0.77	0.69
3	0.79	0.70
4	0.79	0.70
5	0.82	0.76
6	0.86	0.81

4.4 SUMMARY

This chapter presents a novel method of setting up well construction operations as long-term finite-horizon sequential decision-making systems. This is the first time a well construction operation has been structured as an MDP with carefully shaped rewards and an integrated multi-model digital twin, and subsequently utilized for evaluating action sequences. To summarize, this chapter:

- Discusses the requirements and the steps in setting up such systems (formulating an MDP, defining the goal state, efficient reward shaping, and digitally twinning the underlying process) by detailing the development of a hole cleaning decision-making system.
- Discusses the importance of reward shaping for well construction operations to ensure frequent and suitable feedback, thereby facilitating effective policy design. It also demonstrates the use of a non-sparse normalized reward function designed for hole cleaning system for performance tracking and simple action planning.

- Demonstrates the use of digital twins for simulating various action sequences to track the state evolution and reward progression, thereby allowing ranking of the different sequences based on their long-term returns.

Furthermore, more directed search and planning methods such as simulation-based search can be deployed on these systems to enhance system performance considerably. The development and applications of such intelligent decision-making systems are discussed in the next chapter.

Chapter 5: Developing Intelligent Decision-Making and Action Planning Systems

This chapter builds on the Markov Decision Process (MDP) system formulation presented in the previous chapter. The development of intelligent systems for well construction operations that can utilize the underlying digital twinning framework and the reward structure of the MDP setup to simulate and self-learn by strategically generating action sequences is detailed here. The Monte Carlo tree search (MCTS), a simulation-based search technique, is used for action planning. MCTS is further enhanced by incorporating domain-specific heuristics. An action planning system to monitor and improve hole cleaning performance is then developed and subsequently tested on oil well construction data. The heuristic design for policy enhancement considers factors such as safety versus performance trade-offs, distance to the goal state, and feasibility of specific actions from specific states. The action sequence recommended by the system, when implemented, would have resulted in significant performance improvement over the original decision maker's actions, as is quantified by the long-term reward and the final system state.

5.1 Setting up Decision-Engines for Well Construction Operations

Well construction processes are non-holonomic since the wellbore condition at any time (state) is a function of the well's operational past, i.e., all previous wellbore conditions (past states) and previous operations (actions)(Cayeux et al., 2020). The states themselves, depending on the process, can be represented by combinations of parameters such as equivalent circulation density (ECD), cuttings bed height, cuttings concentration in the flow, friction factor, and drilling dysfunction indicators. To adequately represent a process and distinguish different states, each of these parameters can take on many different values. These unique combinations of values for the many state parameters can result in a vast state-space. Similarly, various combinations of values for the many action control variables result in a vast action-space. Some action variables for drilling operations include drillstring rotation speed (RPM), weight on bit (WOB), flowrate, tripping speeds, mud properties (density and rheology), etc. (Robert F. Mitchell & Miska, 2011). Furthermore, the online or near real-time planning requirements impose constraints on computation time. Decision-time algorithms that can plan in limited time by considering the search-space in the vicinity of the current state are therefore needed to address these requirements. SBS algorithms, such as flat Monte Carlo (MC) and Monte Carlo tree search (MCTS), have been successfully used for planning in systems with large state- and action-space (e.g., game AI engines for chess and Go, as discussed). The game AI engines utilize the MCTS in conjunction with deep neural networks (for policy and value evaluations) to identify, shortlist and sequentially simulate legal actions from a given position (state) for both players. Multiple episodes of such self-play are used to improve the policy incrementally and finally select the most promising line of play (an optimal action sequence). Likewise, the utilization of such SBS techniques for action planning during the various well construction operations can result in improved efficiency and operational performance.

5.1.1 Monte Carlo tree search

The MCTS is an SBS algorithm that combines MC search with an incremental tree structure. Successive MC simulations (by using a forward model of the process) are utilized for iteratively expanding the search tree and evaluating the various nodes in the tree structure. A node represents a state and contains information about its parent node, possible next actions, the number of current implementations of each action, and the average value associated with each action implementation thus far. Instead of building the entire tree, a few promising lines of play are developed further, resulting in asymmetric tree growth. The selective growth of the search tree is brought about by using two distinct action selection policies: the tree policy and the rollout policy (James et al., 2017; Vodopivec et al., 2017).

Tree policies can be either greedy (i.e., focusing on exploiting what is already known), or try to balance exploring new or potentially promising paths of the search space with greedy exploitation. This balance is commonly referred to as the exploration-exploitation trade-off. One such policy can be devised by treating every state within the tree as a multi-armed bandit (MAB) problem where the Upper confidence bound (UCB1) algorithm is utilized for action selection within the tree structure (Browne et al., 2012). The resulting algorithm is referred to as Upper confidence bound for trees (UCT). The UCT guarantees convergence to an optimal policy (given enough time) since the exploration factor (C_{exp}) not only ensures exploration of unvisited parts of the search space, but the exploration term ($\sqrt{\frac{2 \cdot \ln N(s)}{N(s,a)}}$) also gets less exploratory with increasing number of visits (Kocsis et al., 2006). Equation (48), represents the basic UCT policy, where $N(s)$ is the total number of visits to the state s, $N(s,a)$ represents the number of times action a has been taken from state s. $Q(s,a)$ is the exploitation term representing the average value associated with implementing action a from state s. $Q_{\mathrm{UCT}}(s,a)$ is the upper confidence bound or the urgency term, and the next action within the search tree is selected based on maximizing this term over the action space A_s from the state s (equation (49)). The rollout policy, by default, is a uniform-random policy.

$$Q_{\mathrm{UCT}}(s,a) = Q(s,a) + C_{exp} \cdot \sqrt{\frac{2 \cdot \ln N(s)}{N(s,a)}} \tag{48}$$

$$a_{n+1} = max_{a_i \in A_s}(Q_{UCT}(s, a_i)) \quad (49)$$

Primarily, MC control (a model-free RL technique) is applied to simulated episodes of experiences (model-based RL) from a root node, to grow the search tree iteratively and improve the action plan by backpropagating feedback. A single MCTS iteration consists of the following four phases, as detailed in **Figure 45** (Browne et al., 2012):

- **Selection** from nodes already in the search tree using the tree policy
- **Expansion** of the tree at the leaf node by adding one (or more) node(s)
- **Simulation** or rollout of actions, using the rollout policy, until the terminal condition is met (either reaching a terminal state or the end of the planning time horizon, T)
- **Backpropagation** or backing the rewards up the expanded tree to update the values of different state-action pairs ($Q(s, a)$) encountered during the episode

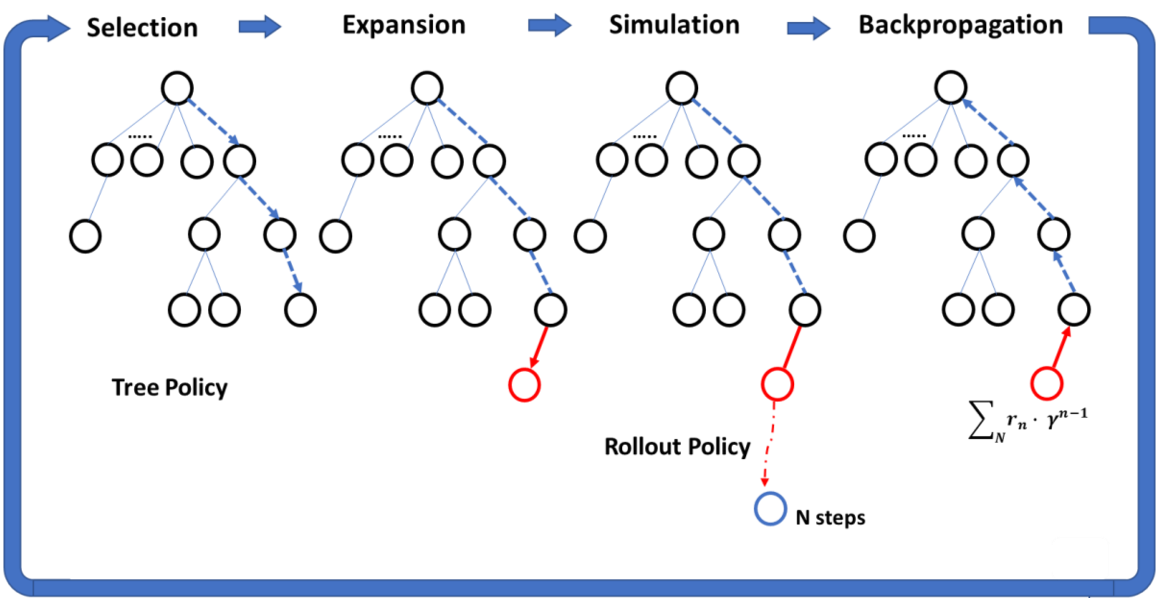

Figure 45 Monte Carlo tree search algorithm (modified from Browne et al., 2012).

As the number of simulations increases over time, the tree expands, and any inherent bias is removed. Every MCTS episode commences from the root node (from which an action plan or action sequence needs to be determined), and traverses the tree based on the most recently acquired knowledge (which is incorporated in the Q values). Thus, MCTS is fundamentally a generalized policy iteration (GPI) algorithm, where the policy or action plan is iteratively evaluated and improved, as shown in **Figure 46**. (Sutton & Barto, 2018; Vodopivec, 2018). Even with naïve or vanilla policies (such as the standard UCT and uniform random), the MCTS works well and starts to move the results towards optimality.

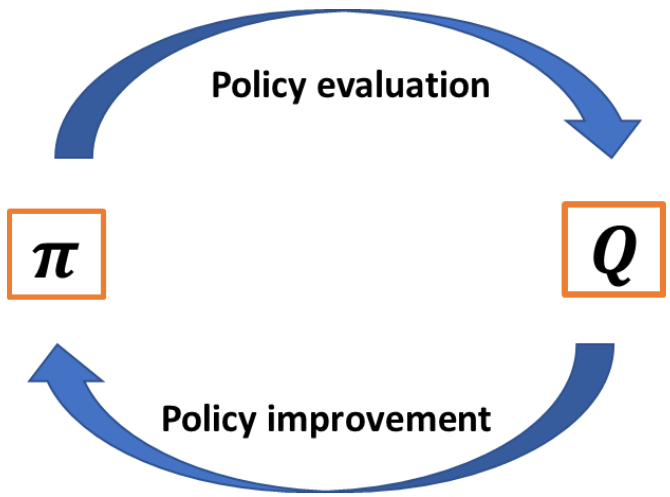

Figure 46 Generalized policy iteration (Sutton and Barto, 2018).

Although the vanilla MCTS blends the generality of random sampling with the exactness of tree search, its convergence rate can be relatively low. Therefore, in practice, the two MCTS policies have been enhanced by incorporating prior-knowledge or handcrafted strategies. This has resulted in different methods, such as progressive widening, progressive bias, using prior-knowledge, and Rapid action value estimation (RAVE) (Browne et al., 2012; Chaslot et al., 2008; Gelly and Silver, 2011). All these strategies require evaluation of some heuristic function, which can either be learned (using deep neural networks) or designed using domain-knowledge or be a combination of both. The heuristic function devised for most other applications depends on factors such as the proximity of the state to the goal state, values associated with patterns, previous action values, how dangerous or safe is the state as compared to the adversary's positions, etc.(Chaslot et al., 2008; Efroni et al., 2019; Silver et al., 2018).

5.1.2 Structuring well construction operations as sequential decision-making systems

The goal of well construction is to drill and complete a well safely, quickly, efficiently, and economically in line with a drilling program. As previously stated, accomplishing these objectives requires efficient planning and informed decision-making at each step of every well construction process. Additionally, due to the non-holonomic property of well construction operations, any action implemented at the current time will not only affect the immediate system state but also influence the long-term evolution of the system. This necessitates the development of intelligent decision-making systems, the foundation of which is a Markov Decision Process (MDP) framework. An MDP is composed of the tuple $(\{S, A, P, R\})$ and a policy (π) that address the following elements of finite-horizon long-term sequential decision-making (LaValle, 2006; Puterman, 1994):

- Identification of appropriate parameters to quantify the **state** (s_t) of the system, and defining the desired or **goal states** (s_{goal}) based on the operation's objective;
- Identification of relevant control variables or **actions** (a_t) that can affect the system state;
- Building the **state-space** (S) and the **action-space** (A) such that $s_t \in S$ and $a_t \in A$ for all s_t and a_t;

- Incorporating problem-specific **heuristics** ($\pi_{heuristic}$) to identify legitimate and promising actions from every state;
- Building models (**digital twins**) of the underlying processes to simulate the state transitions ($\boldsymbol{P^{a}_{ss'}}$) brought about by different actions;
- Defining a method to quantify the various state action transitions, for instance, by using **reward functions** (R) to calculate long-term **value functions** (Q);
- Selection of a suitable action-planning technique to formulate a **plan** (π – the suggested sequence of actions for successive decision epochs).

For a process to be Markovian, it must satisfy the Markovian property, i.e., any transition from a given state depends only on the current state and the immediate action. In other words, the current state completely summarizes the system's operational past. As previously discussed, this is true of well construction operations; therefore, the Markovian property assumption is valid. The MCTS algorithm is particularly well-suited for well construction action planning because of its ability to handle vast search-spaces efficiently. The UCT policy assists with asymmetric tree growth along promising paths while balancing exploration and exploitation of the search space. Although MCTS is inherently aheuristic, it still permits the use of domain-knowledge-derived heuristics for speeding up the search. Also, the GPI property of MCTS ensures that over time better plans (action sequences) are found. **Figure 47** shows the proposed structure for well construction decision-making systems.

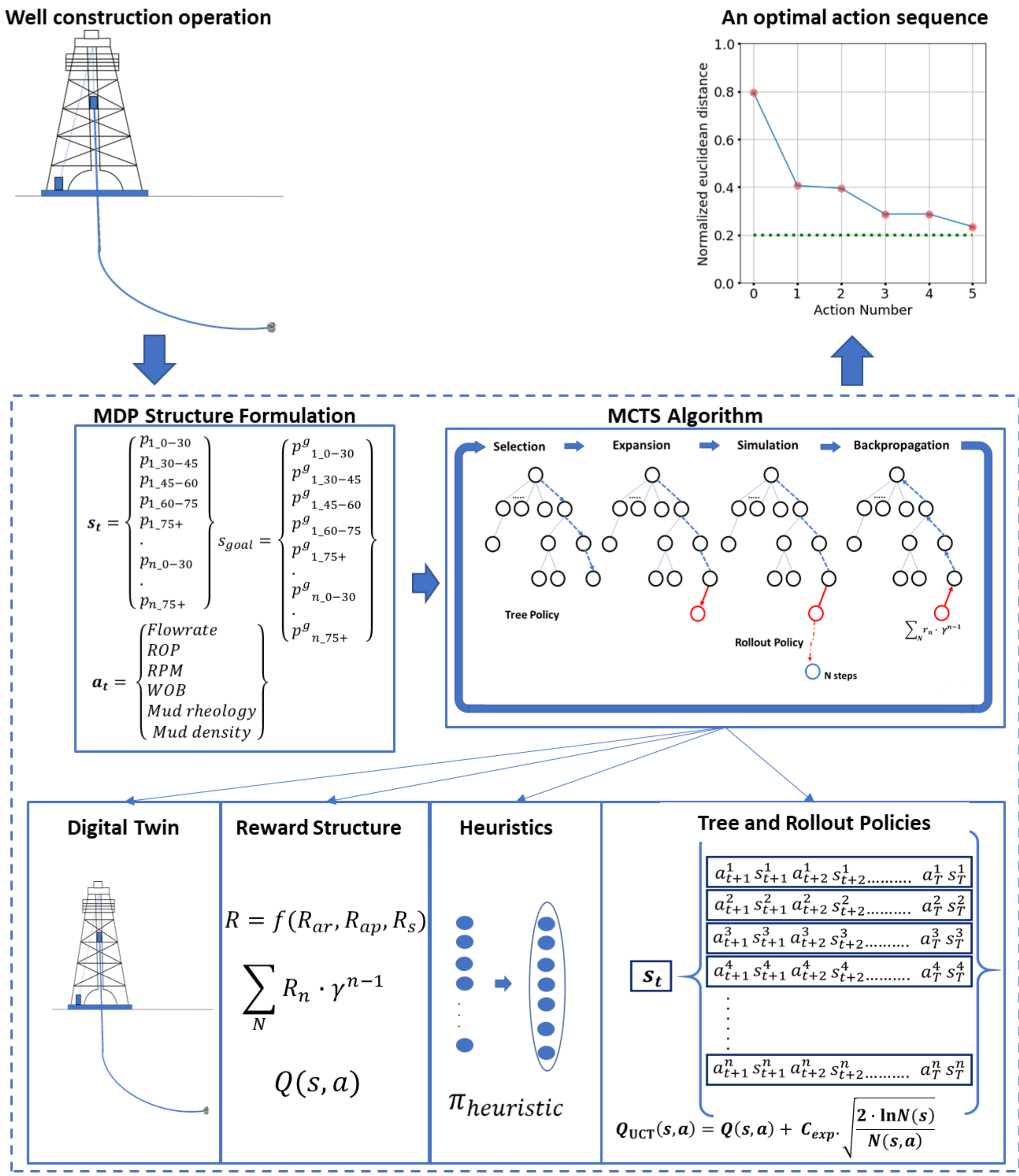

Figure 47 Structure of the proposed decision-engine.

5.2 DESIGN OF A SYSTEM FOR HOLE CLEANING ACTION PLANNING USING THE MCTS

As discussed in the previous chapters, effective and safe hole cleaning requires keeping the cuttings bed height low enough to prevent issues in any stage of well construction operation. Moreover, the equivalent circulation density (ECD) needs to be managed within a drilling margin. To this effect, a step-by-step method for formulating an MDP for the hole cleaning decision-making and planning system is detailed in Section 4.2. To summarize:

- The state of the system, at any decision epoch, is represented by functional values of cuttings bed height and the ECD over the different inclination intervals $\{[0,30),[30,45),[45,60),[60,75),[75+)\}$. The functional values defined for all state components are such that 0 represents the goal state for each.
- Hole cleaning and ECD management are influenced, to varying degrees, by multiple factors, some of which can be actively controlled in real-time in the field. Factors such as drilling mud properties (particularly density and rheology), drilling parameters (such as drillstring RPM and flowrate), and rate of cuttings generation (which is a function of ROP) significantly influence hole cleaning performance, and can be actively controlled in the field (Gul et al., 2020; Nazari et al., 2010). The action set is a combination of discrete values of these control variables.
- A digital twin was built by integrating the available well initializations (data streams such as well plans, well surveys, well geometry information, etc.) with analytical implementations of the hydraulics and cuttings transport models, and a rule-based rig state detection engine.
- A reward function that outputs a normalized feedback (in the $[0,1]$ interval) for every state-action transition was designed by considering the rewards and penalties associated with state and action values and changes in them.

5.2.1 MCTS setup for hole cleaning

Action planning with MCTS requires solving a sub-MDP starting from the current system state (root-node) in a finite amount of time. The hole cleaning digital twin is utilized as the forward-simulation model to simulate the results of different actions on the wellbore condition, and the feedback obtained using the reward function is accumulated and backpropagated. Vanilla MCTS, however, has some limitations:

- The agent is rewarded only when a terminal or a goal state is reached, i.e., sparse rewarding;
- From any state within the tree, all actions in its action-space (A_s) are evaluated by the UCT policy regardless of their practicability for the operation;
- The rollout policy is random uniform, i.e., all actions (irrespective of their feasibility) have an equal probability of being selected.

These limitations result in the requirement to conduct more simulations to expand the search tree to the extent that it can be meaningfully used for trajectory evaluation, thereby slowing down the search. To address these issues this research makes the following changes to the vanilla MCTS:

- Definition of a non-sparse reward function, such that the reward for every state-action transition during the rollout step is utilized for updating all tree nodes' Q values. This is addressed by the reward function shaping strategy, which was discussed in detail in the previous chapter;
- Using a heuristic function to improve the tree policy;
- Using a heuristic function to reduce the randomness in the rollout policy.

5.2.1.1 Heuristic function development

A domain-knowledge based heuristic $\pi_{heuristic}$ is carefully crafted by balancing the following criteria:

- **Safety and performance metric (A_{sp})**, to prevent well control issues (such as kicks and lost circulation events) from occurring, as well as to ensure efficient cuttings bed removal and ROP maximization for optimal drilling performance;
- **Performance metric**, to ensure efficient cuttings bed removal and ROP maximization for optimal drilling performance;
- **Sequential metric (A_{sq})**, to ensure smoother or sequential changes in values of action control variables;
- **Feasibility constraints (A_{fe})**, to suggest realistic changes in values of the action control variables;
- **Proximity metric (A_{px})**, to prioritize actions based on Euclidean distance to the goal state.

Balancing safety and performance are accomplished by incorporating guidelines for well control, hole cleaning, and drilling optimization. **Figure 48** is a simplistic representation of some such rules as a decision-tree. The result is a set of feasible actions A_{sp} satisfying the safety and performance requirements.

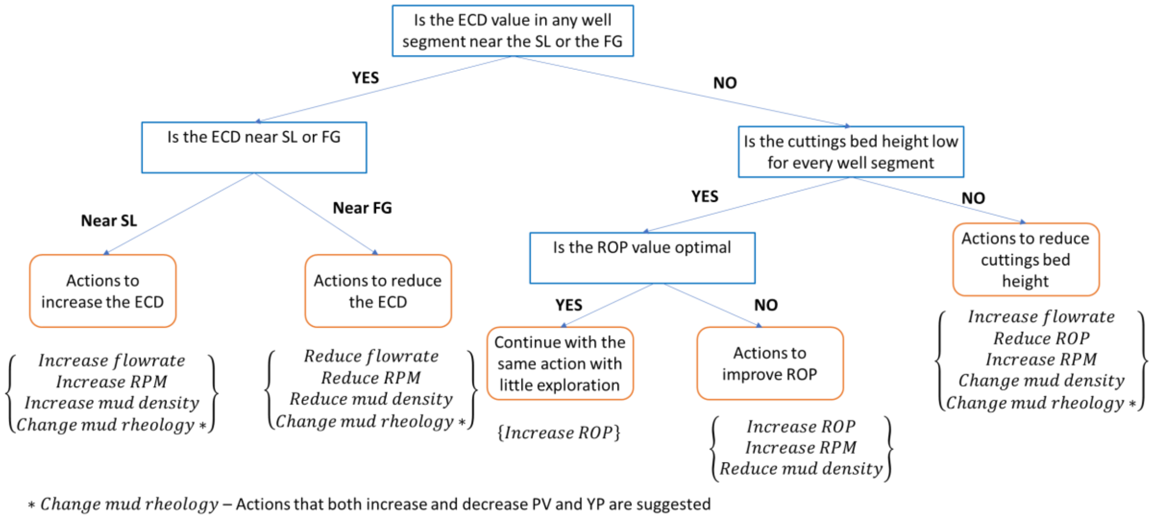

Figure 48 A simplistic representation of an action selection decision-tree for satisfying safety and performance metrics.

Similarly, to satisfy the sequential metric and the feasibility constraints, action sets A_{sq} and A_{fe} are evaluated, respectively. **Figure 49** is a simple representation for estimating A_{sq} for a system with an action set containing three control variables (RPM, flowrate, and mud density). A_{sq} consists of actions in the vicinity of the most recent action. The reasoning behind such selection is to dissuade sudden changes in control variables, thereby constraining the rate of change of control variable values to safe limits. Changing mud properties (both density and rheology) is a time-consuming process; it cannot be performed in near real-time during conventional drilling or circulation operations (note that the effective density can be changed quickly in managed pressure drilling operations, where circulation takes place in a closed system where hydrostatic pressure can be quickly raised using a choke system). However, while planning for the circulation operation, adjusting mud properties is a crucial element of efficient hole cleaning. The purpose of defining A_{fe} is to incorporate such information.

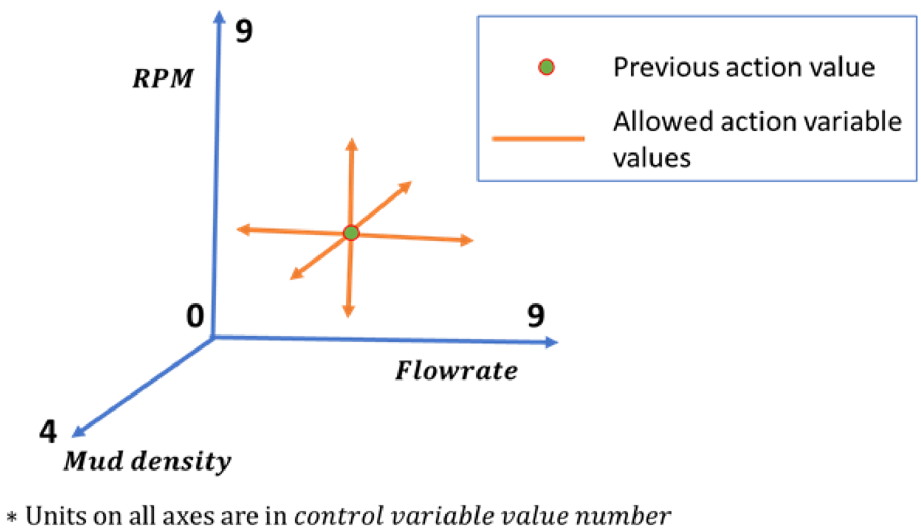

Figure 49 Method for estimating the action set associated with sequential metric.

To calculate the proximity metric, first, the normalized Euclidean distance for the current state (from s_{goal}), $d_{norm-euc}$, is computed using equation (50). s_i is the i^{th} element of the state vector s, and s_{i_max} is the maximum magnitude for the i^{th} state vector component. The $d_{norm-euc}$ is then compared with the radius of a 'greed sphere'. This greed sphere is defined based on a normalized Euclidean distance of 0.5 from the goal state, and it is an indication of whether the states are far away from the goal state.

$$d_{norm-euc} = \frac{\sqrt{\sum_{i=i}^{N} s_i^2}}{\sqrt{\sum_{i=i}^{N} s_{i\_max}^2}} \tag{50}$$

Figure 50 shows an example of this by considering a three-parameter system state (H_i, H_j *and* ECD_i). The near-goal states (s''_{goal}) represent the states for which the magnitudes of all state vector components are either 0 or 1.

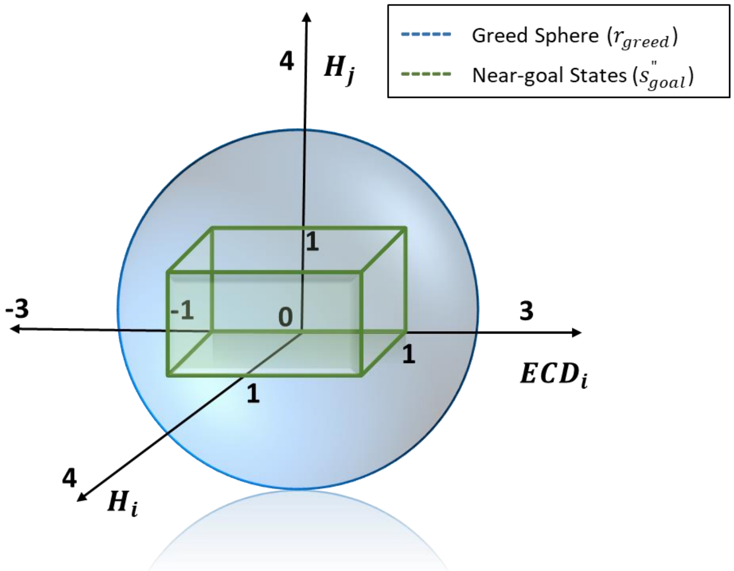

Figure 50 Method for estimating the action set associated with proximity metric.

The action selection strategy is given by equation (51). In case the current state is at or near the goal state, the same action as the most recent action (a_{-1}) is selected. However, if the current state is further out than the greed sphere, more aggressive actions are included in the action set A_{px}. Aggressive actions represent greater magnitude changes in values of action control variables relative to the most recent action.

$$A_{px} = \begin{cases} a_{-1}\,, & \boldsymbol{d_{norm-euc}} \leq s''_{goal} \\ a_{reg}\,, & s''_{goal} < \boldsymbol{d_{norm-euc}} < r_{greed} \\ a_{agg}\,, & \boldsymbol{d_{norm-euc}} \geq r_{greed} \end{cases} \tag{51}$$

Finally, the different action sets are combined, as shown in equation (52), to output heuristic values for any action a in the action space A_s.

$$\pi_{heuristic\_a} = \begin{cases} 1\,, & if\ a \in A_{sp} \cap A_{sq} \cap A_{fe} \cap A_{px} \\ 0\,, & otherwise \end{cases} \tag{52}$$

Thus, $\pi_{heuristic}$ assigns a probability of either 0 or 1 to all the available actions in the action-space for a given state.

5.2.1.2 MCTS structure

For finite-horizon action planning (T decision epochs into the future) in a limited amount of time t_{max}, the system starting in state s_0 proceeds according to the algorithm shown in **Figure 51(a)**. The root node $node_0$ corresponds to the starting state s_0, $node_{leaf}$ is the leaf node reached at the end of the selection phase in a given episode, and $node_{exp}$ is the randomly expanded node from the leaf node. The rollout phase then proceeds to plan until T epochs are reached (with root node as epoch 0), where $node_T$ is the final state (may or may not be the goal state), and G_T is the net discounted return. Equation (53) shows the calculation for G_T, where $\gamma(\leq 1)$ is the discount factor, r_k is the reward associated with the k^{th} state-action transition, and $|exp|$ is the level for $node_{exp}$ in the tree. Finally, the backup function updates the Q value associated with all nodes from the $node_{exp}$ until $node_0$ by averaging this return value.

$$G_T = \sum_{k=|exp|}^{T} r_k . \gamma^{k-1} \tag{53}$$

```
while t_curr < t_max , do
    node_leaf ← Selection(node_0),
    node_exp ← Expansion(node_leaf),
    node_T, G_T ← Rollout(node_exp),
  Backup(node_exp, G_T)
return (actionSequence)
```

```
actionSequence
i = 0 , n = node_0
while i ≤ T , do
      actionSequence.append(bestChild(n.a))
   n ← bestChild(n)
   i ← i + 1
```

Figure 51 (a) MCTS algorithm (b) Action sequence selection method.

As previously discussed, MCTS builds an asymmetric search tree in the allocated time (t_{max}), after which an action sequence is given as output, based on the method shown in **Figure 51(b)**. The ‘best child’ from any node is its child-node corresponding to the action with the highest average Q value. Each node in the search tree contains the following information and can be represented by equation (54):

- The current system state (s_t)
- The most recent action (a_{t-1})
- The action space of the node (A_{s_t})
- The total number of visits to the node so far (N_{s_t})
- All implemented actions and the resulting transitions, i.e., all child nodes ($\{a_i : node_i\}$)
- The total value associated with all iterations passing through the current state ($\sum_{children\ i} Q(s_t, a_i)$)
- The parent node ($node_{t-1}$)

$$node_t = \begin{pmatrix} s_t \\ a_{t-1} \\ A_{s_t} \\ N_{s_t} \\ Children\text{: } \{a_i : node_i\} \\ \sum_{children\ i} Q(s_t, a_i) \\ node_{t-1} \end{pmatrix} \tag{54}$$

The average value ($Q(s_t, a_t)$) associated with a state-action transition is calculated as the mean state-action value over all of its subsequent state's (s_{t+1}) children (a_j).

$$Q(s_t, a_t) = \frac{\sum_{children\ j} Q\left(s_{t+1}, a_j\right)}{N(s_t, a_t)} \tag{55}$$

The tree policy is modified by including the $\pi_{heuristic}$ in the exploration term of the UCT formula (Moerland et al., 2018), as shown by equation (56).

$$\pi_{tree} = argmax_{a \in A_s} \left[Q(s_t, a) + \pi_{heuristic\_a} . C_{exp} . \sqrt{\frac{2 \cdot \ln N_{s_t}}{N_{(s_t, a)}}} \right] \tag{56}$$

Since the value of the exploitation term ($Q(s_t, a)$) is in the [0,1] range, C_{exp} is key in determining the number of simulations that would be required to make the values of the exploration ($C_{exp} \cdot \sqrt{\frac{2 \cdot \ln N_{s_t}}{N_{(s_t,a)}}}$) and the exploitation terms comparable. **Figure 52** shows the plots for exploration terms calculated for different C_{exp} values as a function of the number of child node visits, given a total of 100 visits to the parent node(N_{s_t}). For the exploitation-heavy cases with C_{exp} values 0.25 and 0.5, the values of the two terms become comparable almost immediately, i.e., there is minimal exploration. On the other hand, for the exploration-heavy cases with C_{exp} values of 2 and 4, it takes a significant number of simulations to start exploiting its knowledge of the system. For the system developed in this research a C_{exp} value of 1 is thus selected.

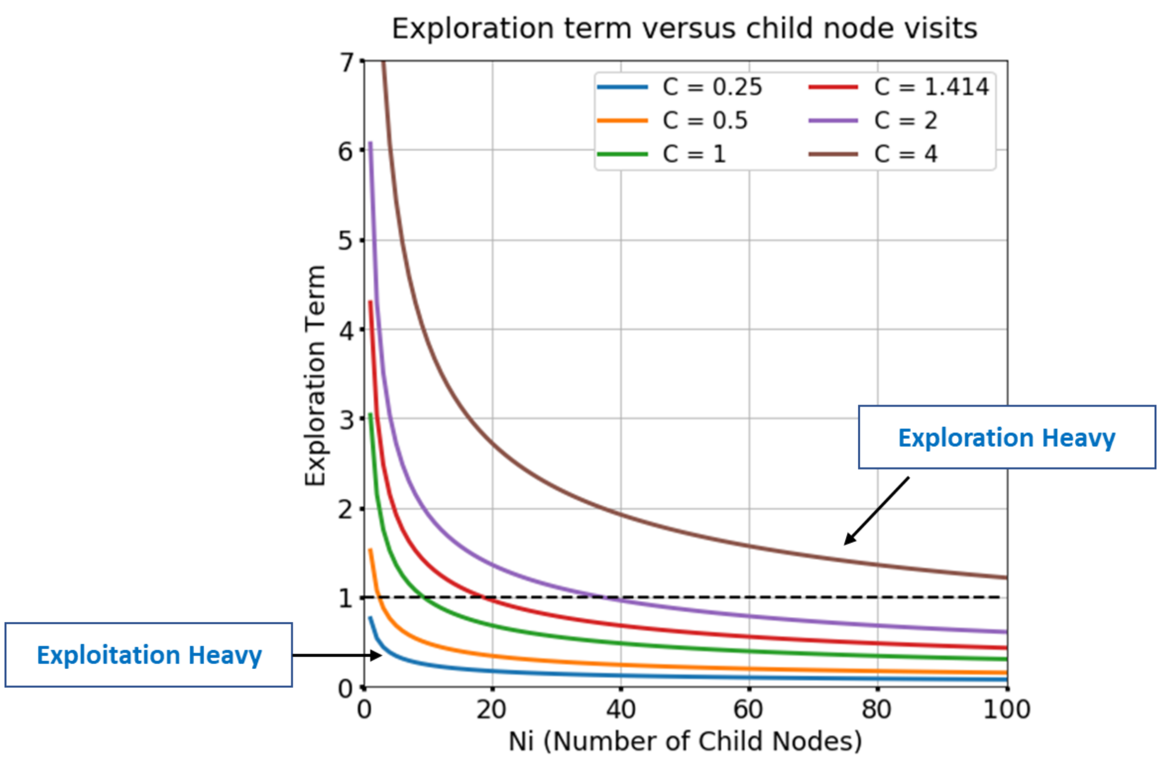

Figure 52 Calculation of exploration terms for different C_{exp} values as a function of the number of child node visits, given a total of 100 visits to the parent node.

During the rollout phase from any node, a uniform random selection policy is followed on a reduced action space (which is constructed based on equation (57)).

$$A_{rollout} = \bigcup_{a \in A_S} \pi_{heuristic\_a}.\, a \tag{57}$$

5.3 Application of the System

The developed action planning system for hole cleaning was evaluated by performing post-mortem analysis on the real-world oil well cases discussed in Section 4.3, that exhibited hole cleaning issues. The analyses were performed by suggesting action sequences from some critical points during well construction. The final states associated with these plans were then compared with the actual well performance. As previously discussed, the dataset included the well's directional survey data, well profile information (casing, BHA and bit details), one-second surface sensor data, and mud check information. A hole cleaning digital twin, as discussed in Chapter 2, was developed by integrating the various models with the relevant data sources.

5.3.1 Well profile and summary of issues

The well had a short vertical section with a shallow kick-off point around 300 feet MD. The inclination angle reached 30 degrees at approximately 750 feet MD, and 75 degrees (horizontal section) around 1250 feet MD. After this, the well remained near horizontal until it reached its total depth (TD) of 2500 feet MD. The well did not report any issues while drilling, however, while pulling out of hole (POOH), and while running casing, some problems were encountered that indicated likely poor hole cleaning. During back-reaming operations while POOH, an increase in torque was logged at multiple depths, and while circulating during this phase, the well unloaded broken up clay particles as well as softball-sized chunks of clay particles at multiple depths. While running in the casing (9.625 in.), some resistance was encountered, and pulldowns had to be used to set the casing in place. Also, during cementing operations while pumping slurry, intermittent losses were observed, the casing string locked up and had to be pulled free. These issues encountered at the different stages of well construction suggested poor hole cleaning. **Figure 53** depicts the optimal (green-shaded zone), the sub-optimal but safe (yellow-shaded zone), and the unsafe (red-shaded zone) regions for both the ECD and the cuttings bed height. A detailed discussion around their derivation was presented in Section 4.3.1.

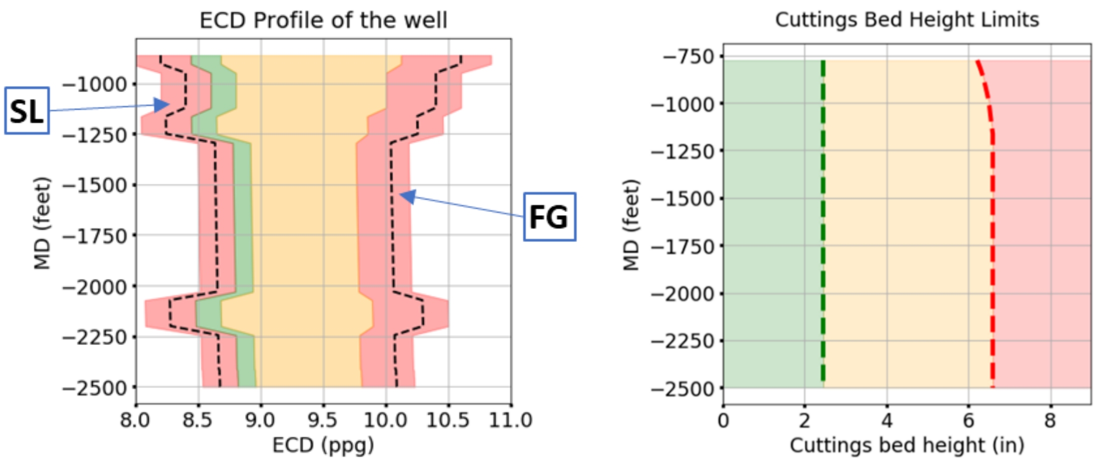

Figure 53 (a) ECD limits for the well considering an uncertainty factor (DF) of ten percent in the SL and FG values (b) Limits for the cuttings bed height for the given well profile(negative sign indicates downward depth into the sub-surface).

5.3.2 Performance tracking and action planning

The system was set up in the MDP framework by using the procedure discussed in Chapter 4. **Table 9** shows the number and ranges of values associated with the different control variables utilized for defining the action-space, and **Table 10** shows the different weights assigned for reward calculations. A detailed discussion around these values was presented in Section 4.3.2.

Table 9 Action-space definition for the hole cleaning action planning system.

Control Variable	**Number of Discrete Values**	**Range of Values**
Flowrate (GPM)	10	[0, 1800]
Drilling ROP (ft/hr.)	10	[0, 900]
Drillstring RPM (rev/min)	10	[0, 180]
Mud Density (ppg)	5	[8.5, 9.7]
Mud Plastic Viscosity (cP)	5	[7, 42]
Mud Yield Point (lb./100ft^2)	5	[7, 42]

Table 10 Weight assignments for the hole cleaning action planning system.

$W_s = [1,1,1,1,1,1,1,1,1]$	
$W_{ap} = [1,1,1,1,1,1]$	
$W_{ar} = [0,1,0,0,0,0]$	
$W_{s\_norm} = 0.50$	
$W_{ap\_norm} = 0.20$	
Drilling	**Circulation**
$W_{ar\_norm} = 0.30$	$W_{ar\_norm} = 0.00$

5.3.2.1 Performance tracking

State transitions were monitored, and associated rewards were calculated to track the performance of the system. The state of the system at the end of the drilling operations (during second BHA run) is represented by equation (46), and can be visualized by **Figure 54**. The mud properties for drilling the last section of the well were: mud density of 9.06 ppg, PV of 11 cP, and YP of 36.5 lbf/100 ft^2.

$$s_{TD} = \begin{Bmatrix} H_{30-45} \\ H_{45-60} \\ H_{60-75} \\ H_{75+} \\ ECD_{0-30} \\ ECD_{30-45} \\ ECD_{45-60} \\ ECD_{60-75} \\ ECD_{75+} \end{Bmatrix} = \begin{Bmatrix} 0 \\ 3 \\ 4 \\ 4 \\ 1 \\ 1 \\ 1 \\ 1 \\ 1 \end{Bmatrix} \quad (58)$$

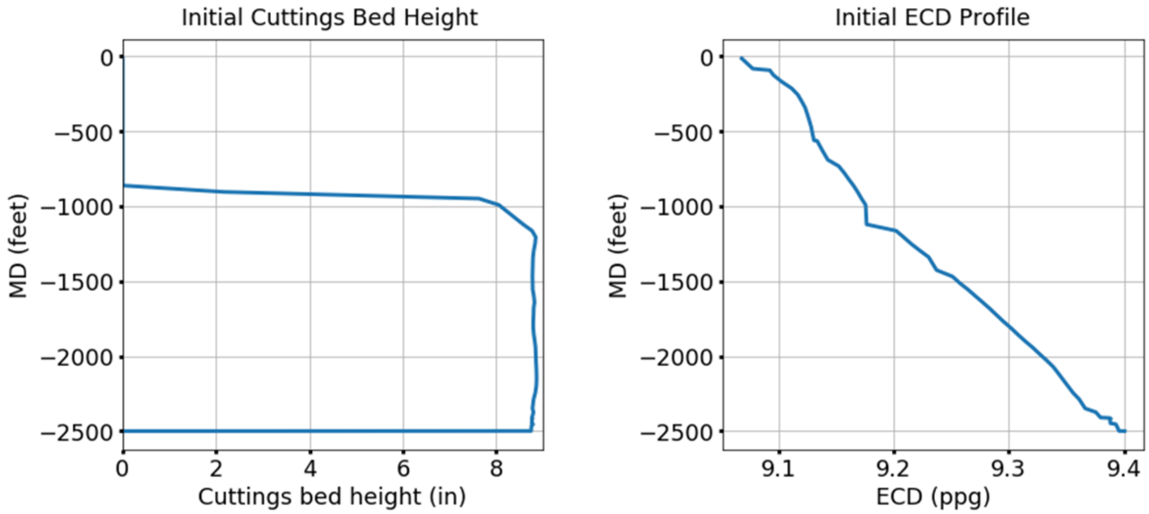

Figure 54 The state of the borehole at the end of the drilling operation during the second BHA run.

The final cuttings bed was around 9-inch, which is significantly higher than the limits specified in **Figure 53(b)**. Therefore, to ensure safe tripping operations without getting stuck, and to prepare the well for casing and cementing operations, these cuttings needed to be removed. A 50-minute circulation cycle was then performed, the resulting state of which is represented by equation (59), and **Figure 55**. The final cuttings bed height was still close to the allowed limit, and therefore non-optimal, explaining the issues encountered during tripping, casing, and cementing.

$$s_{TD\_circ} = \begin{Bmatrix} 0 \\ 2 \\ 3 \\ 3 \\ 1 \\ 1 \\ 1 \\ 1 \\ 1 \end{Bmatrix} \tag{59}$$

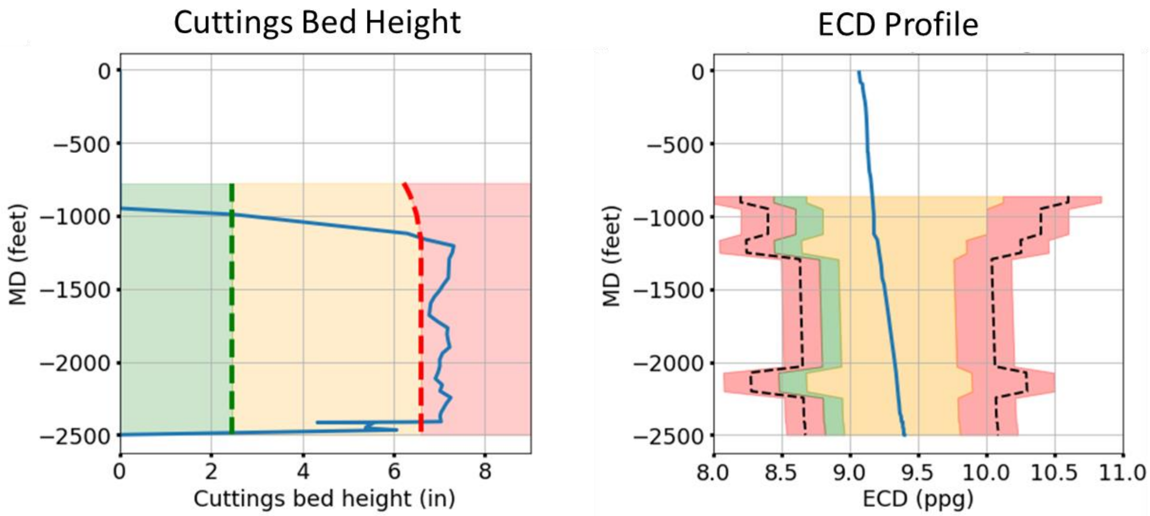

Figure 55 State of the borehole at the end of the circulation cycle (a) The cuttings bed profile (b) The ECD profile.

5.3.2.2 Action planning

The developed decision-making system was then used for planning the circulation cycle. The goal of the system, as previously discussed, is to reduce the cuttings bed height to safe limits while maintaining the ECD within the drilling margin (i.e., bed height and ECD need to be managed to in or around the green-shaded zones defined in **Figure 53**).

The following metrics are used to evaluate the different action sequences:

- The final system state;

- The average return value of the action sequence (V), which is the mean of total accumulated reward over the given trajectory that results from following the action sequence;

$$V = \frac{\sum_{t=1}^{T} R_t}{T} \tag{60}$$

- Progression of the normalized Euclidean distance of the system's states with actions.

For the well's actual circulation operation, the final state represented by equation (59) was considerably far from the goal state. The V value for this action sequence was evaluated to be 0.74. The progression of the normalized Euclidean distance of the system state is shown in **Figure 56**. The green line at 0.2 corresponds to those states which have an absolute Euclidean distance of around two. With the definition of the state vector for this system, the theoretical maximum Euclidean distance is evaluated as 10.44, as detailed in equation (61). For the ratio in equation (50) to be 0.2, the maximum value for the current state's Euclidean distance can be two. For such states, the values of either four of their components have magnitude one, or one of their components has a magnitude of two, while the rest of the components are zero.

$$\sqrt{\sum_{i=i}^{9} s_{i\_max}^{2}} = \sqrt{\mathbf{4(4^2) + 5(3^2)}} = \mathbf{10.44} \tag{61}$$

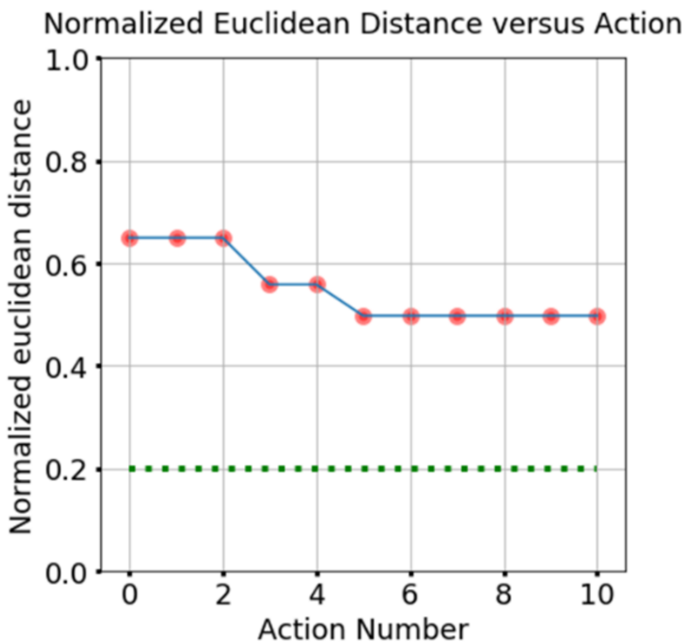

Figure 56 Progression of the normalized Euclidean distance of the system states during the actual well circulation operation.

The purpose of this 0.2 line is purely to serve as a visual aid, such that states closer to the line represent states closer to the goal state.

5.3.2.2.1 Plan 1

Using the initializations defined in **Table 9** and **Table 10**, and with a C_{exp} value 1, the decision-engine was used to plan ahead for eight decision epochs (40-minutes) starting from the state s_{TD} (equation (46)). Equation (62) represents the action sequence (a_{seq1}) recommended by the system. Selecting the right mud properties at the beginning of the circulation cycle is essential, since changing them is a time-consuming process. It is, therefore, highly impractical to adjust them in the middle of the circulation cycle. To this effect, the system suggested changing the mud properties (at the beginning of the circulation cycle) to mud density of 8.9 ppg, PV of 17.5 cP, and YP of 10.5 lbf/100 ft^2 from mud density 9.06 ppg, PV 11 cP, and YP 36.5 lbf/100 ft^2 initially.

$$a_{seq1} = \left\{\begin{pmatrix}1000\\0\\80\\8.9\\17.5\\10.5\end{pmatrix}, \begin{pmatrix}1200\\0\\100\\8.9\\17.5\\10.5\end{pmatrix}, \begin{pmatrix}1400\\0\\120\\8.9\\17.5\\10.5\end{pmatrix}, \begin{pmatrix}1600\\0\\160\\8.9\\17.5\\10.5\end{pmatrix}, \begin{pmatrix}1800\\0\\160\\8.9\\17.5\\10.5\end{pmatrix}, \begin{pmatrix}1600\\0\\160\\8.9\\17.5\\10.5\end{pmatrix}, \begin{pmatrix}1400\\0\\160\\8.9\\17.5\\10.5\end{pmatrix}, \begin{pmatrix}1400\\0\\160\\8.9\\17.5\\10.5\end{pmatrix}\right\} \tag{62}$$

The predicted output state of the system is shown in **Figure 57**. The cuttings bed is almost entirely removed (as represented by the blue line), and the ECD values are very close to the desired regions throughout the well. Equation (63) represents the final state of the system.

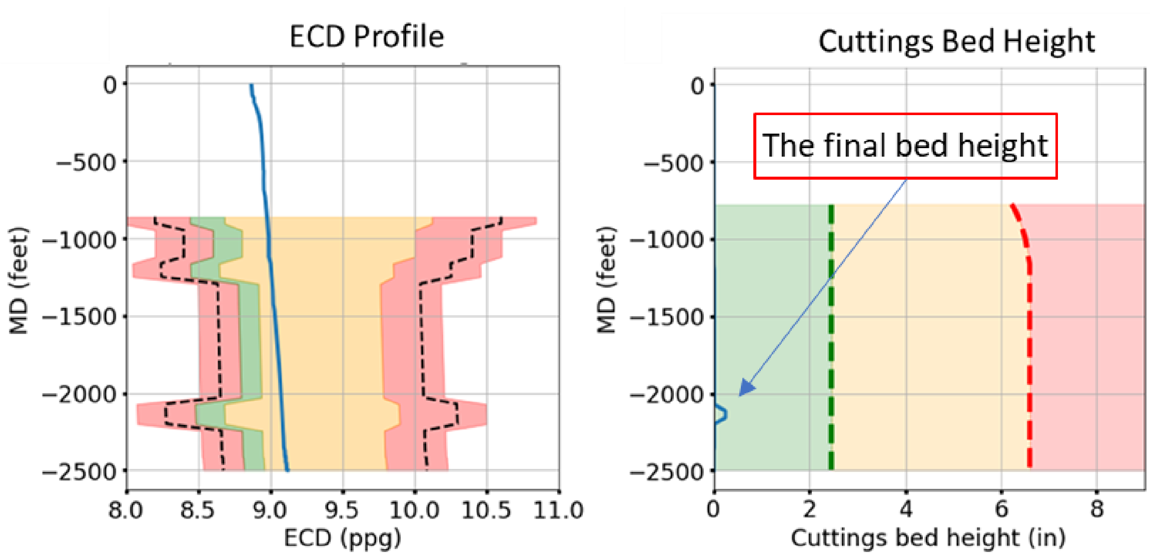

Figure 57 (a) ECD profile (b) Cuttings bed height (output state) for a_{seq1}.

$$s_{TD\_circ1} = \left\{\begin{matrix}0\\0\\0\\0\\1\\1\\1\\1\\1\end{matrix}\right\} \tag{63}$$

Figure 58 illustrates the progression of the system with actions for the sequence a_{seq1}. **Figure 58 (a)** shows the reduction in the cuttings bed height with different actions, and **Figure 58 (b)** represents the progression of the normalized Euclidean distance with actions.

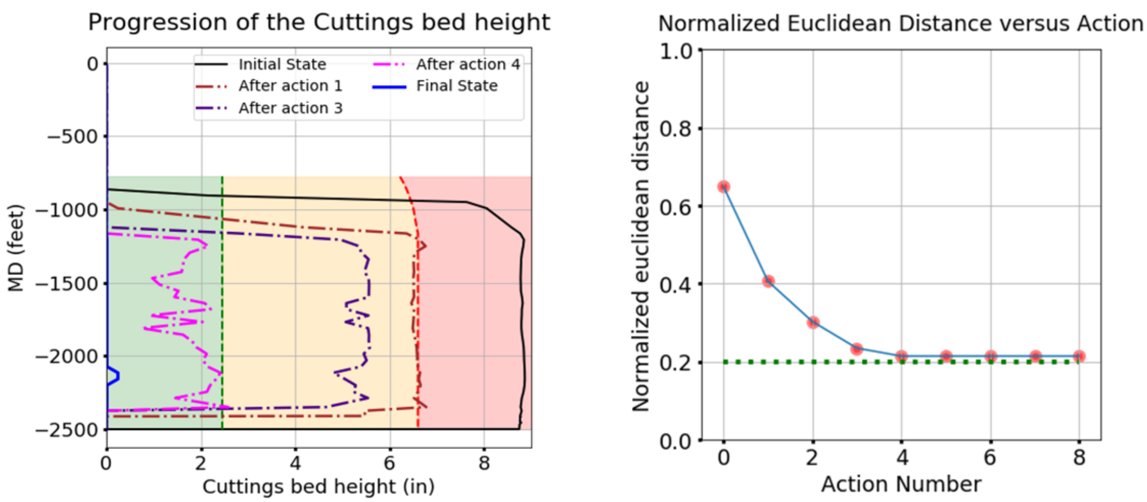

Figure 58 a) Progression of the cuttings bed (b) Progression of the normalized Euclidean distance of the system states for a_{seq1}.

By the fourth action, the system has already moved close to the 0.2 line (by cuttings bed being reduced to the goal state), where it stays until the end. **Figure 59** shows the progression of the rewards associated with this action sequence. Thus, the V value calculated for a_{seq1} is 0.82.

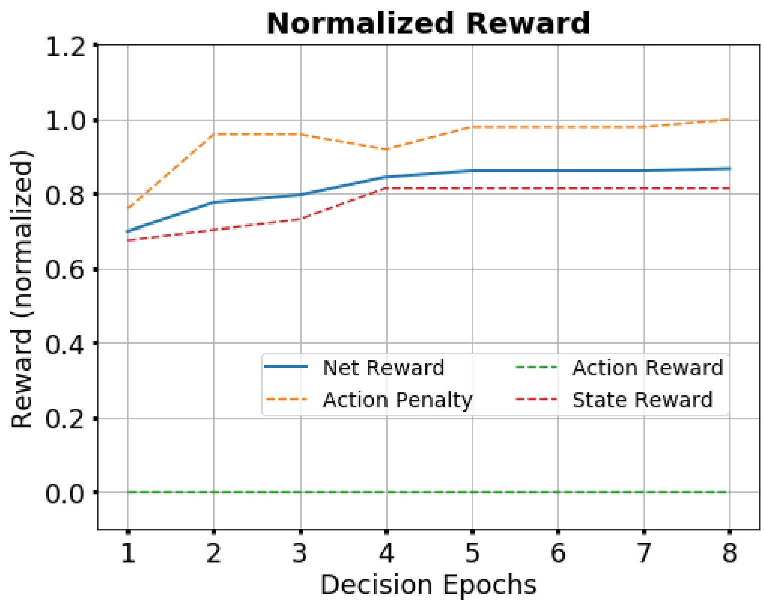

Figure 59 Progression of the rewards associated with a_{seq1}.

An interesting observation in the action sequence is the system actively trying to manage the ECD by reducing the flowrate, after the cuttings bed has been removed. Initially, the system suggests increasing the flowrate and the RPM, which helps with cuttings bed removal (as can be seen by the reduced Euclidean distance), and then later tries to reduce the ECD.

5.3.2.2.2 Plan 2

Another planning operation was performed by changing the flowrate and RPM thresholds, as shown in **Table 11**. No changes were made to the mud density and rheology thresholds, and the weights associated with the different reward components were also unaltered.

Table 11 Modified flowrate and RPM thresholds for varying the action-space.

Control Variable	**Number of Discrete Values**	**Range of Values**
Flowrate (GPM)	10	[0, 1500]
Drillstring RPM (rev/min)	10	[0, 150]

Equation (64) represents the action sequence (a_{seq2}) output by the planning system, over a 40-minute (eight decision epochs) interval. Due to the truncated flowrate and RPM thresholds, the system suggests different mud density and rheology than for a_{seq1} to help with the cuttings removal.

$$a_{seq2} = \begin{Bmatrix} 833 \\ 0 \\ 67 \\ 9.24 \\ 10.5 \\ 10.5 \end{Bmatrix}, \begin{Bmatrix} 1000 \\ 0 \\ 83 \\ 9.24 \\ 10.5 \\ 10.5 \end{Bmatrix}, \begin{Bmatrix} 1167 \\ 0 \\ 83 \\ 9.24 \\ 10.5 \\ 10.5 \end{Bmatrix}, \begin{Bmatrix} 1333 \\ 0 \\ 100 \\ 9.24 \\ 10.5 \\ 10.5 \end{Bmatrix}, \begin{Bmatrix} 1333 \\ 0 \\ 117 \\ 9.24 \\ 10.5 \\ 10.5 \end{Bmatrix}, \begin{Bmatrix} 1500 \\ 0 \\ 133 \\ 9.24 \\ 10.5 \\ 10.5 \end{Bmatrix}, \begin{Bmatrix} 1500 \\ 0 \\ 150 \\ 9.24 \\ 10.5 \\ 10.5 \end{Bmatrix}, \begin{Bmatrix} 1333 \\ 0 \\ 150 \\ 9.24 \\ 10.5 \\ 10.5 \end{Bmatrix} \quad (64)$$

The final state of the system (s_{TD_circ2}), represented by equation (65), is shown in **Figure 60**.

$$s_{TD\_circ2} = \begin{Bmatrix} 0 \\ 0 \\ 0 \\ 0 \\ 1 \\ 1 \\ 1 \\ 1 \\ 1 \end{Bmatrix} \quad (65)$$

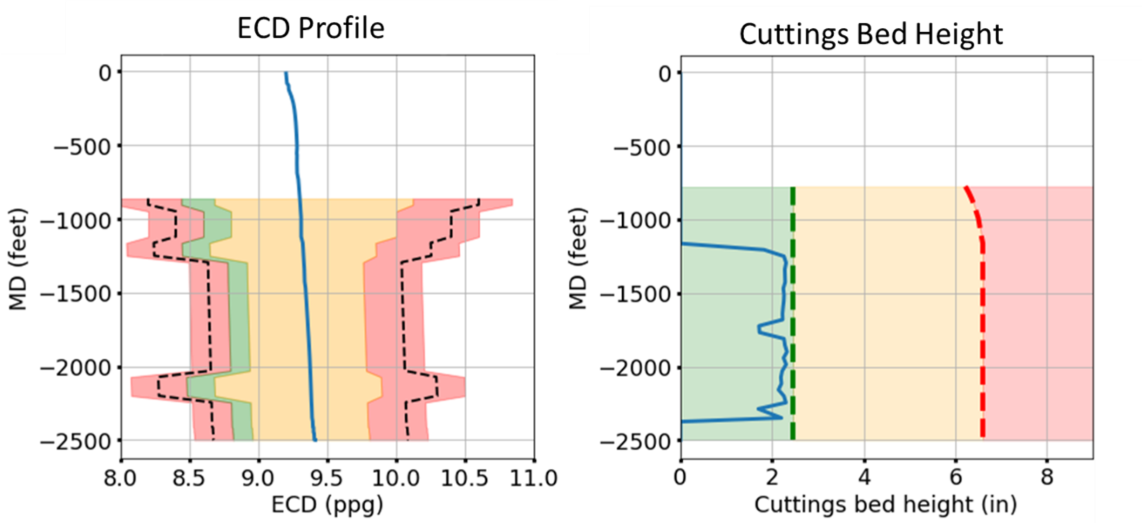

Figure 60 (a) ECD profile (b) Cuttings bed height (c) Progression of the normalized Euclidean distance of the system states for a_{seq2}.

The normalized Euclidean distance does decrease with time, but it only reaches the 0.2 line on the seventh action (**Figure 61(b)**). An interesting observation in **Figure 61(a)** is that the cuttings bed is not entirely removed but is reduced to the goal state (green-shaded zone) values.

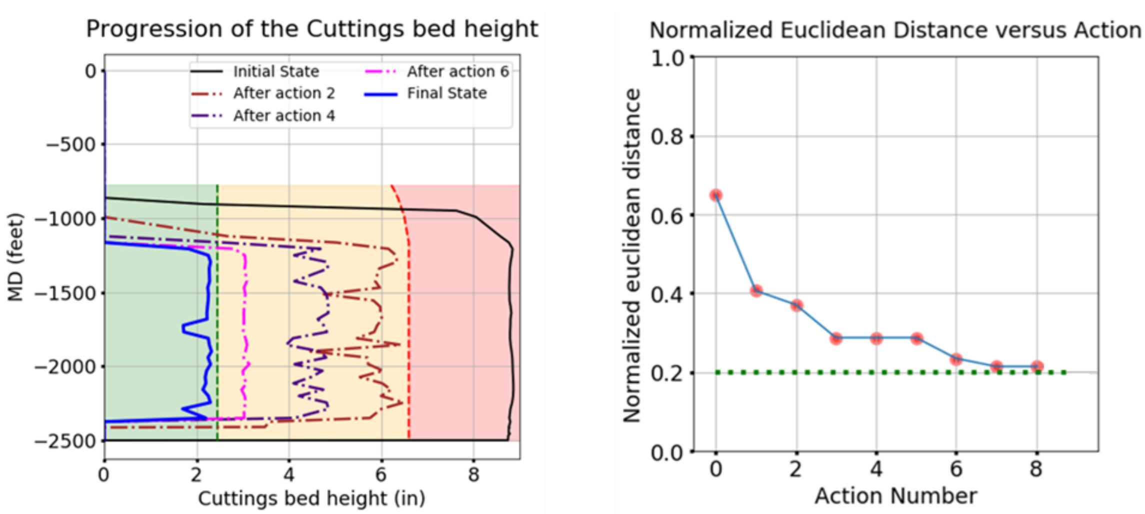

Figure 61 (a) Progression of the cuttings bed (b) Progression of the normalized Euclidean distance of the system states for a_{seq2}.

The ECD is also in the safe-but-suboptimal region, but it is much higher than for the first case due to a higher suggested mud density. Although, the final state representations for both the plans (a_{seq1} and a_{seq2}) are the same, the average V value calculated for a_{seq2} is 0.79, which is lower than for a_{seq1}. The progression of rewards for the sequence a_{seq2} is shown in **Figure 62**.

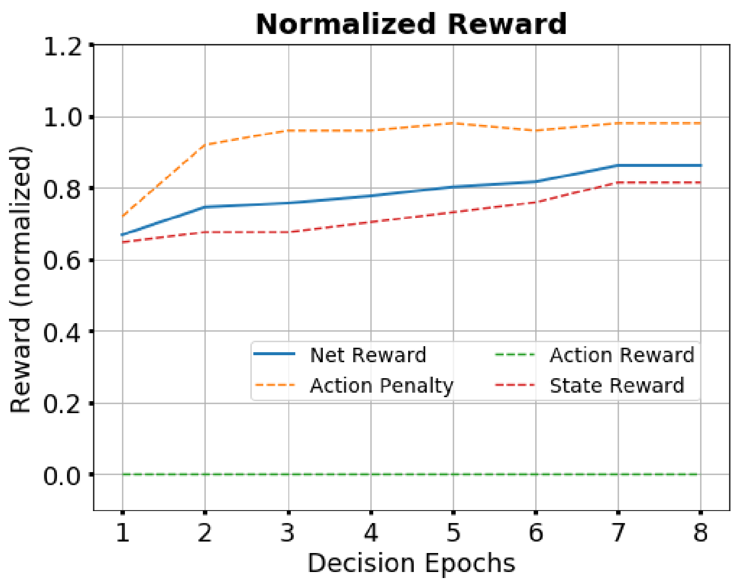

Figure 62 Progression of the rewards associated with a_{seq2}.

5.3.2.3 Discussion

For both the plans, a_{seq1} *and* a_{seq2}, the decision-engine was able to self-learn by simulating multiple episodes of experience and output action sequences that would have helped move the system towards the goal states. To summarize:

- The non-holonomic nature of drilling operations combined with the decision engine's long-term planning capabilities allow for more robust plans. An example of this is the system selecting appropriate mud properties at the beginning of the circulation cycle by evaluating multiple steps into the future. Both plans that were generated result in a better outcome than the actual plan generated and implemented by a human decision-maker.

- Tuning the weights associated with the different reward components allows prioritizing different objectives or different sections of the well over others.
- Utilizing the domain-knowledge enriched MCTS allows for faster and more efficient planning, and well-defined heuristic functions make such planning systems implementable in the field. Exhaustively evaluating all nodes in the search tree to the eighth level (eight decision epochs or 40-minutes) would require over a hundred million simulations, as well as require storing the results of each state-action transition. This would be highly computationally and memory inefficient. MCTS, on the other hand, requires a number of simulations that are many orders of magnitude lower (only a few thousand in total), and all state-action transition results do not need to be stored. For the cases discussed in this paper, the planning algorithm, without any parallel processing or multi-threading on a standard laptop using an unstreamlined python code, was able to generate these plans in under an hour.
- Planning with higher C_{exp} values does result in the convergence of the state's Euclidean distance towards the 0.2 line, but it requires many more simulations. On the other hand, lower C_{exp} values introduce an element of bias depending on the order in which the nodes are added to the tree, which itself depends on the random rollout policy for MC simulations.

5.4 SUMMARY

This chapter discusses a method for the development of intelligent decision engines for well construction operations by utilizing an MDP formalism (detailed in Chapter 4) with the MCTS for action planning. This method is demonstrated by implementing a hole cleaning action planning system and comparing its performance against a human decision maker's performance. To summarize:

- MCTS planning systems allow for a hybrid approach to managing conflicting objectives by combining the advantages of the exploration-exploitation trade-off offered by the MCTS, with domain-knowledge derived heuristics, thereby helping make better decisions.
- A combination of the digital twin and a non-sparse reward function, with backpropagation of the episodic returns, allows the system to learn from simulated experience. A non-sparse reward structure ensures that the feedback received by the agent is frequent and meaningful, thereby speeding up the policy improvement process.
- The underlying tree and rollout policies of the MCTS algorithm can be enhanced by using well-defined process-specific heuristics. This assists in improving the convergence rate of the system towards an optimal action sequence. For the hole cleaning system, the heuristic was designed to balance safety, performance, feasibility, and proximity constraints.
- Utilizing such systems can aid in overall performance improvement by eliminating the need to wait on decisions, as well as suggesting optimal drilling parameters for the given wellbore condition.

Chapter 6: Conclusions and Recommendations

The dissertation attempted to address the problem of inherent bias that can result because of human-centered decision-making in the well construction domain by proposing a framework for the development of intelligent decision-engines.

6.1 Conclusions and Major Contributions

The development of such decision-engines requires addressing the following three key elements:

- **Digital twinning** of the underlying well construction process, which is discussed in Chapter 3. *Here, a novel three-step framework (identification of the objectives, building the digital twin, and performance tracking and scenario analysis) was developed for setting up twinning systems to help analyze potential drilling scenarios for action planning*. This robust cyclic methodology builds and uses the twinning system for single-step scenario analysis. Hence, more informed decision-making is achieved, which improves operational performance and drilling efficiency. The presented approach also opens the doors for the digital twinning of any well construction operation.
- **MDP formulation** or setting up the decision-engine, as is detailed in Chapter 4. *Here, a novel method for designing well construction operations as finite-horizon sequential-decision making systems for long-term action planning was detailed.* The concept of digital twinning is combined with a well-crafted non-sparse normalized reward function to quantify states and evaluate state-action transitions. Such representation of well construction operations allows for an unbiased quantification and comparison of different

action sequences or scenarios, thereby allowing ranking of the different sequences based on their long-term returns.

- **Planning** or solving the MDP formulation to find an optimal action sequence or plan, which is discussed in Chapter 5. The concept of self-play used by game AI engines (such as in Google DeepMind's AlphaGo and AlphaZero) was adapted for well construction operations. Here, a drilling agent continually improves the policy (or the action plan) by backpropagating returns from simulated episodes of experience that are generated using the digital twin. The MCTS algorithm, enhanced by domain-specific heuristics to help speed up the learning, was utilized for action planning. *The development of such intelligent sequential decision-making systems for well construction operations that use heuristics and an exploration-exploitation trade-off to guide the search towards promising regions of the search space is novel.*

This methodology was demonstrated through the chapters by building such a system for **hole cleaning advisory,** which inherently is a multi-step decision-making problem. Such a system tracks the performance by simulating different hole cleaning actions and provides decisions regarding action planning. For the real well applications presented, using the action plans output by this system would have significantly reduced the cuttings bed height (to within safe limits for performing tripping, running casing and cementing operations) while maintaining the ECD to within the drilling margin. This was, in part, accomplished by the ability of the decision-engine to intelligently generate, evaluate and learn by simulating multiple scenarios, multiple steps into the future, which enabled it to suggest the optimal mud rheology at the beginning of the plan. Such complex multi-step scenario analysis and evaluation would have been difficult for a human decision-maker to perform, as was demonstrated by the original sequence of actions taken. Moreover, the designed heuristic function utilized in the MCTS helped reduce the required number of simulations by a thousand-fold as compared to the vanilla MCTS, thereby improving the convergence rate and the memory efficiency.

Hence, completely automated decision making in terms of hole cleaning was achieved and validated. *The automated process of classifying hole cleaning system states, defining controllable action variables, simulating, and learning from the quantification of multiple viable hole cleaning action sequences, and finally selecting the best course of action, is another novel contribution of this work.*

6.2 Recommendations

6.2.1 Applications

- The methodology presented in the dissertation is readily applicable across a multitude of field operations. For instance, such decision engines can be developed for well construction applications, such as well control, drilling parameter optimization, tripping automation, and cementing.
- Furthermore, in the long-term, such decision engines can be integrated into a rig's control system to help automate monitoring, planning, and control of action variables such as drilling rate, drillstring rotation speed, tripping speed, flowrate, and mud properties, thereby fully automating drilling operations and avoiding any human-centric bias.

6.2.2 Technical improvements

- Value function approximation techniques can be used for quantifying the state-space by treating the state-space as a continuous set, with discrete action-space.

- Policy-gradient methods or actor-critic reinforcement learning methods can be used to find the best action for any given state by treating both the state- and action-space as continuous.
- Real-time downhole sensor data, when available, can be incorporated to enhance the digital twin models.
- The speed of the search of the action-space can be improved multifold by utilizing techniques such as:
  - Multi-threading and parallel processing by running several instances of the MCTS simultaneously to build and learn from multiple trees in parallel
  - Implementing the underlying code more optimally in a C or C++ environment, as opposed to in python

APPENDICES

Appendix A: List of Symbols and Abbreviations

A.1 SYMBOLS

Symbol	**Meaning**
A	Action-space
A_{bit}	Area of the drill bit
A_{fe}	Action set associated with feasibility constraints (for hole cleaning heuristic)
A_{flow}	Annular flow area available to the drilling mud
A_{px}	Action set associated with proximity metric (for hole cleaning heuristic)
$A_{rollout}$	Reduced action space for a state during the rollout phase of the MCTS
A_s	Action space from state s
A_{s_t}	The action space of the node associated with state s_t
A_{sp}	Action set associated with safety and performance metrics (for hole cleaning heuristic)
A_{sq}	Action set associated with sequential metric (for hole cleaning heuristic)
a_{-1}	The most recently executed action
a_{agg}	Aggressive actions representing greater magnitude changes in values of action control variables relative to the most recent action
a_{reg}	Regular actions representing small changes in action control variables with respect to the most recent action
a_{seq1}	Action sequence recommended by the decision engine for the first planning case
a_{seq2}	Action sequence recommended by the decision engine for the second planning case
a_t	Action executed by the agent at time t
C_{ang}	Correction factor (in the hole cleaning model) to account for the inclination angle

C_{exp}	The exploration factor in the UCT formula
C_{geo_d}	Correction factor (in the hole cleaning model) for geometry (hydraulic diameter)
C_{geo_inc}	Correction factor (in the hole cleaning model) for geometry (inclination angle)
C_{geo_pv}	Correction factor (in the hole cleaning model) for geometry (mud rheology)
C_{MW}	Correction factor (in the hole cleaning model) for the mud weight
C_{rpm}	Correction factor (in the hole cleaning model) for drillpipe rotation
C_{size}	Correction factor (in the hole cleaning model) for the size of the cuttings
$C_{vertical}$	Correction factor (in the hole cleaning model) for vertical section
c_{cutt}	Concentration of cuttings in the flow
D_i	Diameter of the drillstring element
D_o	Diameter of the borehole (or the casing)
D_{o_k}	Outer diameter of the kth control volume segment ($inches$)
D_{TVD}	Total vertical depth (m)
d_{cc}	Center to center distance (between the drillstring and the borehole)
$d_{norm-euc}$	Normalized Euclidean distance for the current state
dP	The frictional pressure drop in a control volume element
dx	Change in a control volume element's total measured depth
dz	Change in a control volume element's total vertical depth
$ECD_k^{absolute}$	Absolute ECD value in the kth control volume segment (ppg)
ECD_{avg}	The average ECD value for an inclination interval (ppg)
$ECD_{inc.}$	Functional value of ECD in the inclination interval segment $inc.$
ecc	The eccentricity of the drillstring element in the borehole
$\|exp\|$	The level at $node_{exp}$ is in the tree
f_f	Friction factor associated with the flow of drilling mud in the drillstring and the annulus

$flowrate$	Rate of flow of the drilling mud through the drillstring controlled by the mud pump on the surface (measured in GPM)
G_T	Net discounted return to T decision epochs
g	Acceleration due to gravity (9.81 m/s^2)
H	Normalized cuttings bed height for an inclination interval
$H_{inc.}$	Functional value of the cuttings bed height in the inclination interval segment $incl.$
$H_k^{absolute}$	Absolute cuttings bed height in the kth control volume segment (inches)
H_k^{norm}	Normalized cuttings bed height in the kth control volume segment
$incl$	Inclination angle range (degrees)
$N(s)$	Total number of visits to the state s
$N(s,a)$	Number of times action a has been taken from state s
N_{seg}	Number of control volume segments within an inclination interval segment
N_{s_t}	Total number of visits to the node associated with state s_t
$n_{interval}$	Number of discrete values possible for a given control variable
$node_0$	Root node corresponding to the starting state s_0
$node_{exp}$	Randomly expanded node from the leaf node during the expansion phase of the MCTS
$node_{leaf}$	Leaf node reached at the end of the selection phase of the MCTS
$node_t$	Node at decision epoch t
P	Transition probability set
$P_{frictional_{pressure\_loss\_D_{MD}}}$	Frictional pressure drop in the annulus (Pa) at a measured depth H
$P_{hydrostatic\_D_{TVD}}$	Hydrostatic Pressure (Pa) at a vertical depth of TVD_H
$P_{ss'}^a$	Transition probability of a system in the state s to the state s' when an agent executes action a
p_i	i^th^ parameter component of the state vector
${p^g}_i$	Goal state value of the i^th^ parameter component of the state vector

Q	Flowrate of the drilling mud
$Q(s,a)$	Average value associated with implementing action a from state s
$Q_{UCT}(s,a)$	The upper confidence bound or the urgency term in the UCT formula
Q^{π}	State-action value function
R	Reward set
$R_{ECDincl.}$	State reward component associated with ECD in the inclination interval $incl.$
$R_{Hincl.}$	State reward component associated with cuttings bed height in the inclination interval $incl.$
R_{PV}	Action Penalty component associated with changing mud PV
R_{ROP}	Action Penalty component associated with changing ROP
R_{RPM}	Action Penalty component associated with changing RPM
R_{S}	State transition based reward set
R_{S_net}	Non-normalized state reward for the hole cleaning system
R_{YP}	Action Penalty component associated with changing mud YP
$R_{a\_density}$	Action reward component associated with the density value
$R_{a\_flowrate}$	Action reward component associated with the flowrate value
R_{a_PV}	Action reward component associated with the PV value
R_{a_ROP}	Action reward component associated with the ROP value
R_{a_RPM}	Action reward component associated with the RPM value
R_{a_YP}	Action reward component associated with the YP value
R_{ap}	Action transition based penalty set
R_{ap_net}	Non-normalized action penalty for the hole cleaning system
R_{ap_norm}	Normalized action penalty for the hole cleaning system
R_{ar}	Action value based reward set
R_{ar_net}	Non-normalized action reward for the hole cleaning system
R_{ar_norm}	Normalized action reward for the hole cleaning system
$R_{density}$	Action Penalty component associated with changing mud density

$R_{flowrate}$	Action Penalty component associated with changing flowrate
R_{net}	Net normalized reward function for the hole cleaning system
R_{s_norm}	Normalized state reward for the hole cleaning system
$r_{element}$	Radius of the drillstring element
r_{greed}	Radius of the greed sphere for A_{px} evaluation
r_k	Reward associated with the k^{th} state-action transition
r_t	Reward received by the system at time t
S	State-space
s_{TD}	State of the hole cleaning system at the well TD
s_{TD_circ}	State of the wellbore after performing a circulation cycle at TD
s_{TD_circ1}	State of the wellbore after performing a circulation cycle at TD following a_{seq1}
s_{TD_circ2}	State of the wellbore after performing a circulation cycle at TD following a_{seq2}
s_{goal}	Goal or desired state for the hole cleaning system
s''_{goal}	The states near the goal state (for evaluating the A_{px} set)
s_t	State of the system at time t
T	Number of decision epochs to evaluate till in the future
t	Time step or decision epoch t
$t_{evaluation}$	Time interval being considered for evaluation
t_{max}	Time available for MCTS algorithm to plan
V	The average return value of an action sequence
V^{π}	State value function
v_{axial}	Axial flow velocity of the drilling mud in the annulus
$v_{axial\_drillstring}$	Axial component of the drillstring’s velocity
$v_{critical}$	Critical velocity (or CTFV)
v_{cutt}	Velocity of the cuttings in the fluid flow
v_{slip}	Slip velocity

$v_{tangential}$	Tangential component of the drillstring's velocity
$vol_{cuttings}$	Volume of cuttings generated in the given time interval
W_{ap}	Weight set associated with the action transition penalty
W_{ap_norm}	Weight value associated with the normalized action penalty
W_{ar}	Weight set associated with the action value reward
W_{ar_norm}	Weight value associated with the normalized action reward
W_s	Weight set associated with state transition reward
W_{s_norm}	Weight value associated with the normalized state reward
w_{unit}	Unit weight of the drillstring element
$\Delta N_{variable}$	Number of interval changes between consecutive actions
Δw	Difference between the FG and SL of the drilling window (ppg)
α	Dog-leg angle
β	Buoyancy factor
θ	Inclination angle
$\emptyset$	Azimuth angle
φ	Angle between the resultant and the tangential drillstring velocity components
τ	Torque
μ	Friction factor
ρ_{mud}	Density of the drilling mud (ppg)
ρ_{steel}	Density of steel
π	Policy
$\pi_{heuristic\_a}$	Problem specific heuristic (probability of selecting action a)
π_{tree}	Tree policy – the action selected from a given node in the search tree during the selection phase of the MCTS
γ	Discount factor for return calculation

A.2 ABBREVIATIONS

Abbreviation	**Meaning**
CBM	Condition-based maintenance
CRV	Critical resuspension velocity
$CTFV$	Critical transport fluid velocity
DLS	Dog-leg severity
ECD	Equivalent circulation density (ppg)
FG	Fracture gradient (ppg)
GPM	Gallons per minute
$MLWD$	Measurement and logging while drilling
NPT	Non-productive time
$POOH$	Pulling out of hole
PPG	Pounds per gallon
PV	Plastic viscosity (cP)
PWD	Pressure while drilling
ROP	Rate of Penetration (ft/hr.)
RPM	Surface rotation rate of the drillstring (revs/min)
RT	Real-time
SL	Stability limit (ppg)
TD	Total depth of the well (feet)
WOB	Weight on bit (Klbs.)
YP	Yield point (lb./100ft^2)

Appendix B: Development of a Digital Twinning System for Logistics and Planning

During well construction, drilling of a well section or interval is generally followed by circulation cycles for hole cleaning, then casing and cementing operations, and in some cases, by clean-out operations and casing/formation integrity tests. These steps are repeated until the objectives laid out in the drilling program are met, which includes drilling the well to its planned total depth (TD). The unpredictability in reaching TD affects the overall logistics and completion schedule of the well, which, in turn, affects the drilling program. It is, therefore, essential to be able to estimate and optimize the times required for the different well construction operations.

B.1 Determining the Objective of the Twinning System

This section discusses the development of a digital twin for predicting, updating, and optimizing in real-time, the time remaining to drill a section or reach well TD, referred to as 'time to TD'. This time prediction can be made using information such as:

- The operational performance of the offset (historical) wells
- The current position of the drill bit relative to the well plan
- The operational performance of the current well up to its present depth
- Degradation in performance of drilling tools, equipment, or drill bit

B.2 Building the Digital Twin

The following sections describe the different steps involved in building this digital twin.

B.2.1 Identification of system outputs

The first step in estimating time to TD is the identification of components that comprise this time, and the factors affecting these individual components. Time to TD from the standpoint of rig activities is the sum of anticipated times spent performing the different operations (or time spent in different rig states). The following generally comprise time to TD:

- Total anticipated on-bottom drilling time
- Total time for acquiring the directional surveys
- Total expected time for making connections
- Total tripping time (including times for tripping in, tripping out, making up and laying down BHAs)
- Total circulation time
- Total miscellaneous time to capture the times for all other activities and operations not considered above

The anticipated on-bottom drilling time further depends on the following:

- Total distances to be drilled individually by rotary and slide drilling
- The remaining formations to be drilled through and the approximate depths of each
- The estimated average drilling speeds (for both slide and rotary drilling modes) through each remaining formation

Approximation of the total connection and the total survey times requires estimating the remaining number of connections and surveys until the planned TD is reached. Similarly, metrics are designed to extrapolate the estimated circulation and tripping times until the planned TD is reached. To summarize, the time to TD can be calculated using equation (66).

$$T_{well\,TD} = T_{Drilling} + T_{Surveys} + T_{Connections} + T_{Tripping} + T_{Circulation} + T_{Miscellaneous} \tag{66}$$

B.2.2 Determining the required models

The next step is the identification of models required to calculate the individual components. Knowledge derived from offset wells is used in combination with the current well's performance, along with the information about planned tasks, to anticipate future events and estimate the different time components. The following models need to be implemented to accomplish this:

- Rig state detection engine to classify the real-time data into different operational categories such as on-bottom drilling (slide and rotary drilling), tripping (in and out), circulating, reaming, and making connections.
- Slide and rotary drilling predictive models to predict relative amounts of slide and rotary drilling required until the TD, based on the well plan and the learnings from offset wells
- Predictive data-based models to estimate different component times by utilizing an adaptive weighed scheme for combining statistics obtained from real-time data and offset well data, as shown in **Figure 63**.

In the adaptive weighted scheme, the most recently acquired data has the highest weight (W1), while historical data is assigned the lowest weight (W4). The sum of all the weights is 1, and the various times (t_1, t_2, etc.) are not fixed; instead, they are functions of the number of data points collected thus far.

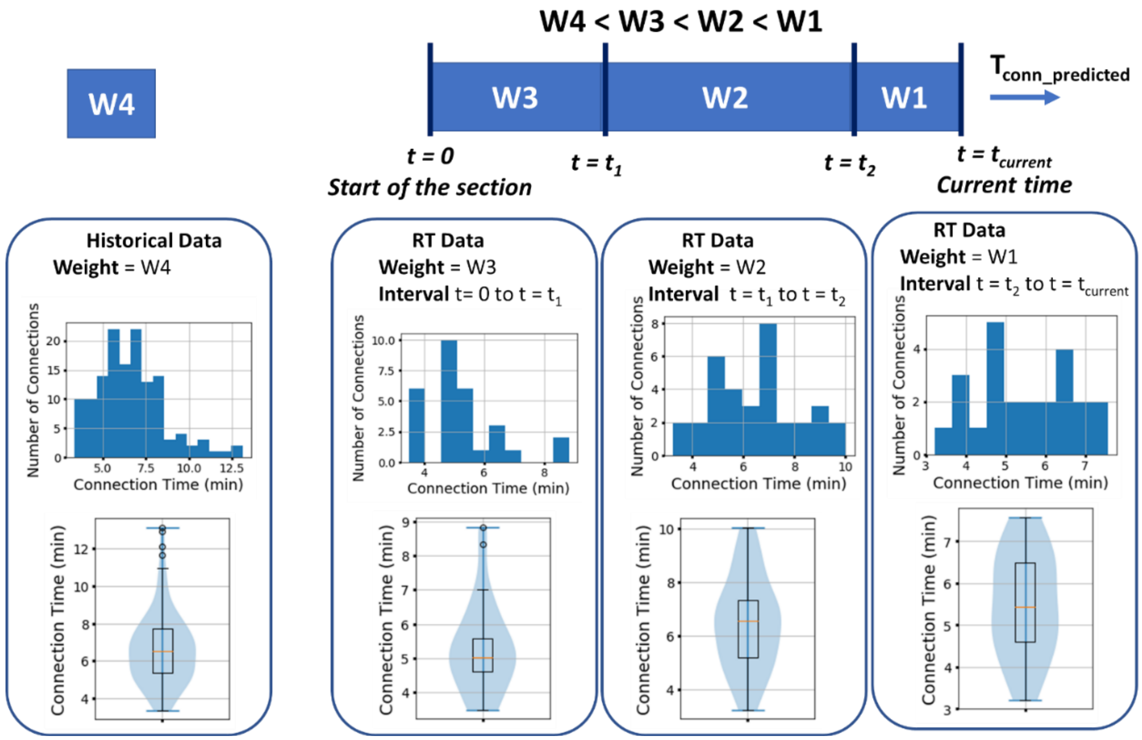

Figure 63 Adaptive weighted scheme for combining data collected at different times (for average connection time approximation).

B.2.3 Identification of the data

The following data streams are required for implementing this digital twin:

- **Real-time drilling data** obtained from the surface sensor measurements, specifically data channels such as drillstring RPM, applied WOB, drilling ROP, flowrate, standpipe pressure, tripping speed, surface torque and hookload measurements
- **Formation top information** (anticipated start and end depths of different formations)
- **BHA and bit information**, obtained from the well plan

- **Well trajectory information**, derived from the well plan and the well survey data, quantified using azimuth and inclination angles at different depths along the well
- **Descriptive statistics**, derived from offset well data, to quantify past performances for the various operations

Figure 64 summarizes the structure of the designed digital twin. First, the offset well data in combination with the current well's well plan, and formation top information is used to derive pre-drill or 'a priori' initializations. Subsequently, these initializations, in conjunction with RT drilling data, are fed into the multi-model digital twin. The twin then estimates the different time components that are summed together to make a time to TD prediction. As a new real-time data point is collected, the various statistics are re-calculated, and a new prediction is made. The differences between this prediction and the actual time are then utilized for tuning the adaptive weights of the prediction model. Therefore, the structure of the developed digital twin ensures that the system is continuously learning and updating itself based on the latest data.

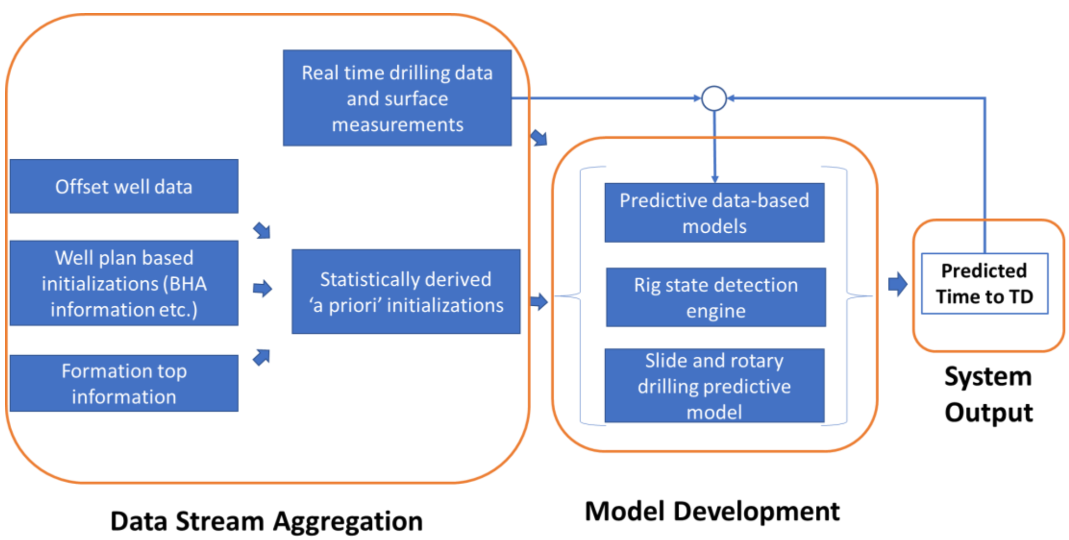

Figure 64 Final structure of the designed digital twin for making time to TD predictions.

B.3 APPLICATION OF THE TWIN FOR PERFORMANCE TRACKING AND SCENARIO ANALYSIS

The developed digital twin was implemented on a dataset comprising four wells; three were used as ‘offset wells’, and the fourth was treated as the ‘test well’. **Figure 65** illustrates the use of the three offset wells to derive a priori initializations for the twin. Initially, the number of collected data points from the test well is low. This results in the times and weights associated with the adaptive weighting tuned to give more importance to the offset well data for making predictions. However, as more real-time data is collected, the twin starts learning, thereby updating the different weights and times.

Figure 65 Utilizing offset well data for deriving a priori initializations.

B.3.1 Performance tracking

The twin was used to make real-time predictions for the time required to reach TD for drilling the horizontal lateral section of the test well. As per the well plan, the lateral section was scheduled to be drilled with a single bit run starting at approximately 11,500 feet till the planned TD of 20,700 feet. However, unexpected tool failures mandated three bit runs (or consequently two trips in and out of the borehole to replace the failed tools). Since these trips were not planned, the initial predictions made by the twin were optimistic. However, the predictions became more realistic once the rig state engine identified the unexpected trips. **Figure 66** shows the results of the predictions on plots between the predicted time versus the actual operation times. **Figure 66(a)** details the individual time predictions for different operations. **Figure 66(b)** shows the total time to TD predictions along with the three bit runs. Another feature of the various time predictions is their ability to adapt rapidly due to:

- Different weights being assigned to different data points at different times (adaptive weighting);
- Continuous real-time re-evaluation of the slide and rotary drilling requirements.

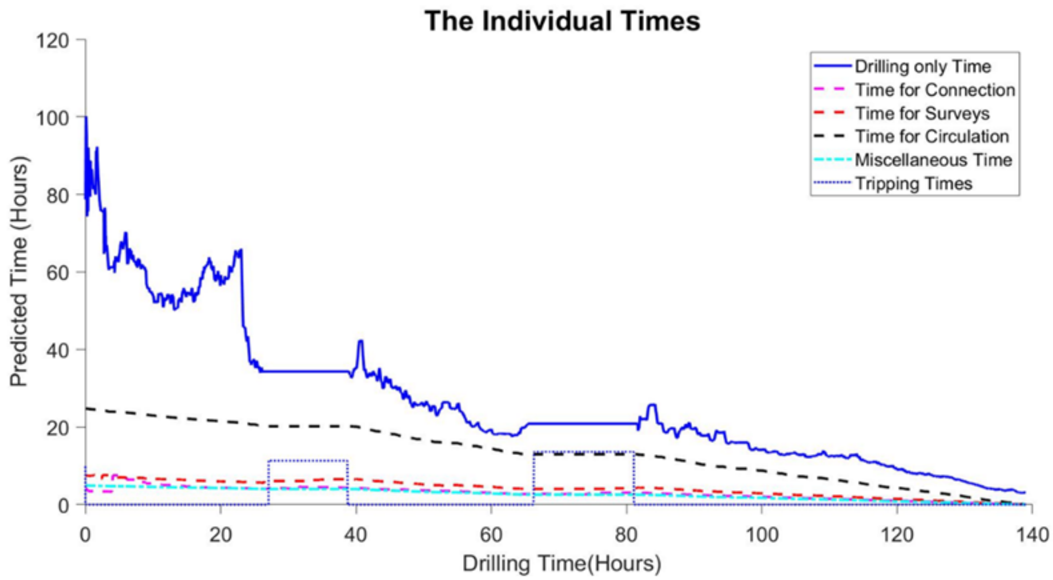

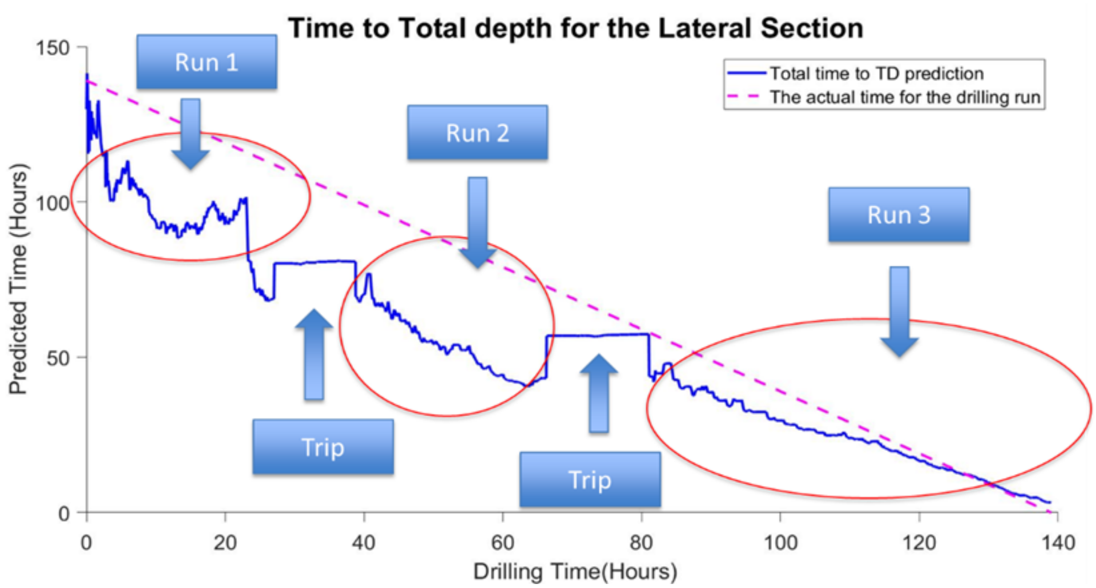

Figure 66 (a) Estimated individual times for different rig states versus time, (b) Total time to TD predictions versus time.

Figure 67 is another way to visualize the predictions by overlaying the predicted and actual remaining times to TD versus the drilled hole depth. The two time jumps around 13,250 feet and 15,850 feet represent the trips to change the failed tools. Spikes are visible in the predicted times in both these instances as soon as the algorithm identifies the beginning of tripping operations. Since a spike accounts for the time related to completing the tripping procedure from the given depth, it is directly proportional to the depth at which tripping starts.

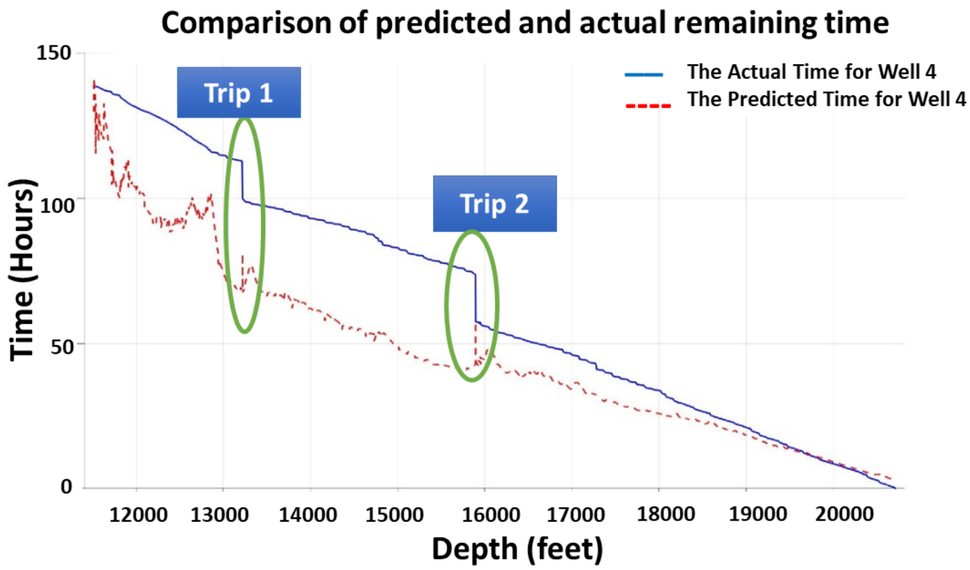

Figure 67 Comparison of the predicted and actual remaining times to TD versus drilled hole depth.

B.3.2 Scenario analysis

Like the hole cleaning advisory twin, this twin also permits scenario analysis to estimate the outcome of different logistical actions on the time to reach TD. Some examples of such logistical decisions include:

- Analyzing the effect of tripping out at a certain depth to change the drill bit
- Examining the impact of different drilling parameters on the various operational times
- Inspecting 'what-if' scenarios with varying values of time components such as tripping speeds or connection times

Some examples of scenarios that were analyzed using basic CBM models and data are summarized in **Figure 68.**

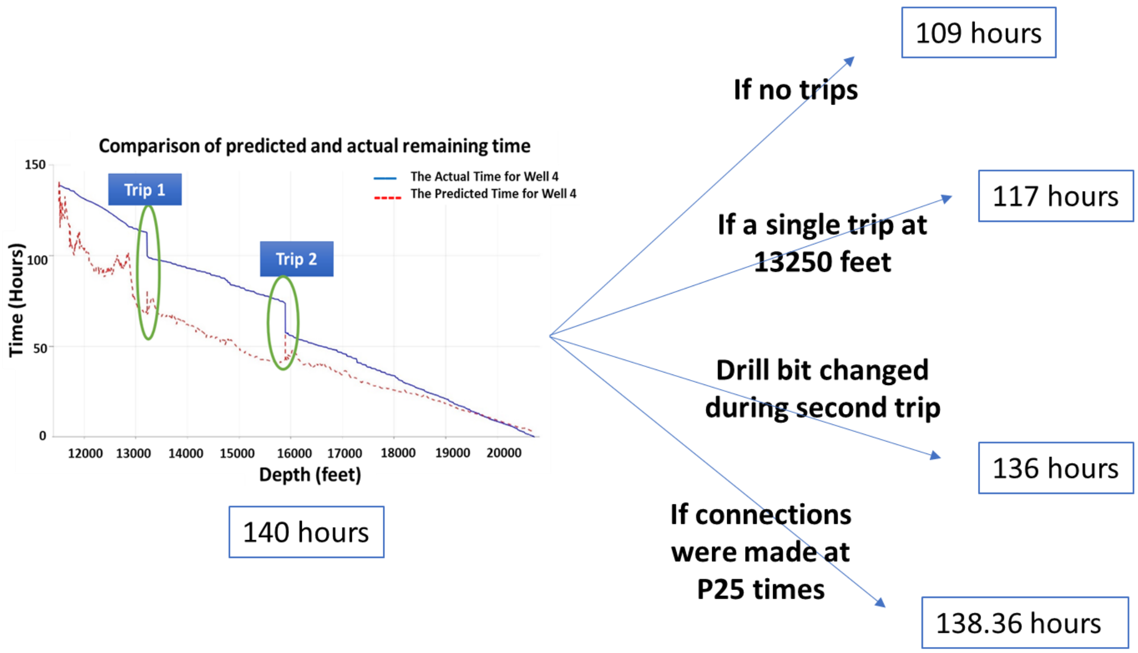

Figure 68 Analyzing post-run 'what-if' scenarios.

Observations include:

- Integrating CBM models such as for estimating bit degradation provides the twin with the ability to estimate the bit condition and remaining useful bit life in RT. This, in turn, allows for evaluating the benefits of continued drilling with a potentially worn bit, versus the time cost of tripping operations to change to a newer bit. The entire horizontal section (over 9,000 feet) was drilled using a single drill bit. However, if the drill bit were changed (to a newer bit) during either of the trips, it would have resulted in reducing the total drilling time. Assuming a linear bit degradation as a function of the depth drilled would have resulted in finishing the last section almost 4 hours faster if the bit were changed during the second trip.

- Operationally, the average time for making a connection while drilling the well was 171 seconds, while the P25 time was 112 seconds (**Figure 69**). Making all connections throughout drilling at 112 seconds would have resulted in the total operation time being reduced by 1.64 hours.

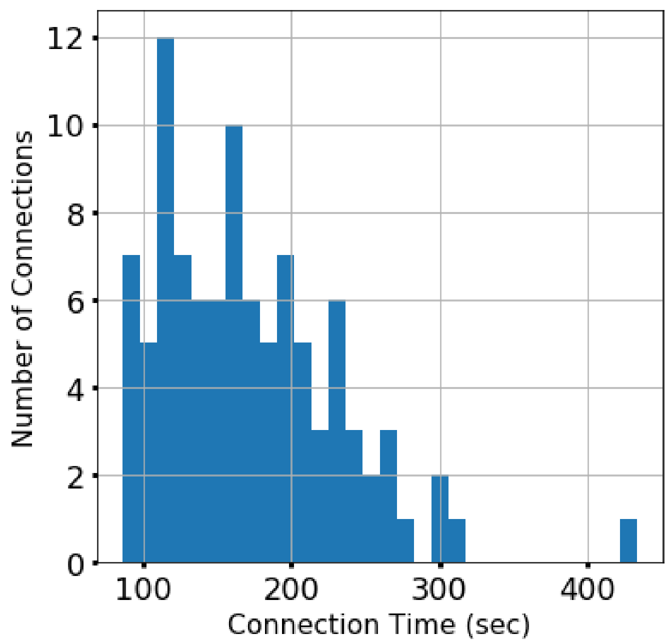

Figure 69 Connection times for the drilling operation.

- This twin is a good starting point for making initial time predictions and estimations and can be further enhanced by using advanced process models. Integrating more comprehensive CBM models for mud motor failure would not only have allowed for the prediction of 'unexpected' tool failures, thereby saving the extra downhole trips (NPT prevention), but also suggested optimal drilling parameters to prolong tool life.

B.4 Summary

This section details another application of the concept of digital twinning for performance tracking and scenario analysis in well construction. Here, an algorithm and its implementation are presented to make predictions in real-time, of the approximate time remaining to TD. This estimation to TD encompasses the rig state detection, descriptive statistical analysis, and estimation of individual rig state times for both historical as well as real-time wells. The underlying algorithm employs an adaptive weighting scheme wherein different weights are assigned to different data based on when it was collected. The predictions are then utilized for analyzing multiple 'what-if' scenarios. The time-based predictions to TD generated by a digital twin can help plan and optimize the logistics on a rig. Moreover, digital twins can help predict and thereby prevent unwanted failures, reducing the likelihood of NPT events. This can bring about significant benefits in terms of reducing well construction time and unnecessary trouble costs.

Appendix C: Monte Carlo Tree Search Enhancements

Many strategies exist that help enhance the vanilla policies of the Monte Carlo tree search (MCTS), some of the more important ones are (Browne et al., 2012; CHASLOT et al., 2008):

- Progressive strategies
- Prior knowledge
- Rapid action value evaluation (RAVE)

These strategies require evaluation of a heuristic, which can either be programmed (be rule-based) or be learned in real-time or be a combination of both.

C.1 Progressive Strategies

For systems with large state and action spaces, progressive strategies can be used to transition between simulation strategy and the selection strategy. A combination of some domain-specific heuristic and the vanilla MCTS selection policy is used. When only a few simulations have been run, a strategy similar to the simulation policy is used. However, as the number of simulations or episodes increase, these strategies converge to the standard UCT selection policy. Progressive widening and progressive bias are two such strategies.

Progressive bias introduces a function of some knowledge-based heuristic into the UCT term, the effect of which decreases as the number of simulations increase. Equation (67) depicts the modified selection policy, where $f(N(s,a)$ is the progressive bias term, which is evaluated using the method shown in equation (68). $H_{N(s,a)}$ is the heuristic representing the domain knowledge (CHASLOT et al., 2008).

$$\pi_{tree} = argmax_{a\in A}\left[Q(s,a) + C_{exp}.\sqrt{\frac{ln\, N_s}{N(s,a)}} + f(N(s,a))\right] \tag{67}$$

$$f\big(N(s,a)\big) = \frac{H_{N(s,a)}}{n(s,a)+1} \tag{68}$$

The heuristic inherently allows for exploration of the most promising node when there is not enough knowledge available, and as the number of simulations increases, $f\big(N(s,a)\big)$ decreases, thereby allowing the $Q(s,a)$ to take over.

Progressive widening, also referred to as progressive unpruning, initially artificially reduces the branching factor during the selection phase. However, as the number of simulations increases, the branching factor is also slowly increased. A heuristic function $H_{N(s,a)}$ is used to evaluate all actions, and eliminate or prune some based on low heuristic scores.

C.2 Prior Knowledge

A method to enhance the selection policy is by introducing some 'prior-knowledge' into the UCT term, as shown in equation (69). The term, $Q(s,a)_{prior}$ is an estimation of the value function based on historical process or simulation data, and N_{prior} is an experimentally tuned parameter to represent an equivalent of the number of visits to a node.

$$\pi_{tree} = argmax_{a\in A}\left[\frac{N(s,a).\,Q(s,a)_{current} + N_{prior}.\,Q(s,a)_{prior}}{N_{prior} + N(s,a)} + C_{exp}.\sqrt{\frac{ln\,N_s}{N(s,a) + N_{prior}}}\right] \tag{69}$$

Instead of selecting a random node, a node is selected based on the prior knowledge heuristic.

C.3 RAVE

Since every episode of the MCTS is independently simulated, the algorithm is unable to generalize between related positions or related actions. The fundamental idea of the RAVE algorithm is to allow the sharing of knowledge between different parts of the search space by using an All moves as first (AMAF) heuristic for every node in the search tree. The underlying concept of AMAF is to update all relevant parts of the search space for every action taken. Equation (70) shows the modifications to the selection policy, and equation (71) shows the method for evaluating the AMAF term for every node in the simulated episode (Silver & Gelly, 2011).

$$\pi_{tree} = argmax_{a \in A} \left[(1 - \beta(N_s)) * \left(Q(s,a) + C_{exp} \cdot \sqrt{\frac{ln\, N_s}{N(s,a)}} \right) + \beta(N_s) * AMAF_{s,(s,a)} \right] \tag{70}$$

$$AMAF = AMAF + \frac{Q - AMAF}{n_{amaf}} \tag{71}$$

Every simulation path in which the action a is implemented, and the system reaches a value Q, the value of the AMAF metric if incrementally changed to account for that state-action transition. $\beta(N_s)$ is an experimentally tuned weighting parameter for a given state and action.

A drawback of the RAVE algorithm is the requirement to keep track of the AMAF values for every node.

Appendix D: Publications

D.1 Published Papers

- Zhou, Y., Baumgartner, T., Saini, G., Ashok, P., Oort, E. van, Isbell, M. R., & Trichel, D. K. (2017, March 14). Future Workforce Education through Big Data Analysis for Drilling Optimization. Society of Petroleum Engineers. doi:10.2118/184739-MS.
- Saini, G., Chan, H., Ashok, P., van Oort, E., & Isbell, M. R. (2018, March 6). Automated Large Data Processing: A Storyboarding Process to Quickly Extract Knowledge from Large Drilling Datasets. Society of Petroleum Engineers. doi:10.2118/189605-MS.
- Saini, G., Chan, H. C., Ashok, P., van Oort, E., Behounek, M., Thetford, T., & Shahri, M. (2018, August 9). Spider Bots: Database Enhancing and Indexing Scripts to Efficiently Convert Raw Well Data Into Valuable Knowledge. Unconventional Resources Technology Conference. doi:10.15530/URTEC-2018-2902181.
- Saini, G., Chan, H. C., Ashok, P., van Oort, E., Behounek, M., Thetford, T., & Shahri, M. (2018, August 9). Spider Bots: Database Enhancing and Indexing Scripts to Efficiently Convert Raw Well Data Into Valuable Knowledge. Unconventional Resources Technology Conference. doi:10.15530/URTEC-2018-2902181.
- Saini, G., Ashok, P., van Oort, E., & Isbell, M. R. (2018, August 9). Accelerating Well Construction Using a Digital Twin Demonstrated on Unconventional Well Data in North America. Unconventional Resources Technology Conference. doi:10.15530/URTEC-2018-2902186.

- Mehta, R.K., Peres, S.C., Shortz, A.E., Hoyle, W., Lee, M., Saini, G, Chan, H, Pryor, M.W. (September 2018). Operator situation awareness and physiological states during offshore well control scenarios. Journal of Loss Prevention in the Process Industries, Volume 55, 2018, Pages 332-337, ISSN 0950-4230, https://doi.org/10.1016/j.jlp.2018.07.010.
- Saini, G. S., Ashok, P., & van Oort, E. (2020, February 25). Predictive Action Planning for Hole Cleaning Optimization and Stuck Pipe Prevention Using Digital Twinning and Reinforcement Learning. Society of Petroleum Engineers. doi:10.2118/199548-MS.
- H. Chan, M. M. Lee, G. S. Saini, M. Pryor and E. van Oort, "Development and Validation of a Scenario-Based Drilling Simulator for Training and Evaluating Human Factors," in *IEEE Transactions on Human-Machine Systems*, vol. 50, no. 4, pp. 327-336, Aug. 2020, doi: 10.1109/THMS.2020.2969014.
- Saini, G.S., Hender, D., James, C., Sankaran, S., Sen, V., and van Oort, E., An Automated Physics-based Workflow for Identification and Classification of Drilling Dysfunctions Drives Drilling Efficiency and Transparency for Completion Design, Paper SPE 200006, SPE Unconventional Resources Conference to be held 28 September – 2 October 2020 in Calgary, Alberta, Canada
- Fallah, A., Gu, Q., Saini, G., Chen, D., Ashok, p., van Oort, E., Karimi Vajargah, A., Hole Cleaning Case Studies Analyzed with a Transient Cuttings Transport Model, SPE-201461-MS, SPE ATCE 2020.

D.2 Planned Journal Publications

- Saini, G., Pournazari, P., Ashok, P., van Oort, E., Intelligent Decision-Making and Action Planning Systems for Well Construction Operations Demonstrated by Application for Hole Cleaning Improvement, *submitted to the Journal of Engineering Applications of Artificial Intelligence*
- Saini, G., Erge, O., Ashok, P., van Oort, E., Structuring Well Construction Operations as Finite Horizon Sequential Decision-Making Systems for Action Planning, *submitted to the Expert Systems with Applications Journal*
- Saini, G., Fallah, A., Ashok, P., van Oort, E., A Generalized Digital Twinning Methodology for Well Construction Operations with Performance Tracking and Scenario Analysis, *submitted to the Information Fusion Journal*

Bibliography

Aadnoy, B. S., Fazaelizadeh, M., & Hareland, G. (2010). A 3D analytical model for wellbore friction. *Journal of Canadian Petroleum Technology*, *49*(10), 25–36. https://doi.org/10.2118/141515-PA

Abbas, A. K., Almubarak, H., Abbas, H., & Dawood, J. (2019, November 11). Application of machine learning approach for intelligent prediction of pipe sticking. *Society of Petroleum Engineers - Abu Dhabi International Petroleum Exhibition and Conference 2019, ADIP 2019*. https://doi.org/10.2118/197396-ms

Abbass, H., Bender, A., Dam, H., Baker, S., Whitacre, J. M., & Sarker, R. (2009). Computational Scenario-based Capability Planning. *GECCO'08: Proceedings of the 10th Annual Conference on Genetic and Evolutionary Computation 2008*, 1437–1444. https://doi.org/10.1145/1389095.1389378

Ahmed, O. S., Aman, B. M., Zahrani, M. A., Ajikobi, F. I., & Aramco, S. (2019). *SPE-197674-MS Stuck Pipe Early Warning System Utilizing Moving Window Machine Learning Approach*.

Ahmed, R., & Miska, S. (2008). Experimental study and modeling of yield power-law fluid flow in annuli with drillpipe rotation. *SPE/IADC Drilling Conference, Proceedings*, *1*, 569–576. https://doi.org/10.2118/112604-ms

Al-Abduljabbar, A. M., Hossain, M. E., Al Gharbi, S., & Al-Rubaii, M. (2018). Optimization of tripping speed to minimize surge & swab pressure. *Proceedings of the SPE/IADC Middle East Drilling Technology Conference and Exhibition*, *2018-Janua*(January), 29–31.

Al-Ghunaim, S. M., Sadiq, B. M., Siam, M., Nassar, I., & Aissa, R. K. (2017). Operations efficiency: Improved well planning methodology based on invisible lost time smart KPIs. *SPE Middle East Oil and Gas Show and Conference, MEOS, Proceedings*, *2017-March*, 1981–2001. https://doi.org/10.2118/183941-ms

Alija, A. S. (2015). ANALYSIS OF DIJKSTRA'S AND A* ALGORITHM TO FIND

THE SHORTEST PATH [Universiti Tun Hussein Onn Malaysia]. In *International Conference on Information and Knowledge Management, Proceedings*. https://doi.org/10.1145/3132847.3132886

Arulkumaran, K., Cully, A., & Togelius, J. (2019). *AlphaStar: An Evolutionary Computation Perspective*. https://doi.org/10.1145/3319619.3321894

Baldino, S., Osgouei, R. E., Ozbayoglu, E., Miska, S., Takach, N., May, R., & Clapper, D. (2015). Cuttings settling and slip velocity evaluation in synthetic drilling fluids. *Offshore Mediterranean Conference and Exhibition, OMC 2015, February 2016*.

Bassal, A. A. (1995). *The effect of Drillpipe Rotation on Cuttings Transport in Inclined Wellbores*.

Bennett, B. (2019). *Graphs: Breadth First Search vs. Depth First Search*. https://medium.com/javascript-in-plain-english/graphs-breadth-first-search-vs-depth-first-search-d9908c560642

Bhaumik, D., Khalifa, A., Green, M. C., & Togelius, J. (2019). *Tree Search vs Optimization Approaches for Map Generation*. http://arxiv.org/abs/1903.11678

Birnie, C. E., Sampson, J., Sjaastad, E., Johansen, B., Obrestad, L. E., Larsen, R., & Khamassi, A. (2019, September 3). Improving the quality and efficiency of operational planning and risk management with ML and NLP. *Society of Petroleum Engineers - SPE Offshore Europe Conference and Exhibition 2019, OE 2019*. https://doi.org/10.2118/195750-MS

Bourgoyne, A. T. (1986). *Applied drilling engineering*. Society of Petroleum Engineers.

Boxall, A. (2016). *Inside McLaren's Secretive F1 Mission Control Room | Digital Trends*. https://www.digitaltrends.com/cars/inside-mclaren-f1-racing-mission-control-room/

Brechan, B., Dale, S. I., & Sangesland, S. (2018). Digital well planning - New cost saving well construction and Life Cycle Well Integrity Model. *Proceedings of the*

Annual Offshore Technology Conference, *4*, 2548–2570. https://doi.org/10.4043/28772-ms

Brechan, Bjorn, & Sangesland, S. (2019, May 13). Digital Well Planning, Well Construction and Life Cycle Well Integrity: The Role of Digital Experience. *SPE Norway One Day Seminar*. https://doi.org/10.2118/195628-MS

Breuer, H. (2018). *The Future of Manufacturing | Digital Twin | Global*. https://new.siemens.com/global/en/company/stories/research-technologies/digitaltwin/the-future-of-manufacturing-plm-red-bull-racing.html

Brown, C., Mccormick, J., & Nunez, A. (2014). Improving the decision making process between drilling and completion using real-time torque and drag modeling. *Proceedings - SPE Annual Technical Conference and Exhibition*, *1*, 627–637. https://doi.org/10.2118/170625-ms

Browne, C. B., Powley, E., Whitehouse, D., Lucas, S. M., Cowling, P. I., Rohlfshagen, P., Tavener, S., Perez, D., Samothrakis, S., & Colton, S. (2012). A survey of Monte Carlo tree search methods. *IEEE Transactions on Computational Intelligence and AI in Games*, *4*(1), 1–43. https://doi.org/10.1109/TCIAIG.2012.2186810

Browne, C., Powley, E., Whitehouse, D., Lucas, S. M., Cowling, P. I., Rohlfshagen, P., Tavener, S., Perez, D., Samothrakis, S., & Colton, S. (2012). A survey of Monte Carlo tree search methods. *IEEE Transactions on Computational Intelligence and AI in Games*, *4*(1), 1–43. https://doi.org/10.1109/TCIAIG.2012.2186810

Burkhardt, J. A. (1961). Wellbore Pressure Surges Produced by Pipe Movement. *Journal of Petroleum Technology*, *13*(6). https://doi.org/10.2118/1546-g

Carter-Journet, K., Kale, A., Zhang, D., Pradeep, E., Falgout, T., & Heuermann-Kuehn, L. (2014). Estimating probability of failure for drilling tools with life prediction. *Society of Petroleum Engineers - SPE Asia Pacific Oil and Gas Conference and Exhibition, APOGCE 2014 - Changing the Game: Opportunities, Challenges and Solutions*, *2*, 1048–1064. https://doi.org/10.2118/171517-ms

Cayeux, E., & Daireaux, B. (2009). Early detection of drilling conditions deterioration using real-time calibration of computer models: Field example from north sea drilling operations. *SPE/IADC Drilling Conference, Proceedings*, *1*, 548–560. https://doi.org/10.2118/119435-ms

Cayeux, Eric, Daireaux, B., & Dvergsnes, E. W. (2011). Automation of drawworks and topdrive management to minimize swab/surge and poor-downhole-condition effects. *SPE Drilling and Completion*, *26*(4), 557–568. https://doi.org/10.2118/128286-pa

Cayeux, Eric, Daireaux, B., Dvergsnes, E. W., & Scelevik, G. (2012). Early symptom detection on the basis of real-time evaluation of downhole conditions: Principles and results from several north sea drilling operations. *SPE Drilling and Completion*, *27*(4), 546–558. https://doi.org/10.2118/150422-PA

Cayeux, Eric, Mesagan, T., Tanripada, S., Zidan, M., & Fjelde, K. K. (2014a). Real-time evaluation of hole-cleaning conditions with a transient cuttings-transport model. *SPE Drilling and Completion*, *29*(1), 5–21. https://doi.org/10.2118/163492-PA

Cayeux, Eric, Mesagan, T., Tanripada, S., Zidan, M., & Fjelde, K. K. (2014b). Real-time evaluation of hole-cleaning conditions with a transient cuttings-transport model. *SPE Drilling and Completion*, *29*(1), 5–21. https://doi.org/10.2118/163492-PA

Cayeux, Eric, Mihai, R., Carlsen, L., & Stokka, S. (2020). An approach to autonomous drilling. *SPE/IADC Drilling Conference, Proceedings*, *2020-March*. https://doi.org/10.2118/199637-ms

Chan, H. C., Lee, M. M., Saini, G. S., Pryor, M., & van Oort, E. (2020). Development and Validation of a Scenario-Based Drilling Simulator for Training and Evaluating Human Factors. *IEEE Transactions on Human-Machine Systems*. https://doi.org/10.1109/THMS.2020.2969014

Chaslot, G., Bakkes, S., Szitai, I., & Spronck, P. (2008). Monte-carlo tree search: A New Framework for Game AI. *Belgian/Netherlands Artificial Intelligence Conference*, 389–390.

Chaslot, G. M. J.-B., WINANDS, M. H. M., HERIK, H. J. VAN DEN, UITERWIJK, J. W. H. M., & BOUZY, B. (2008). Progressive Strategies for Monte-Carlo Tree Search. *New Mathematics and Natural Computation*, *04*(03), 343–357. https://doi.org/10.1142/s1793005708001094

CHASLOT, G. M. J.-B., WINANDS, M. H. M., HERIK, H. J. VAN DEN, UITERWIJK, J. W. H. M., & BOUZY, B. (2008). Progressive Strategies for Monte-Carlo Tree Search. *New Mathematics and Natural Computation*, *04*(03), 343–357. https://doi.org/10.1142/s1793005708001094

Chinesta, F., Cueto, E., Abisset-Chavanne, E., Duval, J. L., & Khaldi, F. El. (2020). Virtual, Digital and Hybrid Twins: A New Paradigm in Data-Based Engineering and Engineered Data. *Archives of Computational Methods in Engineering*, *27*(1), 105–134. https://doi.org/10.1007/s11831-018-9301-4

Cho, H., Shah, S. N., & Osisanya, S. O. (2000). A three-layer modeling for cuttings transport with coiled tubing horizontal drilling. *SPE Reservoir Engineering (Society of Petroleum Engineers), A*, 905–918. https://doi.org/10.2118/63269-ms

Ciccarelli, J., McLachlan, D., Singh, H., & Thomson, R. (2018, October 19). Agile field development planning: A systems approach. *Society of Petroleum Engineers - SPE Asia Pacific Oil and Gas Conference and Exhibition 2018, APOGCE 2018*. https://doi.org/10.2118/191975-ms

Coley, C. (2019). Building a rig state classifier using supervised machine learning to support invisible lost time analysis. *SPE/IADC Drilling Conference, Proceedings, 2019-March*.

Contreras, W., Al-hamrany, A., Wuhaimed, A., Aramco, S., Mathew, B., & Albassam, B. (2020). *IPTC-19657-MS Tripping Performance Analysis and Quantifying Invisible Lost Time What is Tripping ? The Role of Realtime data*.

Cordoso, J. V., Maidla, E. E., & Idagawa, L. S. (1995). Problem detection during tripping operations in horizontal and directional wells. *SPE Drilling and Completion*, *10*(2), 77–83. https://doi.org/10.2118/26330-PA

Crichton, M. T., Moffat, S., & Crichton, L. (2017). Developing a Team Behavioural Marker Framework Using Observations of Simulator-Based Exercises to Improve Team Effectiveness: A Drilling Team Case Study. *Simulation and Gaming*, *48*(3), 299–313. https://doi.org/10.1177/1046878117693266

Cui, X., & Shi, H. (2011). A * -based Pathfinding in Modern Computer Games. *International Journal of Computer Science and Network Security*, *11*(1), 125–130.

Da Cruz Mazzi, V. A., Dumlao, V. C. Q., Mourthé, A. C. L., Elshahawi, H., Kim, I., & Lumens, P. (2020). Machine Learning-Enabled Digital Decision Assistant for Remote Operations. *Proceedings of the Annual Offshore Technology Conference*, *2020-May*. https://doi.org/10.4043/30488-ms

Damski, C. (2019, October 25). Systematic management for drilling process improvement. *Society of Petroleum Engineers - SPE/IATMI Asia Pacific Oil and Gas Conference and Exhibition 2019, APOG 2019*. https://doi.org/10.2118/196413-ms

Danner, G. E. (2020). Using knowledge graphs to enhance drilling operations. *Proceedings of the Annual Offshore Technology Conference*, *2020-May*. https://doi.org/10.4043/30881-ms

Datta, S. P. A. (2016). *Emergence of Digital Twins*. http://arxiv.org/abs/1610.06467

De Oliveira, G. L., Zank, C. A. C., De Costa, A. F. S., Mendes, H. M., Henriques, L. F., Mocelin, M. R., & De Oliveira Neto, J. (2016). Offshore drilling improvement through automating the rig state detection process - Implementation process history and proven success. *SPE/IADC Drilling Conference, Proceedings*, *2016-January*. https://doi.org/10.2118/178775-ms

Duan, M., Miska, S., Yu, M., Takach, N., & Ahmed, R. (2009). Critical Conditions for Effective Sand-Sized-Solids Transport in Horizontal and High-Angle Wells. In *SPE Drilling & Completion* (Vol. 229).

Dunn, M. D., & Payne, M. L. (1986). Design, specification, and implementation of drilling operations database program. *Proceedings - SPE Annual Technical Conference and Exhibition, October 1986*. https://doi.org/10.2523/15360-ms

Efroni, Y., Dalal, G., Scherrer, B., & Mannor, S. (2019). How to Combine Tree-Search Methods in Reinforcement Learning. *Proceedings of the AAAI Conference on Artificial Intelligence*, *33*, 3494–3501. https://doi.org/10.1609/aaai.v33i01.33013494

El Afifi, S., Albassam, B., & Fahmy, F. A. (2015, September 15). Enhance the drilling & tripping performance on automated rigs with fully automated performance measurement. *Society of Petroleum Engineers - SPE Middle East Intelligent Oil and Gas Conference and Exhibition*. https://doi.org/10.2118/176786-ms

Erge, O., Ozbayoglu, E. M., Miska, S. Z., Yu, M., Takach, N., Saasen, A., & May, R. (2014, March 4). The Effects of Drillstring Eccentricity, Rotation, and Buckling Configurations on Annular Frictional Pressure Losses While Circulating Yield Power Law Fluids. *IADC/SPE Drilling Conference and Exhibition*. https://doi.org/10.2118/167950-MS

Erge, O., Ozbayoglu, E. M., Miska, S. Z., Yu, M., Takach, N., Saasen, A., & May, R. (2015). The effects of drillstring-eccentricity, -rotation, and -buckling configurations on annular frictional pressure losses while circulating yield-power-law fluids. *SPE Drilling and Completion*, *30*(3), 257–271. https://doi.org/10.2118/167950-PA

Erge, O., Vajargah, A. K., Ozbayoglu, M. E., & Van Oort, E. (2016). Improved ECD prediction and management in horizontal and extended reach wells with eccentric drillstrings. *SPE - International Association of Drilling Contractors Drilling Conference Proceedings*, *2016-Janua*. https://doi.org/10.2118/178785-ms

Erge, O., & van Oort, E. (2020). Modeling cuttings transport and annular pack-off using local fluid velocities with the effects of drillstring rotation and eccentricity. *SPE/IADC Drilling Conference, Proceedings*, *2020-March*. https://doi.org/10.2118/199587-ms

Etong, N. (2019). *Digital Twins in Commercial Aviation*.

Fazaelizadeh, M. (2013). *UNIVERSITY OF CALGARY Real Time Torque and Drag Analysis during Directional Drilling*.

Feinberg, E. A. (2011). Total Expected Discounted Reward MDPS: Existence of Optimal Policies. *Wiley Encyclopedia of Operations Research and Management Science*, 1–11. https://doi.org/10.1002/9780470400531.eorms0906

Fjellheim, R. (2013). Smart collaboration for decision making in drilling. *Society of Petroleum Engineers - SPE Intelligent Energy International 2013: Realising the Full Asset Value*, 88–92. https://doi.org/10.2118/167391-ms

Forshaw, M., Becker, G., Jena, S., Linke, C., & Hummes, O. (2020). Automated hole cleaning monitoring: A modern holistic approach for NPT reduction. *International Petroleum Technology Conference 2020, IPTC 2020*. https://doi.org/10.2523/iptc-19639-abstract

Gavignet, A. A., & Sobey, I. J. (1989). Model aids cuttings transport prediction. *JPT, Journal of Petroleum Technology*, *41*(9), 916-921 15417. https://doi.org/10.2118/15417-pa

Gelly, S., & Silver, D. (2011). Monte-Carlo tree search and rapid action value estimation in computer Go. *Artificial Intelligence*, *175*(11), 1856–1875. https://doi.org/10.1016/j.artint.2011.03.007

Grieves, M. (2014). *Digital twin: manufacturing excellence through virtual factory Digital Twin*.

Grieves, M., & Vickers, J. (2016). Digital twin: Mitigating unpredictable, undesirable emergent behavior in complex systems. In *Transdisciplinary Perspectives on Complex Systems: New Findings and Approaches* (pp. 85–113). Springer International Publishing. https://doi.org/10.1007/978-3-319-38756-7_4

Grieves, M., & Vickers, J. (2017). *Digital Twin: Mitigating Unpredictable, Undesirable*

Emergent Behavior in Complex Systems. https://doi.org/10.1007/978-3-319-38756-7_4

Griggs, J. W. (2010). *BP GULF OF MEXICO OIL SPILL*. http://www.ktiv.com/Global/story.asp?S=13386062.

Gu, Q., Fallah, A., Chen, D., Ashok, P., & Van Oort, E. (2019). *IPTC-19326-MS Higher Precision Automated Managed Pressure Drilling Control Achieved Through the Addition of a Thermal Model*.

Guan, J., Tang, H., Wang, K., Yao, J., & Yang, S. (2020). A parallel multi-scenario learning method for near-real-time power dispatch optimization. *Energy*, *202*, 117708. https://doi.org/10.1016/j.energy.2020.117708

Gul, S., & van Oort, E. (2020). A machine learning approach to filtrate loss determination and test automation for drilling and completion fluids. *Journal of Petroleum Science and Engineering*, *186*, 106727. https://doi.org/10.1016/j.petrol.2019.106727

Gul, S., van Oort, E., Mullin, C., & Ladendorf, D. (2020). Automated Surface Measurements of Drilling Fluid Properties: Field Application in the Permian Basin. *SPE Drilling & Completion*. https://doi.org/10.2118/201094-pa

Guo, D., Raghavendra, C. S., Yao, K. T., Harding, M., Anvar, A., & Patel, A. (2015). Data driven approach to failure prediction for electrical submersible pump systems. *SPE Western Regional Meeting 2015: Old Horizons, New Horizons Through Enabling Technology*, 967–972. https://doi.org/10.2118/174062-ms

Hemphill, T. (2015). Advances in the calculation of circulating pressure drop with and without drillpipe rotation. *SPE/IADC Drilling Conference, Proceedings*, *2015-Janua*, 760–770. https://doi.org/10.2118/173054-ms

Hindi, K. Al, Boushehri, M., Pingle, D., Kumar, R., Tiwari, A., Wasnik, A., Estarabadi, J., Shoeibi, A., Martocchia, A., & Regan, M. (2018). Quantifying hole cleaning in realtime optimizes drilling performance and demonstarbly reduces NPT and ILT in a complex multilateral well. *SPWLA 2nd Asia Pacific Technical Symposium, APTS*

2018, 1–11.

Hodgson, R. K., & Hassard, P. (2006, April 4). Reducing the Learning Curve Through Use of an Advanced Drilling Simulator. *IADC/SPE Drilling Conference*. https://doi.org/10.2118/98107-MS

Hoffman, R. N., & Atlas, R. (2016). Future observing system simulation experiments. *Bulletin of the American Meteorological Society*, *97*(9), 1601–1616. https://doi.org/10.1175/BAMS-D-15-00200.1

Höhn, P., Freifer, R., & Oppelt, J. (2019). *REALISTIC SCENARIO DRILLING SIMULATION FOR DEEP AND CRITICAL WELLS*. Offshore Mediterranean Conference.

Howell, R., McKenzie, B., Leslie, C., & Poletzky, I. (2019). Advanced drilling simulators for well control training: Bringing together people, procedures and new technology. *SPE/IADC Drilling Conference, Proceedings*, *2019-March*. https://doi.org/10.2118/194181-ms

Hutchinson, M., Elliott, A., Carlson, M., Thornton, B., & Murray, B. (2019). Using simulation to prevent non-productive time. *SPE/IADC Drilling Conference, Proceedings*, *2019-March*.

Isemin, I. A., Nkundu, K. A. B., & Agwu, O. E. (2019). Utilization of big data analytics and advanced formation modelling for detection of kicks in drilling operations. *Society of Petroleum Engineers - SPE Nigeria Annual International Conference and Exhibition 2019, NAIC 2019*. https://doi.org/10.2118/198841-MS

Iyoho, A. W., & Takahashi, H. (1993). Modeling unstable cuttings transport in horizontal eccentric wellbores. *Society of Petroleum Engineers of AIME, (Paper) SPE*, *1*, 1–16.

Jalukar, L. S. (1993). *Study of Hole Size Effect on Critical and Subcritical Drilling Fluid Velocities in Cuttings Transport for Inclined Wellbores*. University of Tulsa.

James, S., Konidaris, G., & Rosman, B. (2017). An analysis of Monte Carlo tree search.

31st AAAI Conference on Artificial Intelligence, AAAI 2017, *July*, 3576–3582.

Jasmin, E. A., Imthias Ahamed, T. P., & Jagathy Raj, V. P. (2011). Reinforcement Learning approaches to Economic Dispatch problem. *International Journal of Electrical Power and Energy Systems*, *33*(4), 836–845. https://doi.org/10.1016/j.ijepes.2010.12.008

Jeong, C., Yu, Y., Mansour, D., Vesslinov, V., & Meehan, R. (2020). A physics model embedded hybrid deep neural network for drillstring washout detection. *SPE/IADC Drilling Conference, Proceedings*, *2020-March*.

Ji, Y., Wang, J., Xu, J., Fang, X., & Zhang, H. (2019). Real-Time Energy Management of a Microgrid Using Deep Reinforcement Learning. *Energies*, *12*(12), 2291. https://doi.org/10.3390/en12122291

Johancsik, C. A., Friesen, D. B., & Dawson, R. (1984). *Torque and Drag in Directional Wells - Prediction and Measurement*.

Johnson, W., & Rao, S. (2020). Using model-based design for digital twins to predict the real-time performance of surface equipment. *SPE/IADC Drilling Conference, Proceedings*, *2020-March*.

Jones, D., Snider, C., Nassehi, A., Yon, J., & Hicks, B. (2020). Characterising the Digital Twin: A systematic literature review. *CIRP Journal of Manufacturing Science and Technology*. https://doi.org/10.1016/j.cirpj.2020.02.002

Kamjoo, A., Maheri, A., Dizqah, A. M., & Putrus, G. A. (2016). Multi-Objective Design under Uncertainties of Hybrid Renewable Energy System Using NSGA-II and Chance Constrained Programming. *INTERNATIONAL JOURNAL OF ELECTRICAL POWER & ENERGY SYSTEMS*, *74*(1), 187–194. https://doi.org/10.1016/j.ijepes.2015.07.007

Kamp, A. M., & Rivero, M. (1999, April 4). Layer Modeling for Cuttings Transport in Highly Inclined Wellbores. *Latin American and Caribbean Petroleum Engineering Conference*. https://doi.org/10.2118/53942-MS

Kang, D.-J., Park, J. H., & Yeo, S.-S. (2009). Intelligent Decision-Making System with Green Pervasive Computing for Renewable Energy Business in Electricity Markets on Smart Grid. *EURASIP Journal on Wireless Communications and Networking*. https://doi.org/10.1155/2009/247483

Karstad, E., & Aadnoy, B. S. (1997, April 4). Analysis of Temperature Measurements during Drilling. *SPE Annual Technical Conference and Exhibition*. https://doi.org/10.2118/38603-MS

Kelessidis, V. C., Ahmed, S., & Koulidis, A. (2015). An improved drilling simulator for operations, research and training. *SPE Middle East Oil and Gas Show and Conference, MEOS, Proceedings*, *2015-January*, 2650–2664. https://doi.org/10.2118/172793-ms

Kenny, P., Sunde, E., & Hemphill, T. (1996). Hole cleaning modelling: What's `n' got to do with it? *Proceedings of the Drilling Conference*, 479–492. https://doi.org/10.2523/35099-ms

Kiran, B. R., Sobh, I., Talpaert, V., Mannion, P., Al Sallab, A. A., Yogamani, S., & Pérez, P. (2020). *Deep Reinforcement Learning for Autonomous Driving: A Survey*.

Kjøsnes, I., Laklingholm, G., Saasen, A., Syrstad, S. O., Agle, A., & Solvang, K. A. (2003). Successful Water Based Drilling Fluid Design for Optimizing Hole Cleaning and Hole Stability. *Proceedings of the Drilling Conference*, 339–346. https://doi.org/10.2523/85330-ms

Klein, S. (2015). *Attacking SameGame using Monte-Carlo Tree Search*.

Kocsis, L., Szepesvári, C., & Willemson, J. (2006). Improved Monte-Carlo Search. *White Paper*, *1*, 22. https://doi.org/10.1007/11871842_29

Korkmaz, M., & Durdu, A. (2018). Comparison of optimal path planning algorithms. *14th International Conference on Advanced Trends in Radioelectronics, Telecommunications and Computer Engineering, TCSET 2018 - Proceedings*, *2018-April*, 255–258. https://doi.org/10.1109/TCSET.2018.8336197

Kumar, A. (2019, April 26). A Machine Learning Application for Field Planning. *Offshore Technology Conference*. https://doi.org/10.4043/29224-MS

Kunath, M., & Winkler, H. (2018). Integrating the Digital Twin of the manufacturing system into a decision support system for improving the order management process. *Procedia CIRP*, *72*, 225–231. https://doi.org/10.1016/j.procir.2018.03.192

Kuznetsova, E., Li, Y. F., Ruiz, C., Zio, E., Ault, G., & Bell, K. (2013). Reinforcement learning for microgrid energy management. *Energy*, *59*, 133–146. https://doi.org/10.1016/j.energy.2013.05.060

Kyllingstad, A., & Nessjøen, P. J. (2011). Condition based maintenance: A new early leak detection system for mud pumps. *SPE/IADC Drilling Conference, Proceedings*, *1*, 420–432.

Lakhanpal, V., & Samuel, R. (2017). A new approach to harness data for measuring invisible lost time in drilling operations. *Proceedings - SPE Annual Technical Conference and Exhibition*.

Larsen, T. I. (1990). *A Study of the Critical Fluid Velocity in Cuttings Transport for Inclined Wellbores*. The University of Tulsa.

Larsen, T. I., Pilehvari, A. A., & Azar, J. J. (1997a). Development of a new cuttings-transport model for high-angle wellbores including horizontal wells. *SPE Drilling and Completion*, *12*(2), 129–134. https://doi.org/10.2118/25872-PA

Larsen, T. I., Pilehvari, A. A., & Azar, J. J. (1997b). Development of a new cuttings-transport model for high-angle wellbores including horizontal wells. *SPE Drilling and Completion*, *12*(2), 129–134. https://doi.org/10.2118/25872-PA

LaValle, S. M. (2006). *Planning Algorithms*. Cambridge University Press. https://doi.org/10.1017/CBO9780511546877

Lesage, M., Falconer, I. G., & Wick, C. J. (1988). Evaluating drilling practice in deviated wells with torque and weight data. *SPE Drilling Engineering*, *3*(3), 248–252.

https://doi.org/10.2118/16114-PA

Li, J., & Walker, S. (2001). Sensitivity analysis of hole cleaning parameters in directional wells. *SPE Journal*, *6*(4), 356–363. https://doi.org/10.2118/74710-PA

Li, L. K., Seng, K. P., Yeong, L. S., Ch'ng, S. I., & Li-Minn, A. (2014). The Boundary Iterative-Deepening Depth-First Search Algorithm. *International Journal of Advances in Computer Science and Its Applications – IJCSIA*, *4*(1), 45–50.

Lim, K. Y. H., Zheng, P., & Chen, C. H. (2019). A state-of-the-art survey of Digital Twin: techniques, engineering product lifecycle management and business innovation perspectives. *Journal of Intelligent Manufacturing*, *February 2020*. https://doi.org/10.1007/s10845-019-01512-w

Lines, L., Mauldin, C., Hill, J., & Aiello, R. (2014). *SPE-170586-MS Advanced Drilling Dynamics Sensor Allows Real-Time Drilling Optimization, Damage Prevention and Condition Monitoring of RSS and LWD BHAs*.

Liu, Y., Yao, K.-T., Liu, S., Raghavendra, C. S., Lenz, T. L., Olabinjo, L., Seren, F. B., Seddighrad, S., & Dinesh Babu, C. G. (2010, April 4). Failure Prediction for Artificial Lift Systems. *SPE Western Regional Meeting*. https://doi.org/10.2118/133545-MS

Liu, Yu, Kibbey, J., Bai, Y., & Wu, X. (2018, March 6). Real-Time Bit Wear Monitoring and Prediction Using Surface Mechanics Data Analytics: A Step Toward Digitization Through Agile Development. *IADC/SPE Drilling Conference and Exhibition*. https://doi.org/10.2118/189602-MS

Lu, Y., Liu, C., Wang, K. I. K., Huang, H., & Xu, X. (2020). Digital Twin-driven smart manufacturing: Connotation, reference model, applications and research issues. *Robotics and Computer-Integrated Manufacturing*, *61*(August), 101837. https://doi.org/10.1016/j.rcim.2019.101837

Macchi, M., Roda, I., Negri, E., & Fumagalli, L. (2018). Exploring the role of Digital Twin for Asset Lifecycle Management. *IFAC-PapersOnLine*, *51*(11), 790–795.

https://doi.org/10.1016/j.ifacol.2018.08.415

Maidla, E., & Haci, M. (2004, April 4). Understanding Torque: The Key to Slide-Drilling Directional Wells. *IADC/SPE Drilling Conference*. https://doi.org/10.2118/87162-MS

Mao, Y., & Zhang, P. (2019). An automated kick alarm system based on statistical analysis of real-time drilling data. *Society of Petroleum Engineers - Abu Dhabi International Petroleum Exhibition and Conference 2019, ADIP 2019*.

Martins, A. L., & Costapinto Santana, C. (1992). Evaluation of cuttings transport in horizontal and near horizontal wells - A dimensionless approach. *SPE Latin American and Caribbean Petroleum Engineering Conference Proceedings*, *1992-March*, 155–161. https://doi.org/10.2523/23643-ms

Mason, C. J., & Chen, D. C. K. (2007). Step changes needed to modernize T&D software. *SPE/IADC Drilling Conference, Proceedings*, *1*, 90–101. https://doi.org/10.2118/104609-ms

Mayani, M. G., Baybolov, T., Rommetveit, R., Ødegaard, S. I., Koryabkin, V., & Lakhtionov, S. (2020a). Optimizing drilling wells and increasing the operation efficiency using digital twin technology. *SPE/IADC Drilling Conference, Proceedings*, *2020-March*.

Mayani, M. G., Baybolov, T., Rommetveit, R., Ødegaard, S. I., Koryabkin, V., & Lakhtionov, S. (2020b). Optimizing drilling wells and increasing the operation efficiency using digital twin technology. *SPE/IADC Drilling Conference, Proceedings*, *2020-March*. https://doi.org/10.2118/199566-ms

Mayani, M. G., Rommetveit, R., Oedegaard, S. I., & Svendsen, M. (2018). Drilling Automated Realtime Monitoring Using Digital Twin Automated monitoring system (AM) of the drilling well using Digital Twin. *Society of Petroleum Engineers*, *November*, 12–15.

McManus, C. D., Leach, P., Wicker, P., & Anderson, S. (2012). Well planning: A risk management process. *Society of Petroleum Engineers - SPE Deepwater Drilling and Completions Conference 2012*, 603–609. https://doi.org/10.2118/156332-ms

Menand, S., Sellami, H., Tijani, M., Stab, O., Dupuis, D. C., & Simon, C. (2006, January 1). *Advancements in 3D Drillstring mechanics: From the Bit to the Topdrive*. https://doi.org/10.2118/98965-ms

Millan, E., & Ringer, M. (2018, March 6). *A New Workflow for Estimating Bit Wear and Monitoring Drilling Efficiency in Real Time During Drilling Operations*. https://doi.org/10.2118/189582-ms

Miller, P., & Gouveia, J. (2019). Applying decision trees to improve decision quality in unconventional resource development. *Proceedings - SPE Annual Technical Conference and Exhibition*, *2019-September*. https://doi.org/10.2118/195811-ms

Minchev, Z. B., & Shalamanov, V. M. (2010). Scenario Generation and Assessment Framework Solution in Support of the Comprehensive Approach. *International Symposium "Analytical Support to Defence Transformation*, *April 2010*, 22;1-22;16.

Mirhaj, S. A., Kaarstad, E., & Aadnoy, B. S. (2016). Torque and drag modeling; Soft-string versus stiff-string models. *Proceedings of the SPE/IADC Middle East Drilling Technology Conference and Exhibition*, *2016-January*. https://doi.org/10.2118/178197-ms

Mitchell, R. F. (1988). Dynamic surge/swab pressure predictions. *SPE Drilling Engineering*, *3*(3), 325–333. https://doi.org/10.2118/16156-PA

Mitchell, Robert F. (2008). Drillstring solutions improve the torque-drag model. *SPE/IADC Drilling Conference, Proceedings*, *1*, 625–642. https://doi.org/10.2118/112623-ms

Mitchell, Robert F., & Miska, S. Z. (2011). *Fundamentals of Drilling Engineering*.

Mitchell, Robert F., & Samuel, R. (2007). How good is the torque-drag model? *SPE/IADC Drilling Conference, Proceedings*, *1*, 232–240.

https://doi.org/10.2523/105068-ms

Mittal, M., Lakhanpal, V., & Samuel, R. (2020). Measuring microinvisible loss milt time in drilling operations. *SPE/IADC Drilling Conference, Proceedings*, *2020-March*, 1–10.

Moerland, T. M., Broekens, J., Plaat, A., & Jonker, C. M. (2018). *A0C: Alpha Zero in Continuous Action Space*. http://arxiv.org/abs/1805.09613

Mussmann, S., & See, A. (2017). *Graph Search Algorithms*.

Mutlu, M., Wassar, T., Franchek, M. A., Omrani, A. E., & Gutierrez, J. A. (2018). Real-time condition and performance monitoring of a subsea blowout preventer pipe ram. *SPE Drilling and Completion*, *33*(1), 50–62. https://doi.org/10.2118/189987-PA

Nadhan, D., Mayani, M. G., & Rommetveit, R. (2018). Drilling with digital twins. *Proceedings of the IADC/SPE Asia Pacific Drilling Technology Conference, APDT*, *2018-Augus*(August), 27–29. https://doi.org/10.2118/191388-ms

Naganawa, S. (2017). *Cuttings-Transport Simulation Combined With Large-Scale-Flow-Loop Experimental Results and Logging-While-Drilling Data for Hole-Cleaning Evaluation in Directional Drilling*. https://doi.org/10.2118/171740-PA

Naganawa, S., & Nomura, T. (2006, April 4). Simulating Transient Behavior of Cuttings Transport over Whole Trajectory of Extended Reach Well. *IADC/SPE Asia Pacific Drilling Technology Conference and Exhibition*. https://doi.org/10.2118/103923-MS

NATO. (2007). *The use of Scenarios in Long Term Defence Planning*. https://plausiblefutures.wordpress.com/2007/04/10/the-use-of-scenarios-in-long-term-defence-planning/

Nazari, T., Hareland, G., & Azar, J. J. (2010, April 4). Review of Cuttings Transport in Directional Well Drilling: Systematic Approach. *SPE Western Regional Meeting*. https://doi.org/10.2118/132372-MS

Nguyen, D., & Rahman, S. S. (1998). A three-layer hydraulic program for effective cuttings transport and hole cleaning in highly deviated and horizontal wells. *SPE Drilling and Completion*, *13*(3), 182–189. https://doi.org/10.2118/51186-PA

Okoli, P., Vega, J. C., & Shor, R. (2019). Estimating downhole vibration via machine learning techniques using only surface drilling parameters. *SPE Western Regional Meeting Proceedings, 2019*. https://doi.org/10.2118/195334-ms

Olaf Blech, J., Fernando, L., & Foster, K. (2017). *Towards Decision Support for Smart Energy Systems based on Spatio-temporal Models*.

Ontanon, S., Synnaeve, G., Uriarte, A., Richoux, F., Churchill, D., & Preuss, M. (2013). A survey of real-time strategy game AI research and competition in starcraft. *IEEE Transactions on Computational Intelligence and AI in Games*, *5*(4), 293–311. https://doi.org/10.1109/TCIAIG.2013.2286295

Ouahrani, L., Abdul Haris, A. N., Suluru, S., Chiha, A., & Al Fakih, A. (2018). Invisible Lost Time measurement and reduction contributes to optimizing total well time by improving ROP and reducing flat time. *Society of Petroleum Engineers - SPE Kingdom of Saudi Arabia Annual Technical Symposium and Exhibition 2018, SATS 2018*. https://doi.org/10.2118/192319-ms

Ozbayoglu, M. E., Saasen, A., Sorgun, M., & Svanes, K. (2008). Effect of pipe rotation on hole cleaning for water-based drilling fluids in horizontal and deviated wells. *Society of Petroleum Engineers - IADC/SPE Asia Pacific Drilling Technology Conference 2008 - "Drilling Technology to Access Future Energy Demand and Environmental Challenges,"* 332–342. https://doi.org/10.2118/114965-ms

Pivano, L., Trong Nguyen, D., & Bruun Ludvigsen, K. (2019). *OTC-29316-MS Digital Twin for Drilling Operations-Towards Cloud-Based Operational Planning*.

Poole, D. L., & Mackworth, A. K. (2017). *Artificial Intelligence: Foundations of Computational Agents* (2nd Editio). Cambridge University Press.

Pournazari, P., Adams, D., Ashok, P., Oort, E. van, & Holliday, K. (2016, September 14). Real-Time Health Monitoring of Top Drives for Offshore Operations Using Physics

Based Models and New Sensor Technology. *SPE Deepwater Drilling and Completions Conference*. https://doi.org/10.2118/180356-MS

Pournazari, P., Ashok, P., Van Oort, E., Unrau, S., & Lai, S. (2015). Enhanced kick detection with low-cost rig sensors through automated pattern recognition and real-time sensor calibration. *Society of Petroleum Engineers - SPE Middle East Intelligent Oil and Gas Conference and Exhibition*.

Power, D. J., Hight, C., Weisinger, D., & Rimer, C. (2000). Drilling Practices and Sweep Selection for Efficient Hole Cleaning in Deviated Wellbores. *Proceedings of the IADC/SPE Asia Pacific Drilling Technology Conference, APDT*, 451–459. https://doi.org/10.2118/62794-ms

Power Digital Solutions, G. (2016). *GE Power Digital Solutions GE Digital Twin*.

Puterman, M. L. (1994). *Markov Decision Processes* (M. L. Puterman (ed.)). John Wiley & Sons, Inc. https://doi.org/10.1002/9780470316887

Qi, X., Luo, Y., Wu, G., Boriboonsomsin, K., & Barth, M. (2019). Deep reinforcement learning enabled self-learning control for energy efficient driving. *Transportation Research Part C: Emerging Technologies*, *99*, 67–81. https://doi.org/10.1016/j.trc.2018.12.018

Rasheed, A., San, O., & Kvamsdal, T. (2019). *Digital Twin: Values, Challenges and Enablers*. https://arxiv.org/abs/1910.01719

Reckmann, H., Jogi, P., Kpetehoto, F. T., Chandrasekaran, S., & Macpherson, J. D. (2010, April 4). MWD Failure Rates Due to Drilling Dynamics. *IADC/SPE Drilling Conference and Exhibition*. https://doi.org/10.2118/127413-MS

Reddy, H. (2013). PATH FINDING - Dijkstra's and A* Algorithm's. *International Journal in IT and Engineering*, 1–15.

Rommetveit, R., Mayani, M. G., Nabavi, J., Helgeland, S., Hammer, R., & Råen, J. (2019). Automatic realtime monitoring of drilling using digital twin technologies enhance safety and reduce costs. *Society of Petroleum Engineers - Abu Dhabi International Petroleum Exhibition and Conference 2019, ADIP 2019*.

Rowatt, J. D., Jourde, A., Pemmasani, V. K., Barbosa, B., Yepez, J.-C., & Thow, P. (2020, February 25). Results from the Introduction of a Well Construction System. *IADC/SPE International Drilling Conference and Exhibition*. https://doi.org/10.2118/199608-MS

Rubiandini R.S., R. (1999). *Equation for Estimating Mud Minimum Rate for Cuttings Transport in an Inclined-Until-Horizontal Well*. https://doi.org/10.2118/57541-ms

Saasen, A., & Løklingholm, G. (2002a). The Effect of Drilling Fluid Rheological Properties on Hole Cleaning. *Proceedings of the Drilling Conference*, 683–687. https://doi.org/10.2523/74558-ms

Saasen, A., & Løklingholm, G. (2002b, April 4). The Effect of Drilling Fluid Rheological Properties on Hole Cleaning. *IADC/SPE Drilling Conference*. https://doi.org/10.2118/74558-MS

Sadlier, A., Says, I., & Hanson, R. (2013, March 5). Automated Decision Support to EnhanceWhile-Drilling Decision Making: Where Doesit fit Within Drilling Automation? *SPE/IADC Drilling Conference*. https://doi.org/10.2118/163430-MS

Saini, G. S., Ashok, P., & van Oort, E. (2020). Predictive action planning for hole cleaning optimization and stuck pipe prevention using digital twinning and reinforcement learning. *SPE/IADC Drilling Conference, Proceedings*, *2020-March*.

Saini, G. S., Ashok, P., van Oort, E., & Isbell, M. R. (2018). Accelerating well construction using a digital twin demonstrated on unconventional well data in North America. *SPE/AAPG/SEG Unconventional Resources Technology Conference 2018, URTC 2018*. https://doi.org/10.15530/urtec-2018-2902186

Saini, G. S., Chan, H. C., Ashok, P., van Oort, E., Behounek, M., Thetford, T., & Shahri, M. (2018, August 9). Spider bots: Database enhancing and indexing scripts to efficiently convert raw well data into valuable knowledge. *SPE/AAPG/SEG*

Unconventional Resources Technology Conference 2018, URTC 2018. https://doi.org/10.15530/urtec-2018-2902181

Saini, G. S., Chan, H. C., Ashok, P., Van Oort, E., & Isbell, M. R. (2018). Automated large data processing: A storyboarding process to quickly extract knowledge from large drilling datasets. *Society of Petroleum Engineers - IADC/SPE Drilling Conference and Exhibition, DC 2018, 2018-March*. https://doi.org/10.2118/189605-ms

Sanchez, R. A., Azar, J. J., Bassal, A. A., & Martins, A. L. (1997). Effect of drillpipe rotation on hole cleaning during directional well drilling. In *Proceedings of the Drilling Conference* (pp. 459–467). https://doi.org/10.2523/37626-ms

Schmidt, M.-T. (2017). *Delivering a Digital Twin*.

Schwarting, W., Alonso-Mora, J., & Rus, D. (2018). Planning and Decision-Making for Autonomous Vehicles. *Annu. Rev. Control Robot. Auton. Syst. 2018*, *1*, 187–210. https://doi.org/10.1146/annurev-control-060117

Shahri, M., Kutlu, B., Thetford, T., Nelson, B., Wilson, T., Behounek, M., Ambrus, A., & Ashok, P. (2018). Adopting physical models in real-time drilling application: Wellbore hydraulics. *Society of Petroleum Engineers - SPE Liquids-Rich Basins Conference - North America 2018, LRBC 2018*. https://doi.org/10.2118/191797-ms

Shahri, M., Wilson, T., Thetford, T., Nelson, B., Behounek, M., Ambrus, A., D'Angelo, J., & Ashok, P. (2018). Implementation of a fully automated real-time torque and drag model for improving drilling performance: Case study. *Proceedings - SPE Annual Technical Conference and Exhibition*, *2018-Septe*. https://doi.org/10.2118/191426-ms

Sheppard, M. C., Wick, C., & Burgess, T. (1987). Designing Well Paths To Reduce Drag and Torque. *SPE Drilling Engineering*, *2*(4), 344–350. https://doi.org/10.2118/15463-PA

Shirangi, M. G., Ettehadi, R., Aragall, R., Furlong, E., May, R., & Dahl, T. (2020). *IADC*

/ SPE-199681-MS Digital Twins for Drilling Fluids : Advances and Opportunities Development of a Digital Twin Automated Machine Learning for Predictive Analytics. 1–15.

Shirkavand, F., Hareland, G., & Olson, W. (2010). The design and development of a drilling simulator for planning and optimizing under-balanced drilling operations. *Journal of Canadian Petroleum Technology*, *49*(6), 68–73. https://doi.org/10.2118/139125-PA

Shokouhi, S. V., & Skalle, P. (2009). Enhancing decision making in critical drilling operations. *SPE Middle East Oil and Gas Show and Conference, MEOS, Proceedings*, *2*, 809–816. https://doi.org/10.2118/120290-ms

Sifferman, T. R., & Becker, T. E. (1992). Hole cleaning in full-scale inclined wellbores. *SPE Drilling Engineering*, *7*(2), 115–120. https://doi.org/10.2118/20422-PA

Silver, D, & Gelly, S. (2011). Monte-Carlo tree search and rapid action value estimation in computer Go. *Artificial Intelligence*, *175*(11), 1856–1875.

Silver, David. (2009). *Reinforcement Learning and Simulation-Based Search in Computer Go*. University of Alberta.

Silver, David, Hubert, T., Schrittwieser, J., Antonoglou, I., Lai, M., Guez, A., Lanctot, M., Sifre, L., Kumaran, D., Graepel, T., Lillicrap, T., Simonyan, K., & Hassabis, D. (2018). *A general reinforcement learning algorithm that masters chess, shogi, and Go through self-play*. http://science.sciencemag.org/

Silver, David, Schrittwieser, J., Simonyan, K., Antonoglou, I., Huang, A., Guez, A., Hubert, T., Baker, L., Lai, M., Bolton, A., Chen, Y., Lillicrap, T., Hui, F., Sifre, L., Van Den Driessche, G., Graepel, T., & Hassabis, D. (2017). Mastering the game of Go without human knowledge. *Nature*, *550*(7676), 354–359. https://doi.org/10.1038/nature24270

Silver, David, Sutton, R. S., & Müller, M. (2012). Temporal-difference search in computer Go. *Machine Learning*, *87*(2), 183–219. https://doi.org/10.1007/s10994-

012-5280-0

Srivastav, R., Enfis, M., Crespo, F., Ahmed, R., Saasen, A., & Laget, M. (2012). Surge and swab pressures in horizontal and inclined wells. *SPE Latin American and Caribbean Petroleum Engineering Conference Proceedings*, *1*, 720–727. https://doi.org/10.2118/152662-ms

Sutton, R. S., & Barto, A. G. (2018). *Reinforcement Learning: An Introduction* (Second edi). The MIT Press , Cambridge, Massachusetts.

Tuegel, E. J., Ingraffea, A. R., Eason, T. G., & Spottswood, S. M. (2011). Reengineering Aircraft Structural Life Prediction Using a Digital Twin. *International Journal of Aerospace Engineering*, *2011*, 14. https://doi.org/10.1155/2011/154798

Vandael, S., Claessens, B., Ernst, D., Holvoet, T., & Deconinck, G. (2015). Reinforcement Learning of Heuristic EV Fleet Charging in a Day-Ahead Electricity Market. *IEEE Transactions on Smart Grid*, *6*(4), 1795–1805. https://doi.org/10.1109/TSG.2015.2393059

Vodopivec, T. (2018). *Monte Carlo Tree Search Strategies* [Maastricht University]. https://core.ac.uk/download/pdf/151301258.pdf

Vodopivec, T., Samothrakis, S., & Ŝter, B. (2017). On monte carlo tree search and reinforcement learning. *Journal of Artificial Intelligence Research*, *60*, 881–936. https://doi.org/10.1613/jair.5507

Walker, R. E., & Mayes, T. M. (1975). Design of Muds for Carrying Capacity. *JPT, Journal of Petroleum Technology*, *27*(07), 893–900. https://doi.org/10.2118/4975-PA

Walker, S., & Li, J. (2000). *The Effects of Particle Size, Fluid Rheology, and Pipe Eccentricity on Cuttings Transport*. 1–10. https://doi.org/10.2118/60755-ms

Wiewiora, E. (2017). Reward Shaping. In *Encyclopedia of Machine Learning and Data Mining* (pp. 1104–1106). Springer US. https://doi.org/10.1007/978-1-4899-7687-

1_966

Williams, C. E., & Bruce, G. H. (1951). Carrying Capacity of Drilling Muds. *Journal of Petroleum Technology*, *3*(04), 111–120. https://doi.org/10.2118/951111-g

You, M., Salama, W., & Alasow, A. (2020). Technology lifecycle management innovation–prognostic health monitoring on downhole drilling equipment. *International Petroleum Technology Conference 2020, IPTC 2020*.

Zeidler, H. U. (1970). *An Experimental Analysis of the Transport of Drilled Particles in an Annulus*.

Zhang, F., Miska, S., Yu, M., Ozbayoglu, E., Takach, N., & Osgouei, R. E. (2015, March 24). Is Well Clean Enough? A Fast Approach to Estimate Hole Cleaning for Directional Drilling. *SPE/ICoTA Coiled Tubing & Well Intervention Conference & Exhibition*. https://doi.org/10.2118/173681-MS

Zhao, Y., Sun, B., Fu, G., Liu, S., Xu, L., & Wang, N. (2019). Early detection of drillstring washout based on hydraulics model and pattern recognition method. *Proceedings of the International Offshore and Polar Engineering Conference*, *2*, 1854–1860.

Zou, L., Patel, M. H., & Han, G. (2000). A New Computer Package for Simulating Cuttings Transport and Predicting Hole Cleaning in Deviated and Horizontal Wells. *Proceedings of the International Oil and Gas Conference and Exhibition in China, IOGCEC*, *1*, 261–272. https://doi.org/10.2118/64646-ms